AGH University

FLUIDIZATION

Author:
mgr inz. Leszek Stepien

Supervisor:
dr hab. inz. Marek Sciazko

Department of Energy nad Fuels

January 2015

Chapter 1

Introduction to fluidization

1.1 Goal of this course

The aim of this course is to provide basic knowledge about fluidization and aerodynamics of gas-solid systems as well as mathematical tools that enable to simulate basic fluidized systems.

1.2 The phenomenon of fluidization

To simply decribe the idea behind fludization process one can say that it is the operation that can change a system a solid particles into fluidlike suspension in gas or liquid. This method of contacting of this two phase mixture have some unusual characteristics that are widely used in many fields of chemical industry. Simplified diagram showing the idea of fluidization is presented in Fig. 1.1. Gas is delivered from the bottom of the reactor, goes through a gas distributor to provide inform distribution through whole profile of bed and flows through packed bed of solids.

At low gas velocities the drag force is to small to lift the bed, which remains fixed. Increasing gas velocity causes solids to move upward and create fluid bed. Depending on the velocity of gas we can distinguish different modes of fluidization (Fig. 1.2) from bubbling fluidization, through turbulent and fast fluidization modes up to pneumatic transport of solids.

Another important issue concerning the fluidization proces is pressure drop through a fixed bed. Fig. 1.3 presents changes in pressure drop with changing gas velocity. At first one can observe increasing pressure drop, up to some level where it becomes constant, despite increasing gas velocity. This change in pressure drop trend can be connected

FIGURE 1.1: Schematic diagram of fluidization
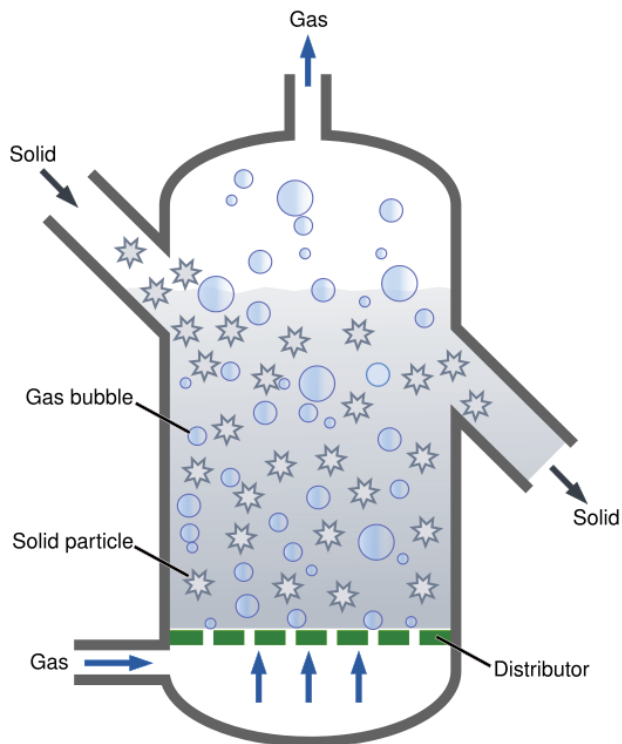
with the creation of dense phase of fluidized bed and that is the moment when the fluidization occurs. The velocity at which the pressure is stabilized is called minimum fludization velocity. Pressure drop is stable in a certain range of velocities, then a slight increase can be observed which precede a drastic decrease in pressure drop. This is due to the entrainment of smaller particles which are suspended in the section over the dense fluidized bed. Further increase in gas velocity will cause more fractions to be carried over which leads to disappearance of dense phase and start of pneumatic transport. Although, as it will be shown later in some cases gas velocities exceeding the terminal velocity can be applied for the so called fast fluidization.

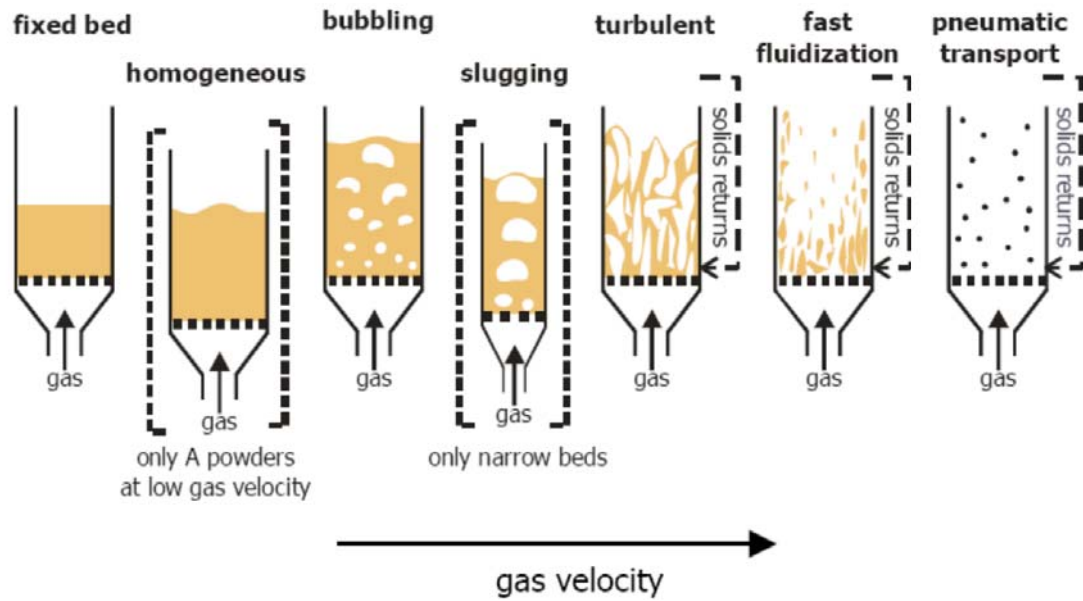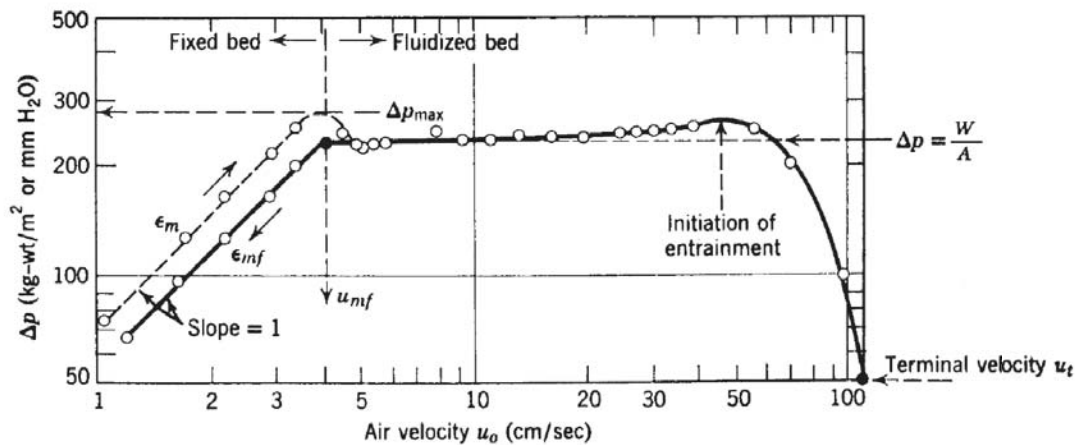FIGURE 1.2: Fluidization type depending on gas velocity

FIGURE 1.3: Pressure drop vs. gas velocity.

1.3   Discussion points

1. Definition of fluidization phenomenon.

2. Various types of beds with gas flowing through a bed of fine particles.

3. Circulating fluid bed characteristics.

4. Liquidlike features of fluid beds

5. Advantages and disadvantages of fluidized beds.

6. Heat transport phenomenon in fluidized bed.

7. Drying process in fluid bed - basic process configuration.

8. Catalytic cracking in fluid bed.

9. Fluid bed boilers for energy generation.

10. Fluid bed pyrolysis and gasification.

Chapter 2

Fluidization velocities

2.1   Characterization of particles

Usually the bed contains particles with a wide range of size and shapes, which causes the necessity to provide a proper and uniform description of size of material forming a bed. If the particles are spherical the bed can be described by means of their diameter distribution, but in real application most particles are nonspherical which yields a question about the way to decribe this kind of beds. There exists a wide range of nonsphericity measures [?]. However, the most wildly used is the one called sphericity (ϕ_s) defined as the ratio of the surface of sphere to the surface of particle with the same volume. For spherical particles $\phi_s = 1$ and for other shapes $0 \leq \phi_s \leq 1$. Sphericity values for some popular particles can be found in [?]. Other important parameter describing nonspherical particles is their specific surface, given as the ratio between surface and volume of the particle:

$$a^{'} = \frac{6}{\phi_s d_{sph}}$$
(2.1)

where d_{sph} is a diameter of the sphere having the same volume as the considered particle. The same concept can be applied to the whole bed of particles:

$$a = \frac{6(1 - \epsilon_m)}{\phi_s d_{sph}}$$
(2.2)

where ϵ_m is the fractional voidage, which usually can be found experimentally for each specific system.

2.2 Particle size distribution

Variety in shapes of particles is not an only problem in describing the bed, because in most cases one also has a bed of particles with different sizes. For this description we can define two functions of size distribution **p** and **P**. Assuming that we have a bed of solids with diameters dp_i, for $i \in (1, 2, \ldots, N)$ then **p** gives the fraction (mass, volume, number) of particles that are of the diameter $d \in (dp_1, dp_{i+1})$. The function **P** gives the so called cumulative distribution, which means the fraction of solids that are smaller than the given value dp. Examples of such distributions are shown in Fig.2.1

FIGURE 2.1: Difference between **P** (left) and **p** (right)
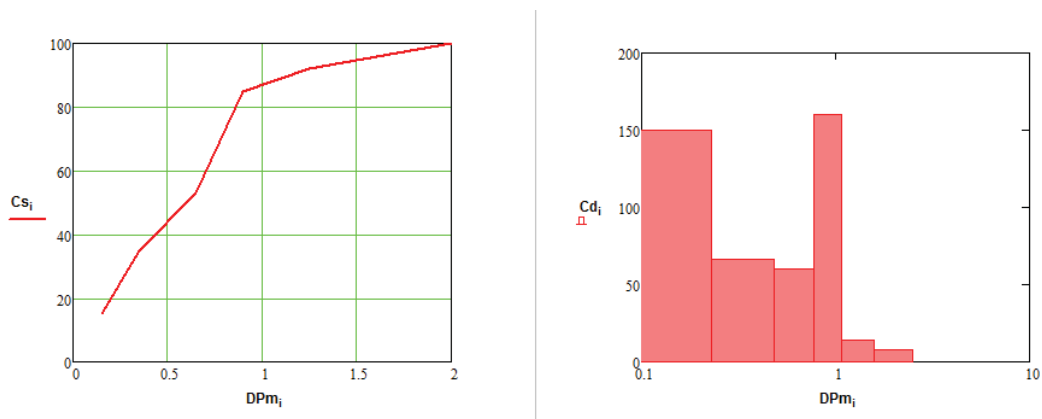
Next issue is to provide an average size than can best describe properties of the system and can be used in further calculations. This is done by harmonic diameter:

$$\overline{dp} = \frac{1}{\sum_{i=1}^{N} \frac{x_i}{dp_i}} \tag{2.3}$$

where x_i is a fraction of solids with diameter $(dp_i, dp_{i+1}$ and $dp_i = \frac{dp_i + dp_{i+1}}{2}$. Then mean specific surface can be obtained using equation (2.1):

$$\overline{a'} = \frac{6}{\phi_s \overline{dp}} \tag{2.4}$$

2.3 Fluidization velocities

First step in the process of description of fluidized bed is to calculate the velocity of gas needed in the system. We can distinguish two basic velocities describing fluidization: minimum and terminal. In this section we present the procedure used to calculate both

of them. All calculations can be performed for a bed with single or multi size particles (in case of multi size bed it is necessary to calculate its mean diameter).

2.3.1 Pressure drop

Pressure drop through fixed bed of solids of uniform size (dp) of the length L is given by Ergun [XX] correlation:

$$\frac{\Delta P}{L} = 150\frac{(1 - \epsilon_m)^2}{\epsilon_m^3}\frac{\mu u_0}{(\phi_s d_p)^2} + 1.75\frac{1 - \epsilon_m}{\epsilon_m^3}\frac{\rho_g u_o^2}{\phi_s dp} \tag{2.5}$$

where μ is gas viscosity, dp is solid diameter, ρ_g is gas density, u_0 is superficial gas velocity.

2.3.2 Minimum fluidizing velocity

At the beginning of this section one has to revise definitions of two dimensionless numbers: Reynolds(2.6) and Archimedes (2.7)

$$Re = \frac{d_p u_{mf} \rho_g}{\mu} \tag{2.6}$$

$$Ar = \frac{d_p^3 \rho_g (\rho_s - \rho_g) g}{\mu^2} \tag{2.7}$$

Now, remembering that the phenomenon of fludization occurs when drag force created by the upward flow of gas is a least equal to the weight of particles in the bed. Mathematically it can be presented with the following equation:

$$\Delta P_{bed} A_t = A_t L_{mf}(1 - \epsilon_{mf})[(\rho_s - \rho_g)g] \tag{2.8}$$

Rearranging and combining with equation (2.5) gives a quadratic in $u_m f$ which can be presented in dimensionless form of the equation (2.9) (for the details see "Problem solving", ex. 3)

$$\frac{1.75}{\epsilon_{mf}^3 \phi_s} Re_{p,mf}^2 + \frac{150(1 - \epsilon_{mf})}{\epsilon_{mf}^3 \phi_s^2} Re_{p,mf} = Ar \tag{2.9}$$

Solving equation (2.9) can be laborious but gives reliable estimation of u_{mf} if sphericity and voidage are known. For rough estimation without knowledge of voidage and sphericity of the system some simplifications can be used. For fine particles expression (2.10) proposed by Wen and Yu [xx] can be used to obtain reynolds number in minimum

fludization conditions:

$$Re_{p,mf} = (33.7^2 + 0.0494Ar)^{1/2} - 33.7 \tag{2.10}$$

2.3.3 Terminal fluidization velocity

Terminal fluidization velocity can be calculated from the equation given in the dimentionless form (2.11)

$$C_D Re_t^2 = \frac{4}{3}Ar \tag{2.11}$$

where C_D is drag coefficient, which can be obtained experimentally or calculated from one of many empirical relationships, C_D is a function of Reynolds number. One of the correlation that enables to calculate drag coefficient for a wide range of Reynolds numbers ($10^{-1} \div 10^6$) was proposed by Kaskas [xx] (2.12

$$C_D(Re) = \frac{24}{Re} + \frac{4}{\sqrt{Re}} + 0.4 \tag{2.12}$$

Substituting (2.12) to (2.11) we obtain equation (2.13). Solving numerically for Re_t we can obtain terminal velocity for the system.

$$Re^2(\frac{24}{Re} + \frac{4}{\sqrt{Re}} + 0.4) = \frac{4}{3}Ar \tag{2.13}$$

To avoid numerical calculations of equation (2.13) some simplification can be used, depending on the type of low in the reactor. For laminar flow we obtain the only analytical solution to the equation (2.13)
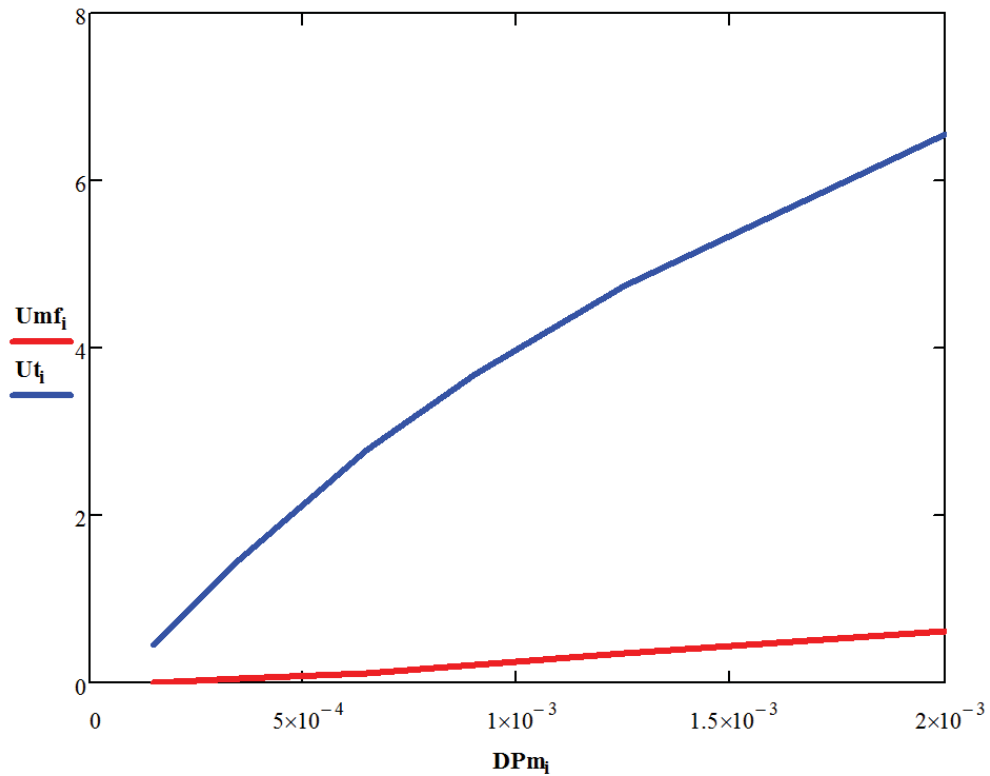
$$C_D = \frac{24}{Re} \text{ for } Re < 0.4 \tag{2.14}$$

For larger Reynolds numbers we can use one of the following approximations:

$$Cd = \frac{10}{\sqrt{Re}} \text{ for } 0.4 < Re < 500 \tag{2.15}$$

$$Cd = 0.43 \text{ for } 500 < Re < 2*10^5 \tag{2.16}$$

An example of minimum fluidization velocity and terminal velocity as a function of particle diameter is presented in Fig. 2.2

FIGURE 2.2: Minimum (red) and terminal (blue) velocity as a function of particle diameter.

2.4 Gas distributor design

The design of fluid bed gas distributors may have a marked influence on the performance of a fluid bed reactor. The primary physical reason for this influence is that the distributor design influences the hydrodynamics and thus the gas/solid contacting pattern in the fluidized bed. Particle and gas properties play a key role in successful design together with the critical pressure drop ratio, and hole size, geometry and spacing; these strongly influence jet penetration, dead zones, particle sifting, attrition and mixing. [Geldart, 1985; Bauer, 1981].

This section deals with the simple algorithm that enables to design a perforated plate distributor using just an orifice theory.

1. Calculate pressure drop across the distributor (**??**):

$$\Delta p_d = (0.2 \div 0.4)\Delta p_b \tag{2.17}$$

where Δp_b can be calculated form (2.5) or (2.8).

2. Calculate the vessel Reynolds number($Re_t = \frac{d_t u_0 \rho_g}{\mu}$, where d_t is tube(reactor) diameter) and select the corresponding drag coefficient from the table below

Re_t	100	300	500	1000	2000	> 3000
$C_{D,or}$	0.68	0.70	0.68	0.64	0.61	0.60

3. Calculate gas velocity through the orifice

$$u_{or} = C_{D,or} * (\frac{2\Delta p_d}{\rho_g})^{1/2} \qquad (2.18)$$

Check the ratio $\frac{u_0}{u_{or}}$ which gives the fraction of open area in the distributor and should be less than 10%.

4. Assume orifice diameter (d_{or} and calculate the number of orifices per unit area of distributor using equation (2.19)

$$u_o = \frac{\pi}{4} d_{or}^2 u_{or} N_{or}. \qquad (2.19)$$

2.5 Discussion and problem solving

1. Dimensionless numbers - define Archimedes and Reynolds number.

2. Describe the procedure of calculating minimum and terminal velocity for a poly-dispersed system.

3. Prove, that starting from combined equations (2.5) and (2.8) and using following assumptions one can obtain equation (2.10).

$$\frac{1}{\phi_s \epsilon_{mf}^3} = 14 \qquad \frac{1 - \epsilon_{mf}}{\phi_s^2 \epsilon_{mf}^3} = 11$$

4. Prove that in steady state condition equation

$$U_s \frac{dU_s}{dz} = \frac{3}{4} C_D \frac{\rho_g}{\rho_s d_p} (U_g - U_s)^2 - g \frac{\rho_s - \rho_g}{\rho_s} \leftrightarrow (2.11). \qquad (2.20)$$

5. Calculate mean diameter for the system of particles presented below

(a)

d_i, mm	$0.1 - 0.2$	$0.2 - 0.5$	$0.5 - 0.8$	$0.8 - 1.0$	$1.0 - 1.5$	$1.5 - 2.5$
%	15	20	18	32	7	8

(b)

d_i, mm	$0.2 - 0.4$	$0.4 - 0.6$	$0.6 - 1.0$	$1.0 - 1.5$	$1.5 - 2.0$	$2.0 - 3.0$
%	32	20	18	15	7	8

6. Calculate minimum fluidization velocity for presented system. Perform the calculation on mean diameter. Check if applying calculated velocity wile cause any fraction to be carried over?

7. Design gas distributor for the given system.

8. Describe Geldart's powder classification.

Chapter 3

Bubbling fluidized bed

3.1 Bubbles in fluidized bed

Knowledge of the general behavior of a fluidized bed is insufficient for some purposes, for example reaction kinetics and heat transfer depend on details of the gas-solids interaction in the bed. Hence, a satisfactory treatment of these phenomena requires a reasonable model representing the gas flow through the bed and its interaction with bed material. As a consequence, the bubble size, rise velocity, shape, distribution, frequency and flow patterns are of key interest. As it was presented in chapter one, increasing the velocity of gas flowing through a bed o solids causes changes fluidization mode (see Fig. 1.2) At relatively low gas velocities we can observe a so called dense bubbling fluidized bed, which is characterized by the presence of regions with low solid concentration which are called bubbles. The dense phase, with higher solid concentration is called emulsion.

3.1.1 Bubble formation

The following calculations are presented in CGS unit system!
Initial diameter of a bubble formed directly above the gas distributor can be calculated form equation (3.1). Note that this equation is true for a gas flowing with higher velocities, causing the bubbles to overlap when formed ($d_{b0} < l_{or}$).

$$d_{b0} = \frac{2.78}{g}(U_0 - U_{mf})^2 \tag{3.1}$$

Bubbles moving upward change their size (grow with height over the distributor). To describe the size of bubbles on the given height of bed we can use to different correlations proposed by Mori and Wen (3.3) or Werther (3.4). Using Mori-Wen model also requires

calculating of the bubble's maximum diameter (3.2) which occurs at the end of dense part of fluid bed.
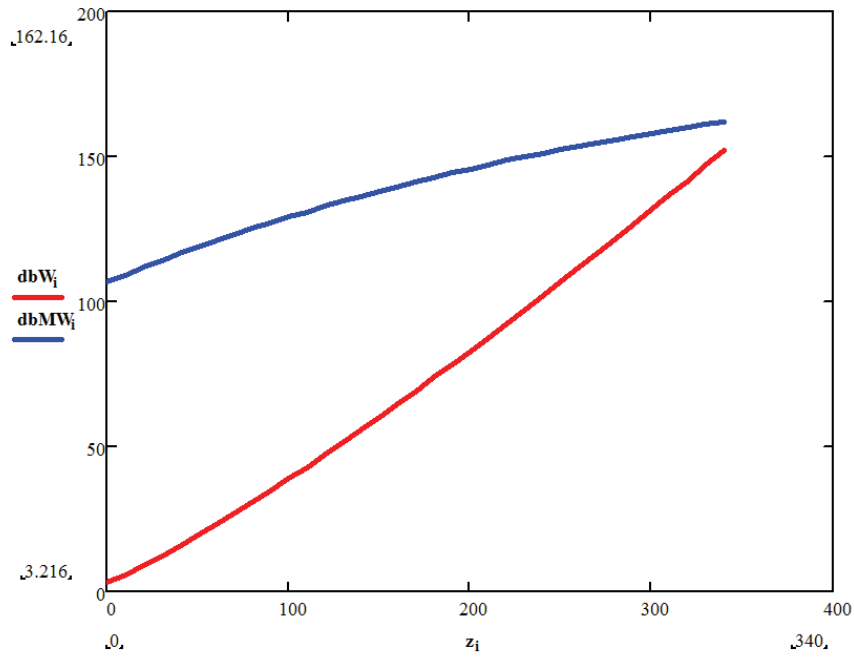
Mori-Wen model:

$$d_{bmax} = 0.65[\frac{\pi}{4}D_t^2(U_0 - U_{mf})]^{0.4} \tag{3.2}$$

$$d_b(h) = d_{bmax} - (d_{bmax} - d_{b0})exp(-0.3\frac{h}{D_t}) \tag{3.3}$$

Werther model

$$d_b(h) = 0.853[1 + 0.272(U_0 - U_{mf})]^{0.333}(1 + 0.0684h)^{1.21} \tag{3.4}$$

FIGURE 3.1: Changes of bubble's diameter[cm] with height of bed [cm] according to Mori-Wen (blue) and Werther (red)

Finally we can calculate the velocity of a single bubble flowing upward:

$$U_{br}(h) = 0.711[g * d_b(h)]^{0.5} \tag{3.5}$$

where $d_b(h)$ is bubble velocity calculated according to Werther.

3.2 Bubbling fluidization

As it was previously mentioned bubbling bed must be treated as a two phase system, with solids in dense phase and gas bubbles in lean phase. From previous paragraph we already know how to asses change of bubbles size in bed and the following part deals with the problem of two phase approach to a bubbling fluid bed. One should remember that bubbles contain very small amounts of solids and are not necessarily spherical. The schematic figure showing elements of such system can be seen in Fig. 3.2.

FIGURE 3.2: Schematic bubble in bubbling bed
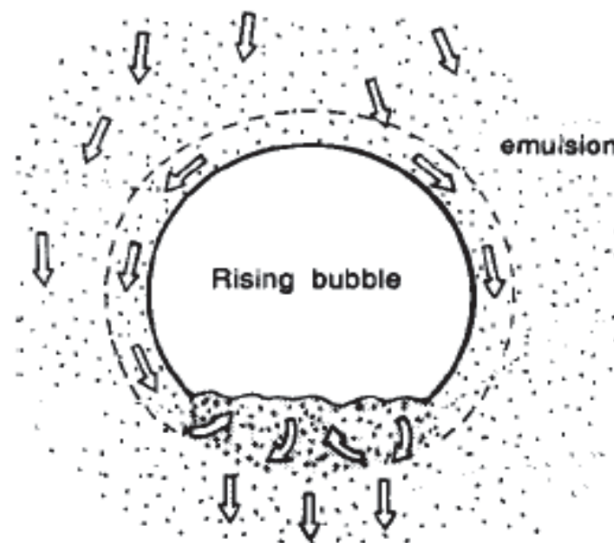
As can be seen the bubbles are approximately hemispherical, with pushed-in bottom. The part directly under the bubble is called a wake, containing significant amount of solids. Moreover every bubble is surrounded by cloud - a part of the emulsion that was penetrated by gas from a rising bubble. Concentration of solid in the cloud is higher than that inside the bubble, but lower than the one in emulsion.

3.2.1 Kuni-Levenspiel model

Kuni-Levenspiel model (later simply called K-L) is based on following assumptions: [http://www.umich.edu/ elements/12chap/html/FluidizedBed.pdf, page 9]

1. All bubbles are of the same size.

2. The solids forming emulsion phase flow downward.

3. Emulsion phase exists at minimum fludizing velocity. The gas occupies the same void fraction in this phase as it had in the entire bed at the minimum fluidization

point. Minimum fluidizing velocity refers to the gas velocity relative to moving solids.

4. In the wake, concentration of solid is said to be the same as in the emulsion phase. However, the wake is turbulent and the average velocities of solids and gas are equal to the upward velocity of a rising bubble.

Fig. 3.3 shows the KL model with its assumptions.

FIGURE 3.3: K-L bed model
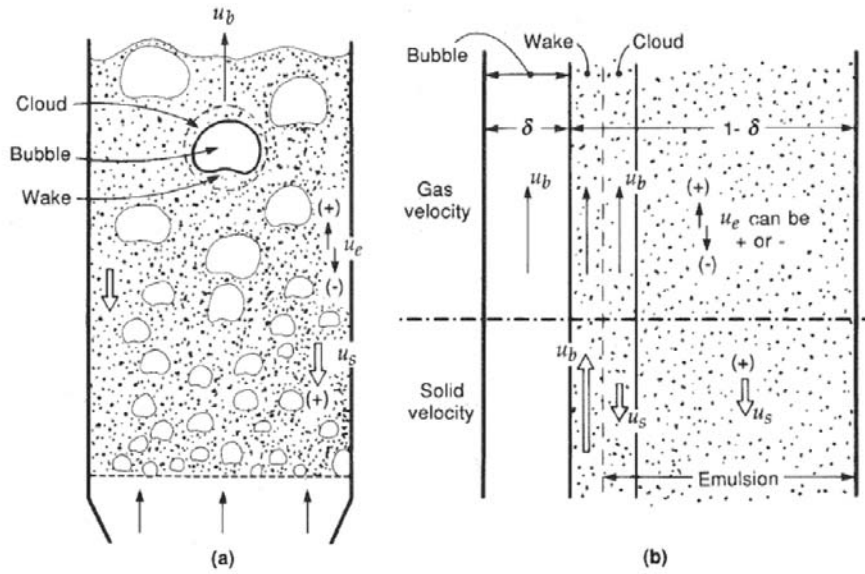
Following algorithm of calculation **K-L model** will use Werther model to obtain size of of bubbles.

1. Calculate bubbles velocity based on single bubble velocity (3.5:

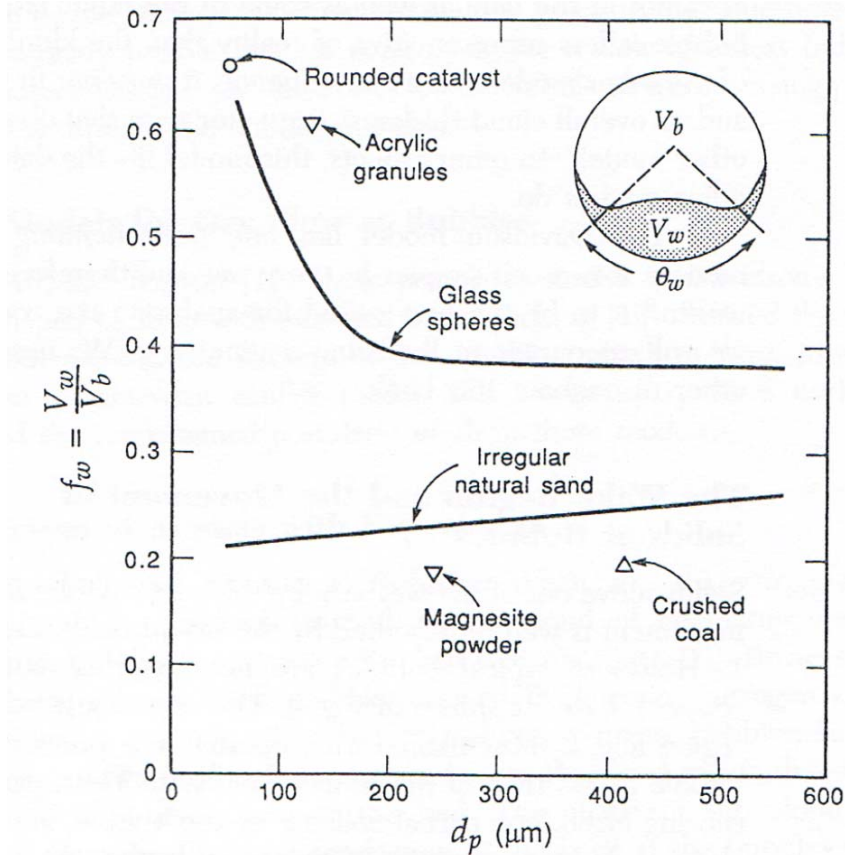$$U_b(h) = U_0 - U_{mf} + U_{br}(h) \tag{3.6}$$

2. Calculate average diameter of bubbles (3.7), using mean value theorem for integration on function $d_b(h)$ (3.4) and average velocity of bubbles (3.8). In this point we have to assume some value of L_f (height of bed).

$$d_{bs}(h) = \frac{1}{L_f} \int_0^{L_f} d_b(h) dh \tag{3.7}$$

$$U_{bs}(h) = U_0 - U_{mf} + 0.711[g * d_{bs}(h)]^{0.5} \tag{3.8}$$

FIGURE 3.4: Wake volume to bubble volume (Kuni, Levenspiel; 1991

3. The downflow velocity of solids, can be calculated based on material balance of solid particles present in the system.

   Total solids = Solids flowing downward in emulsion + solids flowing upward in wakes

$$u_s == \frac{f_w \delta U_b}{1 - \delta - f_w \delta} \tag{3.9}$$

   where f_w is the ratio of wake volume to bubble volume and can be found from the Fig. 3.4

4. Velocity of gas in the emulsion phase comes from the material balance of gas:

   Total gas = Gas in bubbles + gas in wakes + gas in emulsion

$$U_e = \frac{U_{mf}}{\varepsilon_{mf}} - U_s \tag{3.10}$$

5. Volume fraction of bubbles in bed

$$\delta = \frac{U_0 - U_{mf}}{U_{bs} - Umf} \tag{3.11}$$

6. Calculate porosities:

(a) in emulsion phase is assumed to be constant $\varepsilon_e = \varepsilon_{mf}$

(b) average bed porosity:

$$\varepsilon_f = \delta + (1 - \delta)\varepsilon_e \tag{3.12}$$

7. Calculate height of bed (checkpoint if the assumption in (3.7)) was correct.

$$L_f = L_{mf}\frac{1 - \varepsilon_{mf}}{1 - \varepsilon_f} \tag{3.13}$$

3.2.2 Extended K-L model

1. Volume fraction of clouds in bed

$$f_c = \frac{3}{U_{brs}\frac{\varepsilon_{mf}}{U_{mf}} - 1} \tag{3.14}$$

where U_{brs} is a velocity of single bubble (3.5) calculated for average bubble diameter (3.7)

2. Volume fraction of wake is assumed to be constant $f_w = 0.33$.

3. Volume fraction of emulsion

$$f_e = 1 - \delta - f_w\delta - f_c \tag{3.15}$$

4. Fraction of solids in bubbles was specified experimentally $\gamma_b = 0.005$

5. Fraction of solids in clouds and wakes

$$\gamma_c = (1 - \varepsilon_{mf})(f_c + f_w) \tag{3.16}$$

6. Fraction of solids in emulsion

$$\gamma_e = \frac{1 - \varepsilon_{mf})(1 - \delta)}{\delta} - \gamma_b - \gamma_c \tag{3.17}$$

7. Wake velocity is constatnt and equal to the velocity of bubbles (3.8 $U_w = U_{bs}$.

8. Emulsion downflow velocity

$$U_e = \frac{f_w\delta U_{bs}}{1 - \delta - f_w\delta} \tag{3.18}$$

9. Relative gas velocity in emulsion

$$U_{ge} = \frac{U_{mf}}{\varepsilon_{mf}} - U_e \tag{3.19}$$

3.3   Entrainment and elutriation

Fluidized reactor can be divided into two parts, the bottom one called the dense phase which was described in previous sections and dispersed phase, where the concentration of solid decreases. We showed that by using equation (3.13) we can find the height of fluidized bed or to be more specific its dense part. That's were more or less distinct border between the two phases occurs and the bubbles present in the dense phase disappear. The "disappearance" is a reason for the presence of the lean phase in the reactor. This is shown in Fig. 3.5. Spraying of solids into lean phase can have threee different mechanisms (Kuni, Levenspiel):

- bubbles have higher pressure than the surface of bed, so by reaching the top of dense phase they spray solids form its roof into lean phase;

- reaching the surface, bubbles can explode, and then the arising forces cause the solids present in the wake to be sprayed to lean phase;

- two bubbles can coalesce at the surface and create energetic ejection of solids from under the bottom bubble.

The aim of this section is to provide some insight to what happens over the dense part of the bed. Let us first define number of terms necessary to understand the problem. The flux of solids suspended in gas over the dense phase is called an entrainment (G_s). The zone of fluidization vessel above the border between the previously mentioned phases is called a freeboard. The region close to the border between the phases is called the splash zone and that is where the spraying of solids occurs. The entrainment of solids decreases with the increasing height of the freeboard until it reaches some constant level. The height at which it happens is called **TDH** - transport disengaging height. By saturation carrying capacity we understand the largest flux of solids that can entrained by gas above the TDH. Finally elutriation which refers to removal of fine particles from a mixture of solids with different sizes. Larger particles fall back to bed, because they are to heavy to be carried up, but smaller ones are flowing upward with the gas.

Below we present the algorithm that enables to describe the amounts of material in different zones of fluidization vessel.

1. We start with the assumption that the initial velocity of solids U_{bf} sprayed out of the dense phase of the bed is equal to the velocity of bubbles at this height. We use equation (3.6) with the previously calculated height L_f. Here one has to remember that all the velocities were calculated in **CGS unit system** and from now on we have to go back to the **SI units!**

FIGURE 3.5: Mechanism of ejection of solids from dense bed
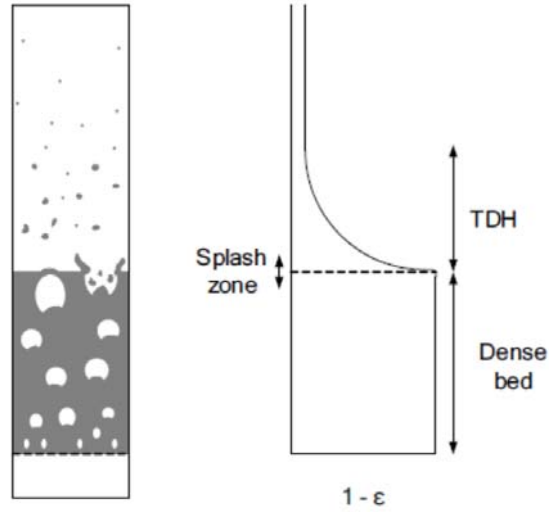
2. The flux of entrained solids $\frac{kg}{m^2 s}$ is calculated by equation:

$$G_s = 0.1\rho_s(1 - \varepsilon_{mf})U_{bf} - U_{mf} \tag{3.20}$$

3. Now we calculate saturation carrying capacity for gas present in the system.

$$E_{sat} = 0.096 U_0 \rho_g Frt(U_t)^{0.633} Ar^{0.121} (\frac{\rho_s}{\rho_g})^{0.013} (\frac{D_t}{D_0})^{-0.05} \tag{3.21}$$

where $Fr_t(U_t)$ is given by (3.22) (Froude number), D_t is reactor diameter and $D_0 = 5.9cm$ and it is reference diameter of experimental fludization vessel

$$Fr_t(U_t) = \frac{U_t^2}{g * d_p} \tag{3.22}$$

4. The distribution of solid flux is given by exponential function of height (3.23) and is presented in Fig. 3.6.

$$E(h) = E_{sat} + (G_s - E_{sat})exp(-ah) \tag{3.23}$$

where $a = 4$ is an experimentally obtained coefficient. As it can be observed in Fig. 3.6 freeboard zone is about 1m high, because that is where we start to observe constant flux of solids.

5. Porosity in lean phase.
We start from calculating the porosity at the height where the freeboard zone ends (3.24) and then we calculate the distribution of porosity with height, assuming that it is related to the flux of solids (3.25). Example of changes in porosity and solid

FIGURE 3.6: Change of solid flux in freeboard zone
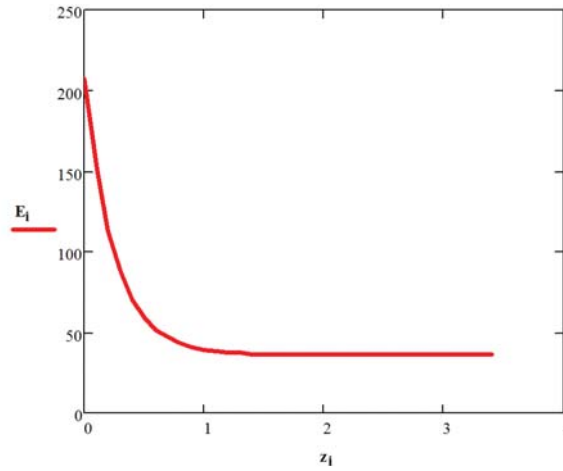
concntration is presented in Fig. 3.7

$$\varepsilon_{sat} = 1 - \frac{E_{sat}}{(U_0 - U_t)\rho_s} \tag{3.24}$$

$$\varepsilon(h) = \varepsilon_{sat} + (\varepsilon_f - \varepsilon_{sat})exp(-ah) \tag{3.25}$$

FIGURE 3.7: Porosity(red) and solid concentration (blue) in freeboard zone
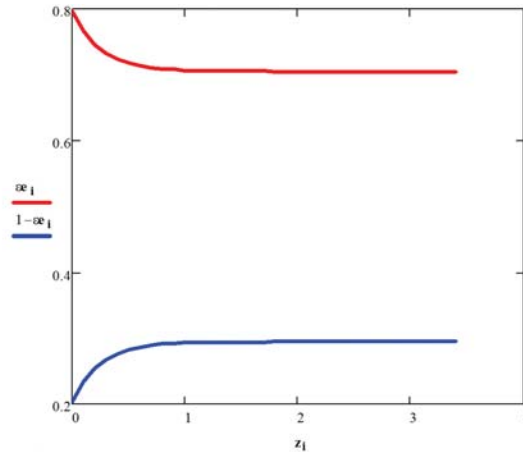
6. Average concentration above the dense phase is calculated with mean value theorem for integrals according to equation (3.26)

$$\varepsilon_{es} = 1 - \frac{1}{L} \int_0^L \varepsilon_{sat} + (\varepsilon_f - \varepsilon_{sat})exp(-ah)dh \tag{3.26}$$

7. Finally we find mass of solids in dense phase (3.27) and mass of solid above the
   dense phase (3.28)

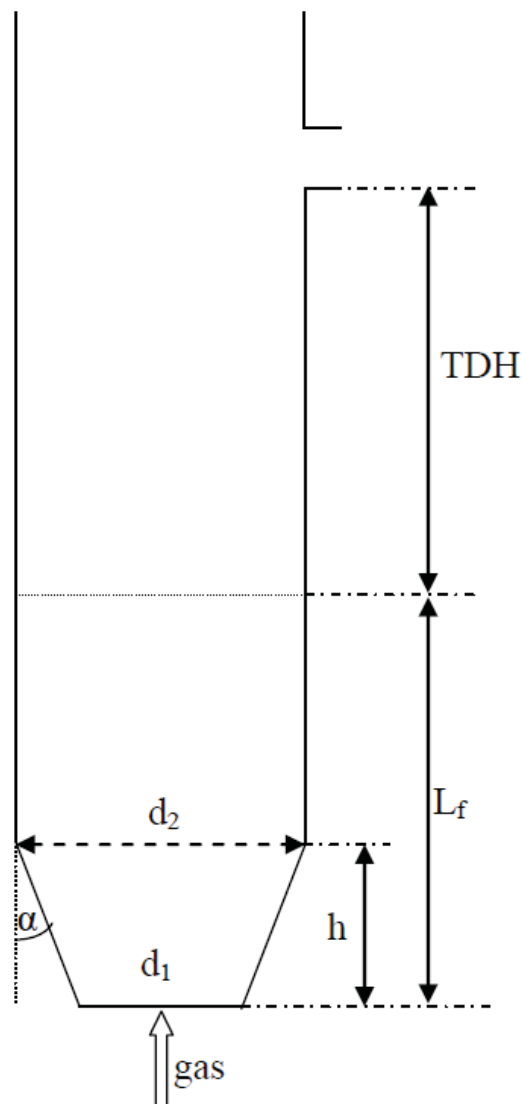$$m_d = L_{mf}(1 - \varepsilon_{mf})\rho_s \frac{\pi D_t^2}{4} \tag{3.27}$$

$$m_d = L_{mf}\varepsilon_{es}\rho_s \frac{\pi D_t^2}{4} \tag{3.28}$$

3.4   Fluid bed dimensions

To complete the description of bubbling fluidized bed one needs to be able to calculate
its dimensions: height and diameter (Fig. 3.8).

FIGURE 3.8: Dimensions ob fluidized bed

Heights of the two zones, dense and lean, featured in figure 3.8 are calculated from Kuni-Levenspiel model (L_f)and entrainment model (TDH) presented in previous paragraph. TDH can be connected with the height at which the outlet to cyclone is mounted. That leaves only diameters of the reactor to be calculated according to the following procedure. To complete this calculation the flow of gas (V_{gas}) MUST be known!

1. Determine the maximum amount of fines that can be carried over from the reactor: p %. Knowing size distribution of the particles in the system, determine the maximum diameter of particles that can be carried over and calculate minimum(u_{mfp}) and terminal (u_{tp})fluidization velocities for this diameter. Choose operation velocity (u_{op} for the bed such that: $u_{mfp} < u_{op} < u_{utp}$).

2. Find the minimum fluidization velocity (u_{max}) for the biggest particles present in the system.

3. Check if $u_{max} < u_{op}$. If the answer is yes, the reactor can have a shape of a simple cylinder and one can calculate tube dimension from eq. (3.29)

$$\frac{V_{gas}}{u_{op}} = \frac{\Pi d_t^2}{4} \qquad (3.29)$$

If the answer is no one need to narrow the bottom part of the reactor in order to increase the initial velocity of gas flowing through reactor. In such case the shape of the reactor will be like the one presented in fig. 3.8. In that case one needs to calculate two different diameters d_1 and d_2.
d_2 is equal to d_t calculated from eq. (3.29) and d_1 comes from the eq. (3.30).

$$\frac{V_{gas}}{u_{max}} = \frac{\Pi d_1^2}{4} \qquad (3.30)$$

4. The height of the narrowing is determined based on the difference $d_2 - d_1$ and the assumptions that the slope of the walls of the reactor ($\alpha < 15\,\text{deg}$). Than the height h is calculated from the eq. 3.31

$$\frac{(d_2 - d_1)/2}{h} = \tan \alpha \qquad (3.31)$$

3.5 Problems and discussions

1. Using extended K-L model describe the bed of solids with a wide size distribution. The conditions of the bed are presented below.

d_i, mm	$0.2 - 0.4$	$0.4 - 0.6$	$0.6 - 1.0$	$1.0 - 1.5$	$1.5 - 2.0$	$2.0 - 3.0$
%	32	20	18	15	7	8

   $\rho_s = 1350 kg/m^3$; $\rho_g = 1.5 kg/m^3$; $U_0 = 50 cm/s$; $\nu = 30 * 10^{-6} Pa * s$; $\varepsilon_{mf} = 0.45$ Estimated height of bed $h = 1.75m$

2. Using extended K-L model describe the bed of solids with a wide size distribution. The conditions of the bed are presented below.

d_i, mm	$0.1 - 0.2$	$0.2 - 0.5$	$0.5 - 0.8$	$0.8 - 1.0$	$1.0 - 1.5$	$1.5 - 2.5$
%	15	20	18	32	7	8

   $\rho_s = 1050 kg/m^3$; $\rho_g = 1.1 kg/m^3$; $U_0 = 200 cm/s$; $\nu = 20 * 10^{-6} Pa * s$; $\varepsilon_{mf} = 0.5$; $\varepsilon_f = 0.796$ Estimated height of bed $h = 1.95m$ Drag coefficient for average diameter of particles: $C_d = 1.53$.

3. Knowing that to obtain the best conversion rate the ration of gas to solid is equal $1.23 m^3/kg$ and the flow of solid material is $m_s = 1200 kg/h$ find the dimensions of the reactor for this process:

   (a) assuming solid distribution from ex. 2 adn maximum of 15% carryover from dense zone.

   (b) assuming that the particle size fits in a range between 0.1mm - 5mm and only particles smaller than 0.25mm can be carried over from the bubbling zone.

Gasification, Producer Gas and Syngas

Samy Sadaka
Assistant Professor -
Extension Engineer

What Is Gasification?

Gasification involves turning organic fuels (such as biomass resources) into gaseous compounds (producer gas or syngas) by supplying less oxygen than is needed for complete combustion of the fuel. Gasification occurs at temperatures between 1112º and 2732º F and produces a low- to medium-energy gas depending upon the process type and operating conditions. Gasification of biomass resources is already being used to produce bioenergy and bioproducts for use in dual-mode engines to produce power (e.g., for irrigation) and to produce heat, steam and electricity. Studies are underway to develop biomass gasification technologies to economically produce hydrogen, organic chemicals and ethanol for use as transportation fuel in cars and trucks and to extend its use as a source of electricity.

What Is the Gasification Mechanism?

During gasification, the fuel (e.g., biomass resources) is heated to a high temperature, which results in the production of volatile compounds (gases) and solid residues (char). The quantity and composition of the volatile compounds depend on the reactor temperature and type, the characteristics of the fuel and the degree to which various chemical reactions occur within the process. The primary reactions that occur in the presence of oxygen result in the conversion of the fuel to carbon monoxide and carbon dioxide. These reactions are very fast and release heat, which provides the energy needed to sustain other gasification reactions. Gasification of solid materials (char) occurs at high temperatures (> 1112º F) and produces gases, tars and ash. Generally, these reactions are carried out in the presence of reactive agents such as oxygen, steam and hydrogen added to the reactor to aid in the chemical conversion of char to volatile compounds. These reactions dominate the gasification process and dictate the final composition of the producer gas or syngas. Their occurrence and extent depend on the operating conditions of the gasifier. Secondary reactions, which occur at temperatures greater than 1112º F and under appropriate pressure conditions, involve the decomposition of the tars to produce carbon and gases.

Gasification, which is incomplete combustion of carbonaceous fuels, can be represented with the following sub-stoichiometric equation:

$$\text{Biomass} + \text{Limited Air} \rightarrow \text{Carbon Monoxide} + \text{Hydrogen} + \text{Methane} + \text{Carbon Dioxide} + \text{Water Vapor} + \text{Nitrogen}$$

Arkansas Is Our Campus

What Are the Differences Between Producer Gas and Syngas?

Producer gas is the mixture of gases produced by the gasification of organic material such as biomass at relatively low temperatures (1292º to 1832º F). Producer gas is composed of carbon monoxide (CO), hydrogen (H_2), carbon dioxide (CO_2) and typically a range of hydrocarbons such as methane (CH_4) with nitrogen from the air. Producer gas can be burned as a fuel gas such as in a boiler for heat or in an internal combustion gas engine for electricity generation or combined heat and power (CHP). The composition of the gas can be modified by manipulation of gasification parameters.

Syngas (synthesis gas) is a mixture of carbon monoxide (CO) and hydrogen (H_2), which is the product of high temperature steam or oxygen gasification of organic material such as biomass. Following clean-up to remove any impurities such as tars, syngas can be used to produce organic molecules such as synthetic natural gas (SNG-methane (CH_4)) or liquid biofuels such as synthetic diesel (via Fischer-Tropsch synthesis).

How Much Air Is Required for the Gasification Process?

For complete combustion, 1.0 pound of bone-dry (0 percent moisture content) biomass needs about 4.58 pounds of air. This is referred to as the stoichiometric air. For gasification reactions, the usual practice is to provide a fraction of the stoichiometric air, which is referred to as an equivalence ratio (ER). With dry biomass, best results are normally achieved at ERs of about 0.25, with a "typical" range of perhaps 0.20 to 0.33. Therefore, for normal gasification, 1.0 pound of biomass needs about 1.15 pounds of air.

What Are the Gasification Reactors?

Several biomass gasification reactor designs have been developed and evaluated and can be generally classified into two broad categories; namely, fixed bed and fluidized bed. Fixed bed reactors are those in which the fuels move either countercurrent or concurrent to the flow of gasification medium (steam, air or oxygen) as the fuel is converted to fuel gas. They are relatively simple to operate and generally experience minimum erosion of the reactor body. There are three basic fixed bed designs – updraft, downdraft and cross-draft gasifiers.

In an updraft fixed bed gasifier (Figure 1), the flows of the fuel and gases are countercurrent to each other. The reactive agent is injected at the bottom of the reactor and ascends to the top while the fuel is introduced at the top and descends to the bottom through zones of progressively increasing temperatures (drying, pyrolysis, gasification and oxidation). Heat from the gasification and oxidation zones rises upward to provide energy for the pyrolysis and drying zones. Gases, tar and other volatile compounds are dispersed at the top of the reactor while ash is removed at the bottom. The syngas typically contains high levels of tar, which must be removed or further converted to syngas for use in applications other than direct heating. Updraft gasifiers are widely used to gasify biomass resources and generally use steam as the reactive agent, but slagging can be severe if high ash fuels are used. They are unsuitable for use with fluffy, low-density fuels.

Downdraft fixed bed gasifiers (Figure 2) are similar to updraft gasifiers, except that the locations of the zones are reversed and, as such, the pyrolysis products are allowed to pass through the high temperature oxidation zone where they undergo further decomposition. The fuel is introduced at the top, and the reactive agent is introduced through a set of nozzles on the side of the reactor. Moisture evaporated from the biomass fuel serves as a reactive agent. The syngas leaves the gasifier from the bottom and contains substantially less tar than from updraft gasifiers, which reduces the need for cleaning and is, therefore, more suitable for a wider variety of applications.

Cross-draft fixed bed gasifiers exhibit many of the operating characteristics of downdraft gasifiers. Air or air/steam mixtures are introduced into the side of the gasifier near the bottom, while the syngas is drawn off on the opposite side. The oxidation and drying zones are concentrated around the sides of the unit. Cross-draft gasifiers respond rapidly to load changes, are relatively simple to construct and produce syngas suitable for a number of applications. However, they are sensitive to changes in the fuel composition and moisture content.
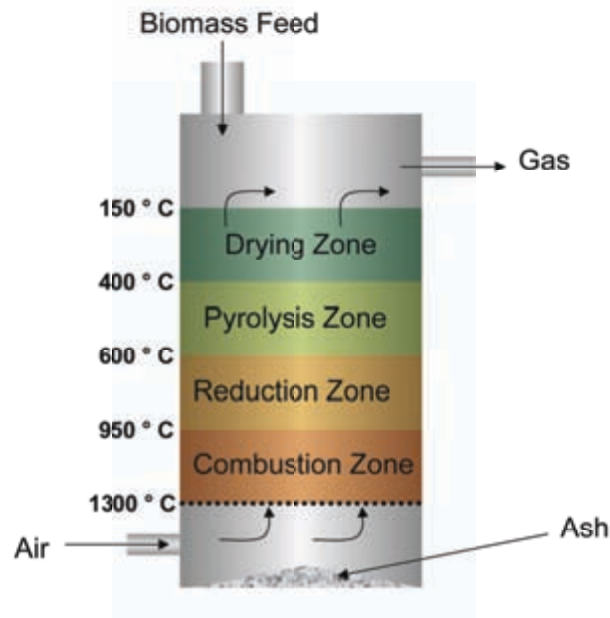
Figure 1. Updraft fixed bed gasifier (Source: G. Foley and G. Barnard. 1985. Biomass Gasification in Developing Countries. Earthscan, London, UK)
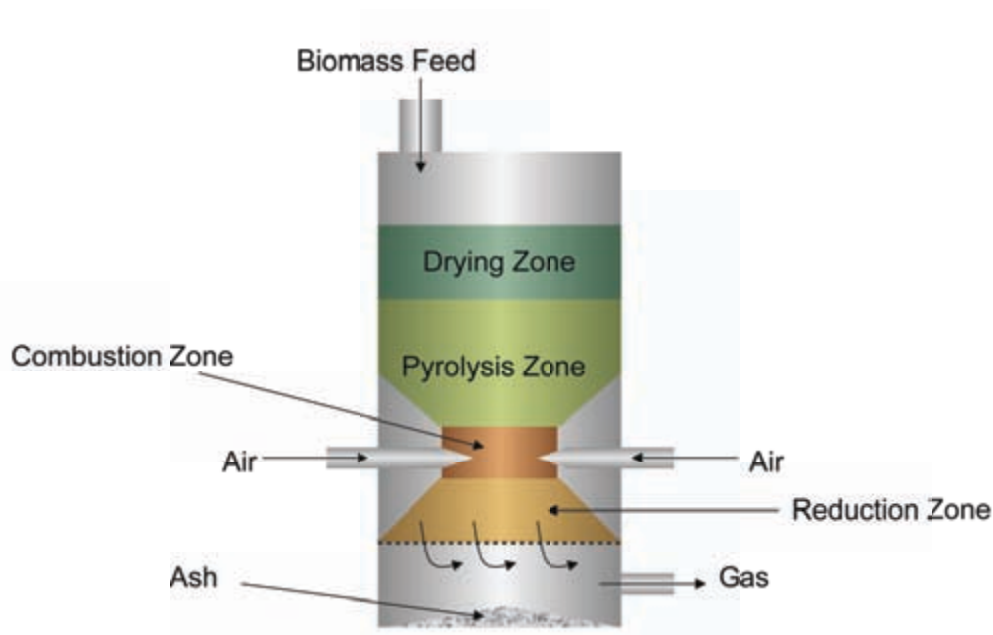

Figure 2. Downdraft fixed bed gasifier (Source: G. Foley and G. Barnard. 1985. Biomass Gasification in Developing Countries. Earthscan, London, UK)

A fluidized bed gasifier has a bed made of an inert material (such as sand, ash or char) that acts as a heat transfer medium. In this design, the bed is initially heated and the fuel introduced when the temperature has reached the appropriate level. The bed material transfers heat to the fuel and blows the reactive agent through a distributor plate at a controlled rate. Unlike fixed bed reactors, fluidized bed gasifiers have no distinct reaction zones and drying, pyrolysis and gasification occur simultaneously during mixing. Compared to other gasifiers, fluidized bed gasifiers have strong gas-to-solids contact, excellent heat transfer characteristics, better temperature control, large heat storage capacity, a good degree of turbulence and high volumetric capacity. But they operate at pressures slightly above atmospheric levels (which requires that leaks be prevented), and they respond slowly to load changes. Due to their complicated and expensive control systems, fluidized bed gasifiers appear to be commercially viable at larger
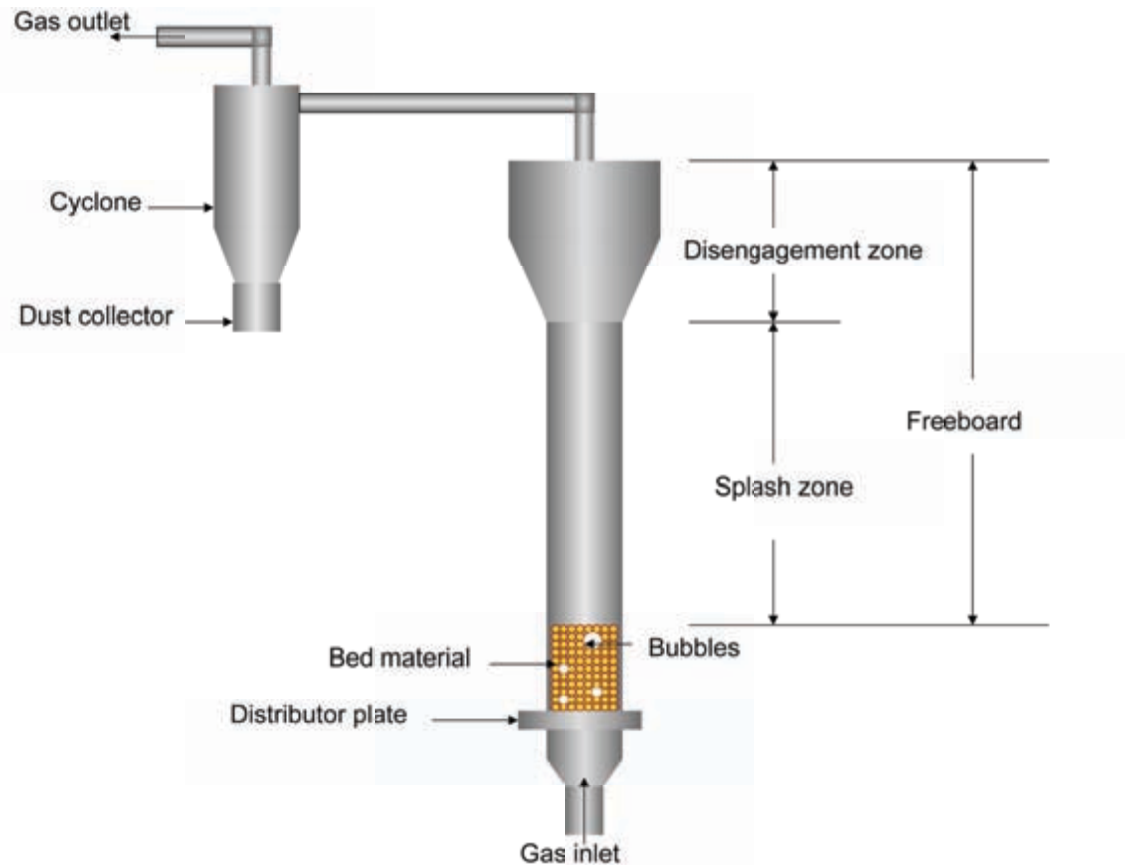
Figure 3. Bubbling fluidized bed gasifier (Source: D. Gelbart. 1986. Gas Fluidization Technology, John Wiley and Sons, New York)

sizes (> 30 MW thermal output). Fluidized bed reactors are classified by their configuration and the velocity of the reactive agent and consist of bubbling, circulating and spouted fluidized beds.

In bubbling fluidized bed gasifiers (Figure 3), fuel is fed into the reactor and gases are introduced at a flow rate that maintains pressure at a level sufficient to keep the fuel particles in suspension. The introduced gases pass through the reactor bed in the form of bubbles that rise and grow in size until they reach the surface of the bed, where they burst. The pressure must be maintained across the bed. Bubbling fluidized bed reactors are categorized as either single or dual fluidized beds. Single fluidized bubbling bed gasifiers have only one bed where the fuel and the reactive agent enter and from which the syngas and char exit. This design results in lower cost and less maintenance relative to multi-bed designs, and the syngas is ready for utilization. However, the energy content of the syngas is lower than achieved in dual-bed designs, inorganic materials in the fuel cannot be separated and pyrolysis occurs at the bottom of the

gasifier leading to nonuniform temperature distribution. Dual- or multi-bed bubbling gasifiers have more than one bed. The first bed is usually used to burn some of the char to produce the energy for the second bed, where pyrolysis occurs. Dual-bed systems produce syngas with higher energy content due to the combustion of the char in a separate chamber, which prevents the combustion gas from diluting the pyrolysis gas. Additionally, inorganic materials in the fuel can be separated and the heat of pyrolysis reactions is evenly distributed, allowing pyrolysis to occur at a relatively uniform temperature. Higher construction costs and greater maintenance are the disadvantages of a dual system.

A circulating fluidized bed gasifier (also called a fast fluidized bed gasifier) is a modified bubbling bed gasifier in which the solids leaving the reactor vessel are returned through an external collection system. Compared to other gasifiers, circulating fluidized bed gasifiers have a higher processing capacity, better gas-solid contact and the ability to handle cohesive solids that might otherwise be difficult to fluidize in

bubbling fluidized beds. Despite these advantages, circulating fluidized beds are still less commonly used because their height significantly increases their cost. A spouted fluidized bed gasifier has a bed of coarse particles partly filling the vessel and a relatively large control opening at the base where gas is injected. With a sufficient flow of gas, particles in the gas can be made to rise as a fountain in the center of the bed and to develop a circling motion on the bed. Additional air added to the base can produce a spouted bed. This type of gasifier has often been used to gasify coal.

What Is the Gasification Medium?

The simplest gasification process uses air as the reactive agent, which converts the excess char into a low energy syngas (142-209 Btu/ft^3) consisting mainly of hydrogen and carbon monoxide diluted with nitrogen from the air. The producer gas is suitable for boiler and engine applications but cannot be transported through pipelines due to its low Btu content. Gasification of char in the presence of steam produces a gas consisting mainly of carbon monoxide, carbon dioxide, hydrogen and methane. Steam can be added from an external source, or it can be obtained from the evaporation of the water in the fuel. Under conditions of low temperatures, low heat rates and high pressure, secondary reactions involving tars occur, but these reactions are not as prevalent under conditions of low pressure, high temperature and high heat rates. Gasification in the presence of steam produces a higher energy syngas relative to using air as the reactive agent.

The use of oxygen rather than air as the reactive agent reduces the amount of nitrogen supplied to the gasification reactions, which creates a medium energy syngas (approximately 321-563 Btu/ft^3) that is much lower in nitrogen and higher in methane, hydrogen and carbon monoxide relative to systems using air. Medium energy syngas can be used for a wide variety of applications and can be transported through a pipeline (due to its relatively low tar content). A drawback to the use of oxygen as a reactive agent is the need for a nearby source of oxygen, which may increase capital and operating costs.

Hydrogen can be used as a reactive agent in gasification, but its use requires high pressure and stringent operating conditions, as well as an external source of hydrogen. Air, steam, oxygen and hydrogen can be used as gasifying agents as shown in Figure 4.

What Are the Factors Affecting Gasification?

A number of factors affect gasification reactions including the temperature, pressure and height of the reactor bed; the fluidization velocity; the equivalence ratio; the air-to-steam ratio; and the characteristics of the fuel.

Increasing the temperature increases the formation of combustible gases, decreases the yield of char and liquids and leads to more complete conversion of the fuel. Hydrocarbon gases (especially methane and ethylene) increase with temperature while the yields of higher hydrocarbons (C_3-C_8: organic chemicals having 3 to 8 carbons) decrease at temperatures above 1202º F. The energy content of the syngas increases steadily up to 1292º F then decreases at higher temperatures.

The rate of char gasification and yields of methane increase with increasing pressure, and the impacts are most significant at high temperatures (1652º-1742º F).

For a given reactor temperature, higher fuel bed heights increase the time fuels are available for reactions to occur (residence time), which increases total syngas yields and increases the concentrations of hydrogen, carbon monoxide, carbon dioxide, methane and ethylene in the syngas.

Fluidization velocity (fluidization is the processing technique employing a suspension of a small solid particle in a vertically rising stream of fluid – usually gas – so that fluid and solid come into intimate contact) affects the mixing of particles within the reactor. Higher velocities increase the temperature of the fuel bed and lead to the production of lower energy syngas.

The equivalence ratio (actual fuel-to-air ratio divided by the stoichiometric fuel-to-air ratio) affects the temperature of the fuel bed. High ratios increase the rate of syngas production, and low ratios result in the production of lower syngas yields and energy
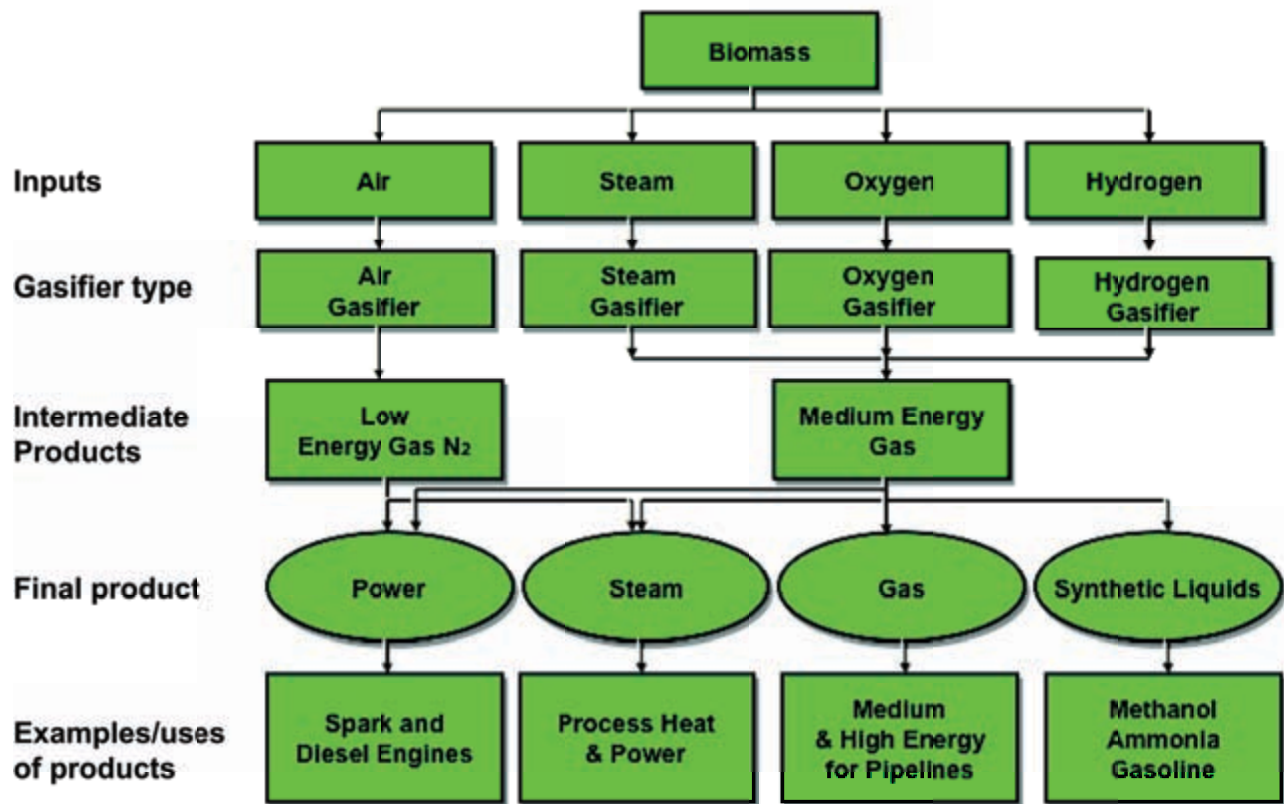
Figure 4. Gasification processes and their products.

content and more tar. Increases in the steam-to-air ratio increases the energy content of the syngas.

What Are the Limitations of the Gasification Process?

Although gasification processes are highly developed, there are still several limitations, particularly with respect to biomass gasification, including the moisture content and size of the fuel particles, the fuel feeding system, the ash deformation temperature, particle mixing and segregation and entrainment (elutriation).

Fuel moisture content differs by fuel type. Fuels with high moisture content lower the reactor temperatures due to the amount of energy needed to dry the fuel, which results in the production of lower energy syngas and lower yields of syngas. The speed at which fuel particles heat up (i.e., the heat rate) decreases as particle size increases, resulting in the production of more char and less tar.

The type of fuel-feeding mechanism required is determined by the size, shape, density, moisture content and composition of the fuel. Mechanisms developed to accommodate the wide variety of biomass fuels include direct feeding in which the feeding mechanism is isolated from the reactor to prevent the back-flow of tar and combustible gases, and over-the-bed feeders, which are usually less troublesome because there is no direct contact between the hot fuel bed material and the feeder. However, the use of over-the-bed feeders is restricted to fuels of higher density and/or larger sized particles and, because of particle emissions, results in the production of a dirty syngas, which must be cleaned before use.

At lower operating temperatures, some minerals in the fuel can cause agglomeration. The temperature at which agglomeration occurs (the ash deformation temperature) depends on the fuel type and its mineral composition. Effective mixing of fuel particles of various sizes is needed to maintain uniform temperature within the reactor.

How Much Energy Can Be Produced by Gasification?

➢ 1 acre of wheat land produces about 3,000 pounds of wheat straw.

➢ 1 pound of wheat straw contains about 7,750 Btu.

➢ 1 pound of straw could produce 23.9 ft^3 of gas with average calorific value of 125 Btu/ft^3.

➢ 1 acre of wheat land could produce 71,700 ft^3 of producer gas.

➢ 1 acre of wheat land could produce 8.9 MMBtu.

➢ 1 acre of wheat straw could replace 410 pounds of propane.

What Types of Biomass Can Be Gasified?

Almost any carbonaceous or biomass fuel can be gasified under experimental or laboratory conditions. However, the real test for a good gasifier is not whether a combustible gas can be generated by burning a biomass fuel with 20 to 40 percent stoichiometric air, but that a reliable gas producer can be made which can also be economically attractive to the customer. Towards this goal the fuel characteristics have to be evaluated and fuel processing done. A gasifier is very fuel specific, and it is tailored around a fuel rather than the other way around.

What Are the Applications of Gasification Technology?

◈ **Production of heat and power**
Power generation can be accomplished via gasification of biomass, followed by a combustion engine, combustion turbine, steam turbine or fuel cell. These systems can produce both heat and power (CHP – Combined Heat and Power) and can achieve system efficiencies in the range of 30 to 40 percent.

◈ **Production of hydrogen**
Hydrogen is currently produced in large quantities via steam reforming of hydrocarbons over a Ni catalyst at 1472º F. This process produces a syngas that must be further processed to produce high-purity hydrogen. The syngas conditioning required for steam reforming is similar to that

required for a biomass gasification-derived syngas; however, tars and particulates are not as much of a concern.

◈ **Production of methanol**
Commercial methanol synthesis involves reacting CO, H$_2$ and steam over a copper-zinc oxide catalyst in the presence of a small amount of CO$_2$ at a temperature of about 500º F and a pressure of about 70 bar (1015 psi). To best use the raw product syngas in methanol synthesis, it is essential to maintain H$_2$/CO of at least 2 and CO$_2$/CO ratio of about 0.6 to prevent catalyst deactivation and to keep the catalyst in an active reduced state.

◈ **Production of gasoline or diesel**
Gasoline and diesel (synthetic fuels) can be produced from syngas via a process named Fischer-Tropsch (FT). The FT synthesis involves the catalytic reaction of H$_2$ and CO to form hydrocarbon chains of various lengths (CH$_4$, C$_2$H$_6$, C$_3$H$_8$, etc.). Gasifier-produced gases with H$_2$/CO ratio around 0.5 to 0.7 are recommended as a feed to the FT process when using iron as a catalyst.

◈ **Production of ethanol**
Anaerobic bacteria are able to grow on syngas components, thus forming acetate and ethanol. The bacterial conversion has the advantages of high selectivity, no thermal equilibrium and fewer problems with catalyst poisoning. The bacterial culture has to be able to convert CO$_2$, CO and H$_2$ into ethanol. The technology has been proven in a pilot plant in Arkansas, where ethanol has been produced from diverse feedstocks for several years. The reaction time from biomass to distilled ethanol has been proven to be short (7-8 minutes) compared to fermentation of sugars, which often lasts one to two days.

References

1. http://bioweb.sungrant.org/At-a-Glance/Biopower/Technologies/Gasification/Default.htm

2. http://bioweb.sungrant.org/General/Biopower/Technologies/Gasification/Default.htm

3. http://bioweb.sungrant.org/Technical/Biopower/Technologies/Gasification/Default.htm

4. http://www.zero.no/transport/bio/gasification

5. Geldart, D. 1986. *Gas Fluidization Technology*, John Wiley and Sons, New York

6. Sadaka, S. S., A. E. Ghaly and M. A. Sabbah. 2002. Two phase biomass air-steam gasification model for fluidized bed reactor: Part I, II, III. *Biomass and Bioenergy* 22: 439-487

• **Professional Reference Shelf (i.e., CD ROM Shelf)**

R12.3   Fluidized-Bed Reactors[1]

*"When a man blames others for his failures, it's a good idea to credit
others with his successes."*

–– Howard W. Newton

The fluidized-bed reactor has the ability to process large volumes of fluid. For the catalytic cracking of petroleum naphthas to form gasoline blends, for example, the virtues of the fluidized-bed reactor drove its competitors from the market.

Fluidization occurs when small solid particles are suspended in an upward-flowing stream of fluid, as shown in Figure R12.3.1.
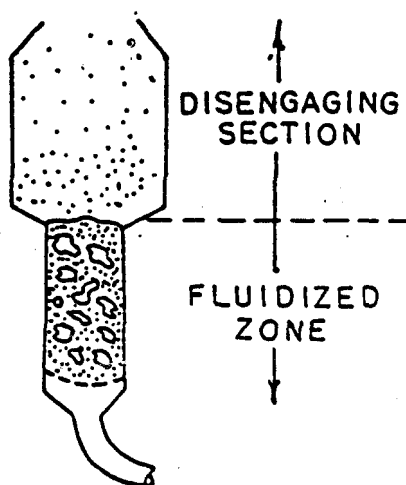
Figure R12.3-1 From Kunii and Levenspiel *Fluidization Engineering*, Melbourne, FL 32901:
Robert E. Krieger Pub. Co. 1969. Reprinted with permission of the publishers

The fluid velocity is sufficient to suspend the particles, but it is not large enough to carry them out of the vessel. The solid particles swirl around the bed rapidly, creating excellent mixing among them. The material "fluidized" is almost always a solid and the "fluidizing medium" is either a liquid or gas. The characteristics and behavior of a fluidized bed are strongly dependent on both the solid and liquid or gas properties. Nearly all the significant commercial applications of fluidized-bed technology concern gas-solid systems, so these will be treated in this section. The material that follows is based upon what is seemingly the best model of the fluidized-bed reactor developed thus far–the bubbling bed model of Kunii and Levenspiel.

---

[1] This material is based on the article by H. S. Fogler and L. F. Brown [*Reactors*, ACS Symposium Series, vol.168, p. 31 1981, H. S. Fogler ed.], which in turn was based on a set of notes by Fogler and Brown.

CD-Ch12FluidizedBed.doc

R12.3.1   An Overview

We are going to use the Kunii-Levenspiel bubbling bed model to describe reactions in fluidized beds. In this model, the reactant gas enters the bottom of the bed and flows up the reactor in the form of bubbles. As the bubbles rise, mass transfer of the reactant gases takes place as they flow (diffuse) in and out of the bubble to contact the solid particles where the reaction product is formed. The product then flows back into a bubble and finally exits the bed when the bubble reaches the top of the bed. The rate at which the reactants and products transfer in and out of the bubble affects the conversion, as does the time it takes for the bubble to pass through the bed. Consequently, we need to describe the velocity at which the bubbles move through the column and the rate of transport of gases in and out of the bubbles. To calculate these parameters, we need to determine a number of fluid-mechanics parameters associated with the fluidization process. Specifically, to determine the velocity of the bubble through the bed we need to first calculate:

1. Porosity at minimum fluidization, ε_{mf}

| The Algorithm |

2. Minimum fluidization velocity, u_{mf}

3. Bubble size, d_b

To calculate the mass transport coefficient, we must first calculate

1. Porosity at minimum fluidization, ε_{mf}

2. Minimum fluidization velocity, u_{mf}

3. Velocity of bubble rise, u_b

4. Bubble size, d_b

To determine the reaction rate parameters in the bed, we need to first calculate

1. Fraction of the total bed occupied by bubbles, δ
2. Fraction of the bed consisting of wakes, $\alpha\delta$
3. Volume of catalyst in the bubbles, clouds, and emulsion, γ_b, γ_c, and γ_e

It is evident that before we begin to study fluidized-bed reactors, we must obtain an understanding of the fluid mechanics of fluidization. In Section R12.3B, equations are developed to calculate all the fluid mechanic parameters (e.g., d_b, u_{mf}) necessary to obtain the mass transfer and reaction parameters. In Section R12.3.3, equations for the mass transfer parameters are developed. In Section R12.3.4, the reaction rate parameters are presented, and the mole balance equations are applied to the bed to predict conversion in Section R12.3.5.

R12.3.2   The Mechanics of Fluidized Beds

In this section we shall first describe the regions of fluidization and calculate the minimum and maximum fluidization velocities. Next, the Kunii-Levenspiel

bubbling bed model is described in detail.[2] Finally, equations to calculate the fraction of the bed comprising bubbles, the bubble size, the velocity of bubble rise, and the fractional volume of bubbles, clouds, and wakes are derived.

R12.3.2A   Description of the Phenomena

We consider a vertical bed of solid particles supported by a porous or perforated distributor plate, as in Figure R12.3-2(a). The direction of gas flow is upward through this bed.
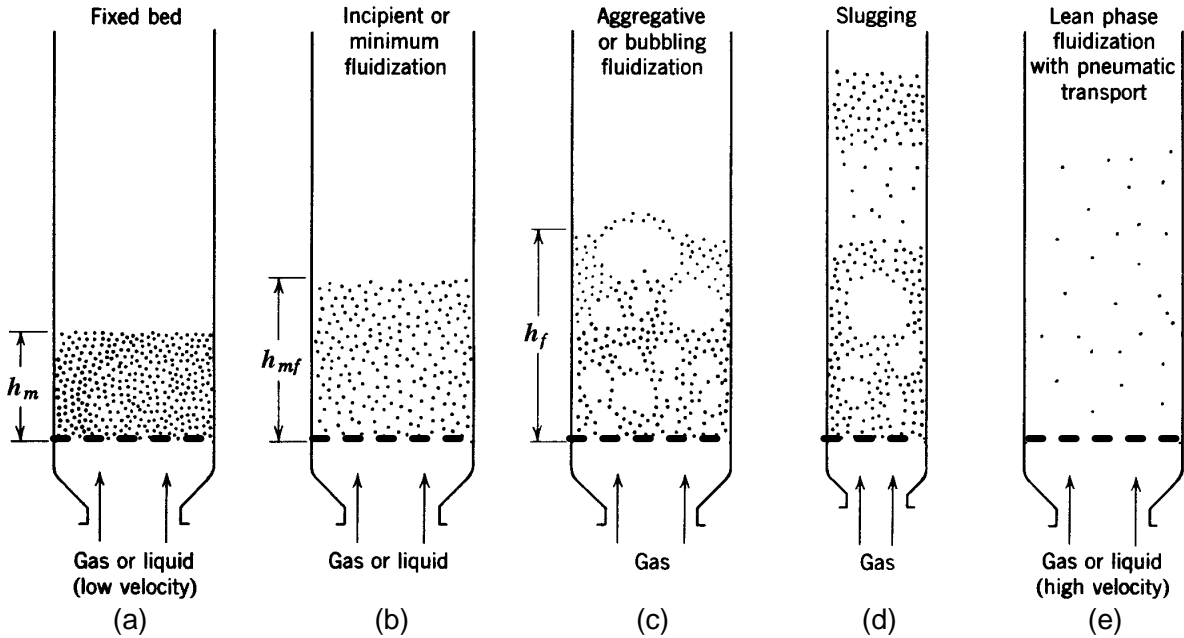
Figure R12.3-2   Various kinds of contacting of a batch of solids by fluid. Adapted from Kunii & Levenspiel, *Fluidized Engineering* (Huntington, NY: Robert E. Krieger Publishing Co., 1977).

There is a drag exerted on the solid particles by the flowing gas, and at low gas velocities the pressure drop resulting from this drag will follow the Ergun equation, Equation (4-22), just as for any other type of packed bed. When the gas velocity is increased to a certain value however, the total drag on the particles will equal the weight of the bed, and the particles will begin to lift and barely fluidize. If ρ_c is density of the solid catalyst particles, A_c is the cross sectional area, h_s, is the height of the bed settled before the particles start to lift, h, is the height of the bed at any time, and ε_s and ε are the corresponding porosities,[3] of the settled and expanded bed, respectively; then the mass of solids in the bed, W_s, is

$$W_s = \rho_c A_c h_s \left(1-\varepsilon_s\right) = \rho_c A_c h \left(1-\varepsilon\right) \qquad \text{(R12.3-1)}$$

---

[2] D. Kunii and O. Levenspiel, *Fluidization Engineering* (New York: Wiley, 1968).
[3] **Note: Nomenclature change in the text and lecture ϕ = porosity, while in this chapter ε = porosity.**

This relationship is a consequence of the fact that the mass of the bed occupied solely by the solid particles is the same no matter what the porosity of the bed. When the drag force exceeds the gravitational force, the particles begin to lift, and the bed expands (i.e., the height increases) thus increasing the bed porosity, as described by Equation (R12.3-1). This increase in bed porosity decreases the overall drag until it is again balanced by the total gravitational force exerted on the solid particles (Figure R12.3-3(b)).

If the gas velocity is increased still further, expansion of the bed will continue to occur; the solid particles will become somewhat separated from each other and begin to jostle each other and move around in a restless manner. Increasing the velocity just a slight amount further causes instabilities, and some of the gas starts bypassing the rest of the bed in the form of bubbles (Figure R12.3-3(c)). These bubbles grow in size as they rise up the column. Coincidentally with this, the solids in the bed begin moving upward, downward, and around in a highly agitated fashion appearing as a boiling frothing mixture. With part of the gas bubbling through the bed and the solids being moved around as though they were part of the fluid, the bed of particles is said to be "fluidized." It is in a state of aggregative, nonparticulate, or bubbling fluidization.

A further increase in gas velocity will result in slug flow (Figure R12.3-3(d)) and unstable chaotic operation of the bed. Finally at extremely high velocities, the particles are blown or transported out of the bed (Figure R12.3-3(e)).

The range of velocities over which the Ergun equation applies can be fairly large. On the other hand, the difference between the velocity at which the bed starts to expand and the velocity at which the bubbles start to appear can be extremely small and sometimes nonexistent. This observation means that if one steadily increases the gas flow rate, the first evidence of bed expansion may be the appearance of gas bubbles in the bed and the movement of solids. At low gas velocities in the range of fluidization, the rising bubbles contain very few solid particles. The remainder of the bed has a much higher concentration of solids in it and is known as the _emulsion phase_ of the fluidized bed. The bubbles are shown as the _bubble phase_. The cloud phase is an intermediate phase between the bubble and emulsion phases.

After the drag exerted on the particles equals the net gravitational force exerted on the particles, that is,

$$\Delta P = g\left(\rho_c - \rho_g\right)(1 - \varepsilon)h \qquad (R12.3-2)$$

the pressure drop will not increase with an increase in velocity beyond this point. (See Figure R12.3-2.) From the point at which the bubbles begin to appear in the bed, the gas velocity can be increased steadily over a quite appreciable range without changing the pressure drop across the bed or flowing the particles out of the bed. The bubbles become more frequent, and the bed, more highly agitated as the gas velocity is increased (Figure R12.3-2(c)); but the particles remain in the bed. This region is bubbling fluidization. Depending on the physical characteristics of the gas, the solid particles, and the distributor plate; and the internals (e.g., heat exchanger

tubes) within the bed, the region of bubbling fluidization can extend over more than an order of magnitude of gas velocities (e.g., 4 to 50 cm/s in Figure R12.3-3). In other situations, gas velocities in the region of bubbling fluidization may be limited; the point at which the solids begin to be carried out of the bed by the rising gas may be a factor of only three or four times the velocity at incipient fluidization.

Eventually, if the gas velocity is continuously increased, it will become sufficiently rapid to carry the solid particles upward, out of the bed. When this begins to happen, the bubbling and agitation of the solids are still present, and this is known as the region of fast fluidization, and the bed is know as *fast-fluidized bed*. At velocities beyond this region, the particles are well apart, and the particles are merely carried along with the gas stream. Under these conditions, the reactor is usually referred to as a *straight through transport reactor* or STTR (Figure R12.3-2(e)).

The various regions described earlier display the behavior illustrated in Figure R12.3-2. This figure presents the pressure drop across a bed of solid particles as a function of gas velocity. The region covered by the Ergun equation is the rising portion of the plot (Section I: $1 < U_0 < 4$ cm/s). The section of the figure where the pressure drop remains essentially constant over a wide range of velocities is the region of bubbling fluidization (Section II: $4 < U_0 \leq 50$ cm/s). Beyond this are the regions of fast fluidization and of purely entrained flow.
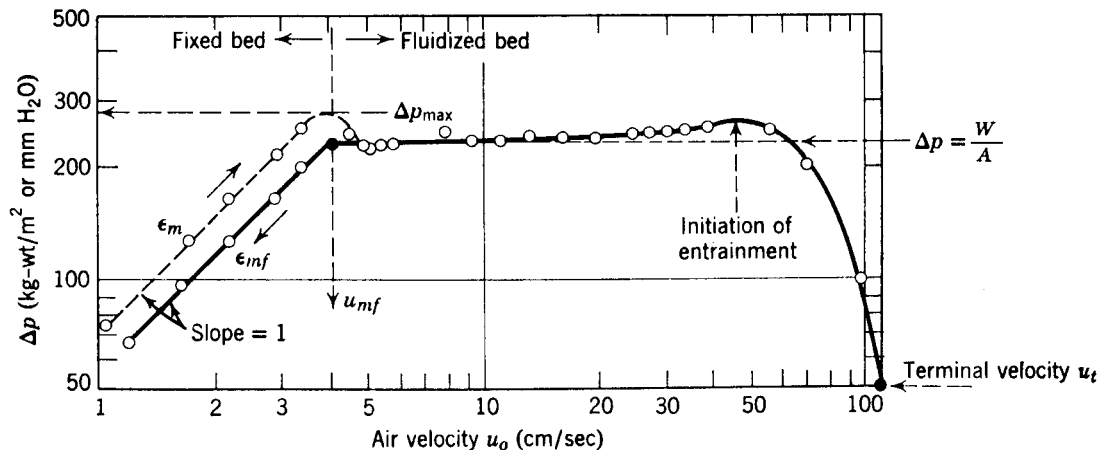

Figure R12.3-3   From Kunii and Levenspiel, Fluidization Engineering (Melbourne, FL: Robert E. Krieger, Publishing Co. 1977). Reprinted with permission of the publishers.

R12.3.2B   The Minimum Fluidization Velocity

Fluidization will be considered to begin at the gas velocity at which the weight of the solids gravitational force exerted on the particles equals the drag on the particles from the rising gas. The gravitational force is given by Equation (R12.3-1) and the drag force by the Ergun equation. All parameters at the point where these two forces are equal will be characterized by the subscript "mf," to denote that this is the value of a particular term when the bed is just beginning to become fluidized.

CD-Ch12FluidizedBed.doc

The combination $[g\,(\rho_c - \rho_g)]$ occurs very frequently, as in Equation (R12.3-1), and this grouping is termed $[\eta]$.

$$(\Delta P/h) = g\,\eta\,(1 - \varepsilon_{mf}) \tag{R12.3-2}$$

The Ergun Equation, Equation (4-22) can be written in the form

$$\frac{\Delta P}{h} = \rho_g U^2 \left| \frac{150(1-\varepsilon)}{\mathrm{Re}_d\,\psi} + \frac{7}{4} \right| \frac{1-\varepsilon}{\psi d_p \varepsilon^3} \tag{R12.3-3}$$

where ψ = shape factor of catalyst particle, sometimes called the sphericity.

At the point of minimum fluidization, the weight of the bed just equals the pressure drop across the bed

$$W_s = \Delta P A_C$$

$$g(1-\varepsilon)\!\left(\rho_c - \rho_g\right)\!h A_c = \rho_g U^2 \left[\frac{150(1-\varepsilon)}{\mathrm{Re}_p\,\psi} + \frac{7}{4} \right] \frac{1-\varepsilon}{\psi d_p \varepsilon^3} A_c h \tag{R12.3-4}$$

For $Re_p < 10$, $\left(Re_p = \dfrac{\rho_g d_p U}{\mu} \right)$, we can solve Equation (R12-5) for the minimum fluidization velocity to give

Calculate u_{mf}

$$u_{mf} = \frac{\left(\psi d_p\right)^2}{150\mu} \underbrace{\left[g\!\left(\rho_c - \rho_g\right) \right]}_{\eta} \frac{\varepsilon_{mf}^3}{1-\varepsilon_{mf}} \tag{R12.3-5}$$

Reynolds numbers less than 10 represents the usual situation, in which fine particles are fluidized by a gas. Sometimes, higher values of the Reynolds number do exist at the point of incipient fluidization, and then the quadratic Equation (R12.3-5) must be used.

Two dimensionless parameters in these two equations for u_{mf} deserve comment. This first is Ψ, the "sphericity," which is a measure of a particle's nonideality in both shape and roughness. It is calculated by visualizing a sphere whose volume is equal to the particle's, and dividing the surface area of this sphere by the actually measured surface area of the particle. Since the volume of a spherical particle is

$$V_p = \pi d_p^3 / 6$$

and its surface area is

$$A_s = \pi d_p^2 = \pi \left[\left(6V_p/\pi\right)^{1/3} \right]^2$$

Calculate ψ

$$\boxed{\psi = \frac{A_s}{A_p} = \frac{\pi\!\left(6V_p/\pi\right)^{2/3}}{A_p}} \tag{R12.3-6}$$

CD-Ch12FluidizedBed.doc

Measured values of this parameter range from 0.5 to 1, with 0.6 being a normal value for a typical granular solid.

The second parameter of special interest is the void fraction at the point of minimum fluidization, ε_{mf}. It appears in many of the equations describing fluidized-bed characteristics. There is a correlation that apparently gives quite accurate predictions of measured values of ε_{mf} (within 10%) when the particles in the fluidized bed are fairly small:[4]

Calculate ε_{mf}

$$\varepsilon_{mf} = 0.586\psi^{-0.72}\left(\frac{\mu^2}{\rho_g\eta d_p^3}\right)^{0.029}\left(\frac{\rho_g}{\rho_c}\right)^{0.021}$$

(R12.3-7)

Another correlation commonly used is that of Wen and Yu

$$\varepsilon_{mf} = (0.071/\psi)^{1/3}$$

(R12.3-8)

and/or

$$\varepsilon_{mf} = \frac{0.091(1-\varepsilon_{mf})}{\psi^2}$$

(R12.3-9)

When the particles are large, the predicted ε_{mf} can be much too small. If a value of ε_{mf} below 0.40 is predicted, it should be considered suspect. Kunii and Levenspiel[5] state that ε_{mf} is an easily measurable value. However, if it is not convenient to do so, Equation (R12.3-7) should suffice. Values of ε_{mf} around 0.5 are typical. If the distribution of sizes of the particles covers too large a range, the equation will not apply because smaller particles can fill the interstices between larger particles. When a distribution of particle sizes exists, an equation for calculating the mean diameter is

$$d_p = \frac{1}{\sum\dfrac{f_i}{d_{p_i}}}$$

(R12.3-10)

where f_i is the fraction of particles with diameter d_{p_i}.

R12.3.2C   Maximum Fluidization

If the gas velocity is increased to a sufficiently high value, however, the drag on an individual particle will surpass the gravitational force on the particle, and the particle will be entrained in a gas and carried out of the bed. The point at which the drag on an individual particle is about to exceed the gravitational force exerted on it is called the maximum fluidization velocity.

---

[4] T.E. Broadhurst and H.A. Becker, *AIChE J.*, *21*, 238 (1975).
[5] D. Kunii and O. Levenspiel, *Fluidization Engineering* (New York: Wiley, 1968).

CD-Ch12FluidizedBed.doc

Maximum velocity through the bed u_t

When the upward velocity of the gas exceeds the free-fall terminal velocity of the particle, u_t, the particle will be carried upward with the gas stream. For fine particles, the Reynolds numbers will be small, and two relationships presented by Kunii and Levenspiel[6] are

$$
\left. \begin{array}{ll}
u_t = \eta d_p^2 / 18\mu & Re < 0.4 \\
u_t = \left(1.78 \times 10^{-2}\, \eta^2 / \rho_g \mu\right)^{1/3} (d_p) & (0.4 < Re < 500)
\end{array} \right\}
\tag{R12.3-11}
$$

We now have the maximum and minimum superficial velocities at which we may operate the bed. The entering superficial velocity, u_0, must be above the minimum fluidization velocity but below the slugging u_{ms} and terminal, u_t, velocities.

$$
u_{mf} < u_0 < u_t
$$

and

$$
u_{mf} < u_0 < u_{ms}
$$

Both of these conditions must be satisfied for proper bed operation.

R12.3.2D   Descriptive Behavior of a Fluidized Bed – The Model Of Kunii And Levenspiel

At gas flow rates above the point of minimum fluidization, a fluidized bed appears much like a vigorously boiling liquid; bubbles of gas rise rapidly and burst on the surface, and the emulsion phase is thoroughly agitated. The bubbles form very near the bottom of the bed, very close to the distributor plate and as a result the design of the distributor plate has a significant effect on fluidized-bed characteristics.

Literally hundreds of investigators have contributed to what is now regarded as a fairly practical description of the behavior of a fluidized bed; chief among these is the work of Davidson and Harrison.[7] Early investigators saw that the fluidized bed had to be treated as a two-phase system – an emulsion phase and a bubble phase (often called the dense and lean phases). The bubbles contain very small amounts of solids. They are not spherical; rather they have an approximately hemispherical top and a pushed-in bottom. Each bubble of gas has a wake that contains a significant amount of solids. These characteristics are illustrated in Figure R12.3-4, which were obtained from x-rays of the wake and emulsion, the darkened portion being the bubble phase.

As the bubble rises, it pulls up the wake with its solids behind it. The net flow of the solids in the emulsion phase must therefore be downward.

---

[6] D. Kunii and O. Levenspiel, *Fluidization Engineering* (New York: Wiley, 1968).

[7] J. F. Davidson and D. Harrison, *Fluidized Particles* (New York: Cambridge University Press, 1963).
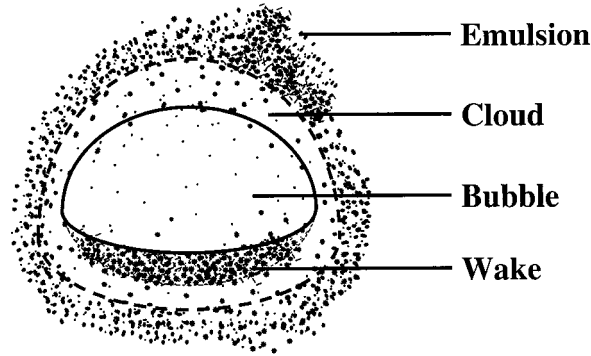
CD-Ch12FluidizedBed.doc

Figure R12.3-4 Schematic of bubble, cloud, and wake.

The gas within a particular bubble remains largely within that bubble, only penetrating a short distance into the surrounding emulsion phase. The region penetrated by gas from a rising bubble is called the cloud.

Davidson found that he could relate the velocity of bubble rise and the cloud thickness to the size of bubble. Kunii and Levenspiel[8] combined these observations with some simplifying assumptions to provide a practical, useable model of fluidized-bed behavior. Their assumptions are presented in Table R12.3-1.

TABLE R12.3-1. ASSUMPTIONS IN THE KUNII-LEVENSPIEL MODEL

(a)   The bubbles are all of one size.

(b)   The solids in the emulsion phase flow smoothly downward, essentially in plug flow.

(c)   The emulsion phase exists at minimum fluidizing conditions. The gas occupies the same void fraction in this phase as it had in the entire bed at the minimum fluidization point. In addition, because the solids are flowing downward, the minimum fluidizing velocity refers to the gas velocity relative to the moving solids, that is,

$$u_e = \frac{u_{mf}}{\varepsilon_{mf}} - u_s \qquad (R12.3-12)$$

(The ε_{mf} is present in this equation because u_{mf} is the superficial velocity, i.e., based on an empty tube cross section.) The velocity of the moving solids, u_s, is positive in the downward direction here, as in most of the fluidization literature. The velocity of the gas in the emulsion, u_e, is taken as a positive in the upward direction, but note that it can be negative under some conditions.

---

[8] D. Kunii and O. Levenspiel, *Fluidization Engineering* (New York: Wiley, 1968).

R12-9

CD-Ch12FluidizedBed.doc

> (d) In the wakes, the concentration of solids is equal to the concentration of solids in the emulsion phase, and therefore the gaseous void fraction in the wake is also the same as in the emulsion phase. Because the emulsion phase is at the minimum fluidizing condition, the void fraction in the wake is equal to ε_{mf}. The wake, however, is quite turbulent, and the average velocities of both solid and gas in the wake are assumed to be the same and equal to the upward velocity of the bubbles

Several of these assumptions had been used by earlier investigators, particularly Davidson and Harrison.[9] With the possible exception of (c), all these assumptions are of questionable validity, and rather obvious deviations from them are observed routinely. Nevertheless, the deviations apparently do not affect the mechanical or reaction behavior of fluidized beds sufficiently to diminish their usefulness.

R12.3.2E   Bubble Velocity and Cloud SSize

From experiments with single bubbles, Davidson and Harrison found that the velocity of rise of a single bubble could be related to the bubble size by

$$u_{br} = (0.71)(gd_b)^{1/2} \tag{R12.3-13}$$

Single bubble

When many bubbles are present, this velocity would be affected by other factors. The more bubbles that are present, the less drag there would be on an individual bubble; the bubbles would carry each other up through the bed. The greater number of bubbles would result from larger amounts of gas passing through the bed (i.e., a larger value of u_0). Therefore, the larger the value of u_0, the faster should be the velocity of a gas bubble as it rises through the bed.

Other factors that should affect this term are the viscosity of the gas and the size and density of the solid particles that make up the bed. Both of these terms also affect the minimum fluidization velocity, and so this term might well appear in any relationship for the velocity of bubble rise; the higher the minimum fluidization velocity, the lower the velocity of the rising bubble.

Adopting an expression used in gas-liquid systems, Davidson and Harrison proposed that the rate of bubble rise in a fluidized bed could be represented by simply adding and subtracting these terms:

Velocity of bubble rise u_b

$$u_b = u_{br} + \left(u_0 - u_{mf}\right)$$

$$\boxed{u_b = u_0 - u_{mf} + (0.71)(gd_b)^{1/2}} \tag{R12.3-14}$$

Bubble Size. The equations for the velocity of bubble rise, Equations (R12.3-13) and (R12.3-14) are functions of the bubble diameter, an elusive value to obtain.

---

[9] J. F. Davidson and D. Harrison, *Fluidized Particles* (New York: Cambridge University Press, 1963).

CD-Ch12FluidizedBed.doc

As might be expected, it has been found to depend on such factors as bed diameter, height above the distributor plate, gas velocity, and the components that affect the fluidization characteristics of the particles. Unfortunately, for predictability, the bubble diameter also depends significantly upon the type and number of baffles, heat exchangers tubes, and so forth, within the fluidized bed (sometimes called "internals"). The design of the distributor plate, which disperses the inlet gas over the bottom of the bed, can also has a pronounced effect upon the bubble diameter.

Studies of bubble diameter carried out thus far have concentrated on fluidized beds with no internals and have involved rather small beds. Under these conditions the bubbles grow as they rise through the bed. The best relationship between bubble diameter and height in the column at this writing seems to be that of Mori and Wen,[10] who correlated the data of studies covering bed diameters of 7 to 130 cm, minimum fluidization velocities of 0.5 to 20 cm/s, and solid particle sizes of 0.006 to 0.045 cm. Their principal equation was

$\boxed{d_b}$

$$\boxed{\frac{d_{bm} - d_b}{d_{bm} - d_{bo}} = e^{-0.3h/D_t}} \qquad (R12.3\text{-}15)$$

In this equation, d_b is the bubble diameter in a bed of diameter D_t, observed at a height h above the distributor plate; d_{bo} is the diameter of the bubble formed initially just above the distributor plate, and d_{bm} is the maximum bubble diameter attained if all the bubbles in any horizontal plane coalesce to form a single bubble (as they will do if the bed is high enough).

The maximum bubble diameter, d_{bm} has been observed to follow the relationship

$\boxed{d_{\text{maximum}}}$

$$\boxed{d_{bm} = 0.652\left[A_c\left(u_0 - u_{mf}\right)\right]^{0.4}} \qquad (R12.3\text{-}16)$$

$$\underset{\text{cm}}{\phantom{d_{bm} = 0.652[}} \quad \underset{\text{cm}^2}{} \quad \underset{\text{cm/s}}{\phantom{(u_0 - u_{mf})}}$$

for all beds, while the initial bubble diameter depends upon the type of distributor plate. For porous plates, the relationship

$$\boxed{d_{b0} = 0.00376\left(u_0 - u_{mf}\right)^2, \text{ cm}} \qquad (R12.3\text{-}17)$$

$\boxed{d_{\text{minimum}}}$ is observed, and for perforated plates, the relationship

$$\boxed{d_{b0} = 0.347\left[A_c\left(u_0 - u_{mf}\right)\big/n_d\right]^{0.4}} \qquad (R12.3\text{-}18)$$

appears to be valid, in which n_d is the number of perforations. For beds with diameters between 30 and 130 cm, these relations appear to predict bubble diameters with an accuracy of about ± 50%; for beds with diameters between 7 and 30 cm, the accuracy of prediction appears to be approximately + 100%, – 60% of the observed values.

---

[10] S. Mori and C. Y. Wen, *AIChE J.*, *21*, 109 (1975).

CD-Ch12FluidizedBed.doc

Werther developed the following correlation based on a statistical coalescence model:[11]

$$\frac{d_b}{\text{cm}} = 0.853 \sqrt[3]{1 + 0.272 \frac{u_0 - u_{ms}}{\text{cm/s}}} \left[1 - 0.0684 \ \frac{h}{\text{cm}}\right]^{1.21} \qquad \text{(R12.3-19)}$$

The bubble size predicted by this model is close to that predicted by Mori and Wen[12] for large diameter beds (2 m) and smaller than that suggested by Mori and Wen for small diameter beds (0.1 m).

R12.3.2F   Fraction of Bed in the Bubble Phase

Using the Kunii-Levenspiel model, the fraction of the bed occupied by the bubbles and wakes can be estimated by material balances on the solid particles and the gas flows. The parameter δ is the fraction of the total bed occupied by the part of the bubbles that does not include the wake, and α is the volume of wake per volume of bubble. The bed fraction in the wakes is therefore $(\alpha\delta)$. (c.f. Figure R12.13-5)
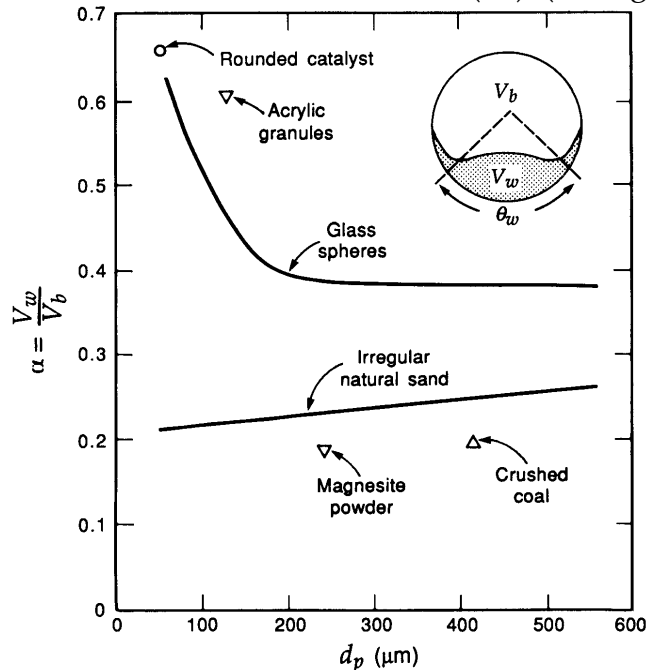
Figure R12.3-5 Wake angle θw and wake fraction of three-dimensional bubbles at ambient conditions; evaluated from x-ray photographs by Rowe and Partridge. Adapted from Kunii & Levenspiel, *Fluidized Engineering*, 2nd ed. (Stoneham, MA: Butterworth-Heinemann, 1991).

The bed fraction in the emulsion phase (which includes the clouds) is $(1 - \delta - \alpha\delta)$. Letting A_c and ρ_c represent the cross-sectional area of the bed and the density of the solid particles, respectively, a material balance on the solids (Figure R12.3-4) gives

---

[11] J. Werther, *ACS Symposium Series.*, *72*, D. Luss & V. W. Weekman, eds. (1978).
[12] S. Mori and C. Y. Wen, *AIChE J.*, *21*, 109 (1975).

CD-Ch12FluidizedBed.doc

$$\begin{array}{c}\text{Solids flowing}\\\text{downward in emulsion}\end{array} = \begin{array}{c}\text{Solids flowing}\\\text{upward in wakes}\end{array}$$

$$A_c \rho_c \left(1 - \delta - \alpha\delta\right)u_s \quad = \quad \alpha\delta u_b \rho_c A_c$$

or

Velocity of solids u_s

$$u_s = \frac{\alpha\delta u_b}{1 - \delta - \alpha\delta} \tag{R12.3-20}$$

A material balance on the gas flows gives

$$A_c u_0 \quad = \quad A_c \delta u_b \quad + \quad A_c \varepsilon_{mf} \alpha\delta u_b \quad + \quad A_c \varepsilon_{mf}\left(1 - \delta - \alpha\delta\right)u_e$$

$$\begin{pmatrix}\text{Total gast}\\\text{flow rate}\end{pmatrix} = \begin{pmatrix}\text{Gas flow}\\\text{in bubbles}\end{pmatrix} + \begin{pmatrix}\text{Gas flow}\\\text{in wakes}\end{pmatrix} + \begin{pmatrix}\text{Gas flow in}\\\text{emulsion}\end{pmatrix} \tag{R12.3-21}$$

The velocity of rise of gas in the emulsion phase is

Velocity of gas in emulsion u_e

$$\boxed{u_e = \frac{u_{mf}}{\varepsilon_{mf}} - u_s} \tag{R12.3-22}$$

(In the fluidization literature, u_s is almost always taken as positive in the downward direction.) Factoring the cross-sectional area from Equation (R12.3-21) and then combining Equations (R12.3-21) and (R12.3-22), we obtain an expression for the fraction δ of the bed occupied by bubbles

Volume fraction bubbles δ

$$\boxed{\delta = \frac{u_0 - u_{mf}}{u_b - u_{mf}\left(1 + \alpha\right)}} \tag{R12.3-23}$$

The wake parameter, α, is a function of the particle size in Figure R12.3-5. The value of α has been observed experimentally to vary between 0.25 and 1.0, with typical values close to 0.4. Kunii and Levenspiel assume that the last equation can be simplified to

$$\delta = \frac{u_0 - u_{mf}}{u_b} \tag{R12.3-24}$$

which is valid for $u_b \gg u_{mf}$, (e.g. $u_b \approx \dfrac{5\ u_{mf}}{\varepsilon_{mf}}$)

Example R12-1 Maximum Solids Hold-Up

A pilot fluidized bed is to be used to test a chemical reaction. The bed diameter is 91.4 cm. You wish to process 28.3×10^3 cm^3 of gaseous material. The average particle diameter is 100 μ. The reactor height is 10 feet. Allowing for a disengaging height of 7 feet, this means we have a maximum bed height of 91.4 cm. The distributor plate is a porous disc.

What is the maximum weight of solids (i.e., holdup) in the bed? Other data:

Color of Pellet: Brown

ψ: 0.7 ρ_g: 1.07×10^{-3} g/cm^3

ρ_c: 1.3 g/cc μ: 1.5×10^{-4} poise

Solution

The amount of solids in the reactor is given by Equation (R12.3-1)

$$W_s = \rho_c A_c h_s \left(1 - \varepsilon_s\right) = \rho_c A_c h \left(1 - \varepsilon\right) \qquad \text{(R12.3-1)}$$

The two parameters which need to be found are ε_{mf} and δ.

A. **Calculation of ε_{mf}**

$$\varepsilon_{mf} = 0.586 \psi^{-0.72} \left(\frac{\mu^2}{\rho_g \eta d_p^3} \right)^{0.029} \left(\frac{\rho_g}{\rho_c} \right)^{0.021} \qquad \text{(R12.3-7)}$$

1. Calculate gravity term

$$\eta = g\left(\rho_c - \rho_g\right) = \left(980 \ cm^2/s\right)\left(1.3 - 0.00107\right)g/cm^3$$

$$= 1270 \ g/(cm)^2 \left(s^2\right)$$

2. Cross-sectional area

$$A_c = \frac{\pi D^2}{4} = (\pi)(91.4 \ cm)^2 / 4 = 6.56 \times 10^3 \ cm^2$$

Superficial velocity

$$u_0 = \left(v_0 / A_c\right) = 2.83 \times 10^4 / 6.56 \times 10^3 = 4.32 \ cm/s$$

Porosity at minimum fluidization (Equation (R12.3-4))

$$\varepsilon_{mf} = (0.586)(0.7)^{-0.72} \left[\frac{\left(1.5 \times 10^{-4} \ g/cm \bullet s\right)^2}{\left(0.00107 \ g/cm^3\right)\left(1270 \ g/cm^2 \bullet s^2\right)\left(10^{-2} cm\right)^3} \right]^{0.029}$$

$$\times \left(0.00107 \ g/cm^3 / 1.3 \ g/cm^3\right)^{0.021}$$

$$\varepsilon_{mf} = 0.58$$

B. **Calculation of Volume Fraction of Bubbles**

$$\delta = \frac{u_0 - u_{mf}}{u_b - u_{mf}\left(1 + \alpha\right)} \qquad \text{(R12.3-23)}$$

Here we see we must calculate u_{mf} and u_b.

R12-14

Step 1. First the minimum fluidization velocity is obtained from Equation (R12.3-3)

$$u_{mf} = \frac{\left[(0.7)\left(10^{-2}\,cm\right)\right]^2}{150}\left(\frac{1270\;g/cm^2 \bullet s^2}{1.5 \times 10^{-4}\;g/cm \bullet s}\right)\left(\frac{0.58^3}{1-0.58}\right)$$

$$u_{mf} = 1.28\;cm/s$$

Step 2. To calculate u_b we must know the size of the bubble d_b., that is,

$$u_b = u_0 - u_{mf} + (0.71)(gd_b)^{1/2} \qquad\qquad (R12.3\text{-}14)$$

Step 3. The average size of the bubble, d_b, is determined by evaluating Equation (R12.3-15) at $(h/2)$.

$$\frac{d_{bm} - d_b}{d_{bm} - d_{b0}} = e^{-0.3h/D_t} \qquad\qquad (R12.3\text{-}15)$$

Where d_{bm} and d_{bo} are given in Equations (R12.3-16) and (R12.3-17) respectively.

Maximum bubble diameter

$$d_{bm} = 0.652\left[A_c\left(u_0 - u_{mf}\right)\right]^{0.4},\;\;cm \qquad\qquad (R12.3\text{-}16)$$

$$d_{bm} = (0.652)\left[\left(6.56 \times 10^3 cm^2\right)(4.32 - 1.28)\;cm/s\right]^{0.4}$$

$$d_{bm} = 34.2\;cm$$

Minimum bubble diameter

$$d_{b0} = 0.00376\left(u_0 - u_{mf}\right)^2,\;cm \qquad\qquad (R12.3\text{-}14)$$

$$d_{b0} = (0.00376)(4.32\;cm/s - 1.28\;cm/s)^2$$

$$d_{b0} = 0.0347\;cm$$

Solving for d_b

$$\frac{34.2 - d_b}{34.2 - 0.0347}\;e^{-0.3h/91.4}$$

$$d_b = 34.2\left(1 - e^{-0.3h/91.4}\right)$$

At h = 45.7 cm $(h/2)$ $d_b = 4.76\;cm$

At the top of the bed (h = 91.4 cm), $d_b = 8.86$ cm

For purposes of the Kunii-Levenspiel model, we shall take the bubble diameter to be 5 cm.

CD-Ch12FluidizedBed.doc

Step 4. We now can return to calculate the velocity of bubble rise and the fraction of bed occupied by bubbles from Equation (R12.3-14) we have

$$u_b = 4.32 \text{ cm/s} - 1.28 \text{ cm/s} + (0.71)\left[\left(980 \text{ cm/s}^2\right)\left(5 \text{ cm}\right)\right]^{0.5}$$

$$u_b = 52.8 \text{ cm/s}$$

From Figure (R12.3-5) we see that a 100 μ size particle corresponds to a value of α of 0.5. Substituting this value into Equation (R12.3-23), the fraction of the bed occupied by the bubble is

$$\delta = \frac{4.32 - 1.28}{52.8 - (1.28)(1.5)}$$

$$\delta = 0.060$$

Thus 94% of the bed is in the emulsion phase plus the wakes.

C. **The Amount of Solids Hold-Up, W_s**

$$W_s = A_c h (1 - \delta)\left(1 - \varepsilon_{mf}\right)\rho_s = \left(6.56 \times 10^3\right)(91.4)(0.94)(0.42)\rho_s$$

$$= \left(2.37 \times 10^5 \text{ cc of solid }\right)\rho_s$$

$$= \left(2.37 \times 10^5\right)(1.3) = 3.08 \times 10^5 \text{ g of solid}$$

or

$$W_s = 678 \text{ lb of solid particles}$$

R12.3.3   Mass Transfer In Fluidized Beds

There are two types of mass transport important in fluidized-bed operations. The first is the transport between gas and solid. In some situations this can affect the analysis of fluidized-bed behavior significantly, and in others it might not enter the calculations at all. In the treatment of this type of transfer, it will be seen that this type of transport is quite similar to gas-solid mass transfer in other types of operations.

The second type of mass transfer is unique to fluidized-bed operations. It concerns the transfer of material between the bubbles and the clouds, and between the clouds and the emulsion (Figures R12.3-3, R12.3-5, and R12.3-6). In almost every type of fluidized-bed operation, there are significant gas-phase concentration differences between the various elements of the fluidized bed. Consequently, calculations involving this type of mass transfer occur in almost every fluidized-bed analysis.
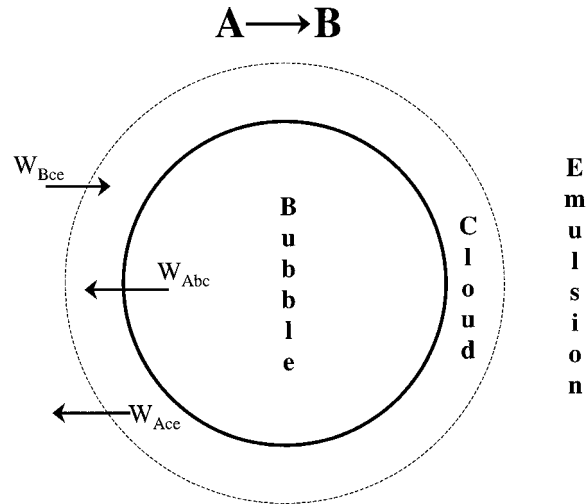
$$A \longrightarrow B$$

Figure R12.3-6 Transfer between bubble, cloud, and emulsion.

R12.3.3A Gas-Solid Mass Transfer

In the bubble phase of a fluidized bed, the solid particles are sufficiently separated so that in effect there is mass transfer between a gas and single particles. The most widely used correlation for this purpose is the 1938 equation of Fröessling (1938) for mass transfer to single spheres given in Chapter 11.

$$Sh = 2.0 + (0.6)(Re)^{1/2}(Sc)^{1/3} \tag{R12.3-25}$$

The relative velocity between the solid particle and the gas used in calculating the Reynolds number will be taken as u_0.

In the emulsion phase, the equation would be one that applied to fixed-bed operation with a porosity in the bed equal to ε_{mf} and a velocity of u_{mf}. The equation recommended by Kunii and Levenspiel:[13]

Transport from gas to single

$$Sh = 2.0 + (1.5)(Sc)^{1/3} \left[(1-\varepsilon)(Re)^{1/2} \right] \tag{R12.3-26}$$

for $5 < Re < 120$, and $\varepsilon < 0.84$

Mass transfer coefficients obtained from these relationships may then be combined with mass transfer among the various phases in the fluidized bed to yield the overall behavior with regard to the transport of mass. Owing to the small particle sizes and high surface area per volume of solids used in fluidized beds, the mass transfer from the gas to the solid surface is usually quite rapid and consequently it seldom limits the reaction.

---

[13] D. Kunii and O. Levenspiel, *Fluidization Engineering* (New York: Wiley, 1968).

CD-Ch12FluidizedBed.doc
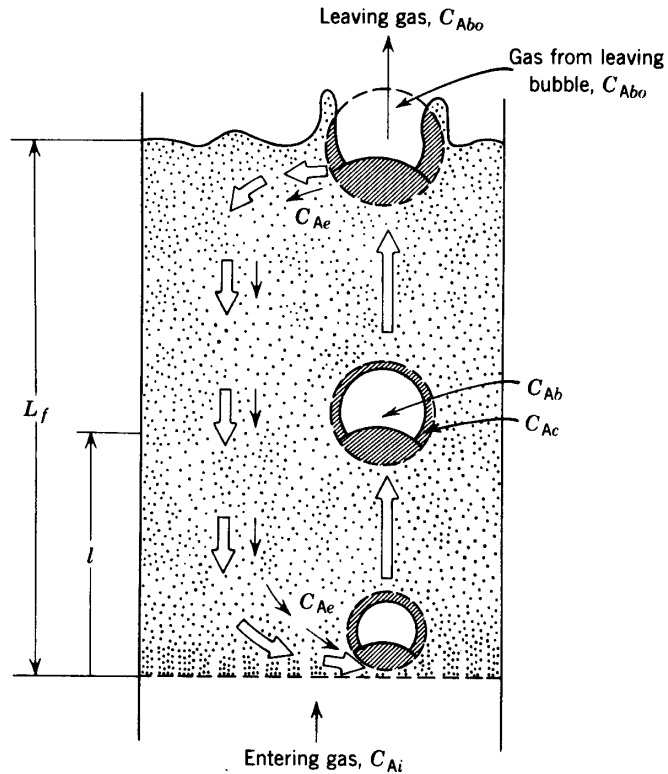
Figure R12.3-7   Sketch of flow pattern in a fluidized bed for downflow of emulsion gas, $u_e/u_0 < 0$ or $u_0/u_{mf} > 6$ to 11. Adapted from Kunii & Levenspiel, *Fluidized Engineering*, Robert E. Krieger Publishing Co., Huntington, New York, 1977.

R12.3.3B   Mass Transfer Between The Fluidized-Bed Phases

For the gas interchange between the bubble and the cloud, Kunii and Levenspiel[14] defined the mass transfer coefficient K_{bc} (s^{-1}) in the following manner:

$$W_{Abc} = K_{bc}\left(C_{Ab} - C_{Ac}\right) \tag{R12.3-27}$$

Where C_{Ab} and C_{Ac} are the concentration of A in the bubble and cloud respectively, (mole/dm^3) and W_{Abc} represents the number of moles of A transferred from the bubble to the cloud per unit time per unit volume of bubble (mole/dm^3/s). The concept of basing all mass transfer (and later, all reaction) on the bubble volume proves to simplify the calculations markedly. For the products, (e.g., B in A $\rightarrow$ B) the rate of transfer into the bubble from the cloud is given by a similar equation

$$W_{Bcb} = K_{cb}\left(C_{Bc} - C_{Bb}\right) \tag{R12.3-28}$$

The mass transfer coefficient K_{bc} can also be thought of as an exchange volume q between the bubble and the cloud.

$$W_{Bcb} = q_b C_{Ab} - q_c C_{Ac} = q_o\left(C_{Ab} - C_{Ac}\right) \tag{R12.3-29}$$

CD-Ch12FluidizedBed.doc

where q_b = Volume of gas flowing from the bubble to the cloud per unit time per unit volume of bubble

q_c = Volume of gas flowing from the cloud to the bubble per unit time per unit volume of bubble

q_o = Exchange volume between the bubble and cloud per unit time per unit volume of bubble (i.e., K_{bc})

$$(q_o = q_c = q_b)$$

Using Davidson's expression for gas transfer between the bubble and the cloud, and then basing it on the volume of the bubble, Kunii and Levenspiel[15] obtained this equation for evaluating K_{bc}:

Mass transfer between bubble and cloud

$$K_{bc} = 4.5\left(\frac{u_{mf}}{d_b}\right) + 5.85\left(\frac{D_{AB}^{1/2}\ g^{1/4}}{d_b^{5/4}}\right),$$
(R12.3-30)

where u_{mf} is in cm/s, d_b is in cm, D_{AB} is the diffusivity (cm^2/s) and g is the gravitational constant (980 cm/s^2).

We note

$$K_{bc} = K_{cb}$$

$K_{bc} \cong 2\ s^{-1}$ and a typical value of K_{bc} is 2 s^{-1}.

Similarly, these authors defined a mass transfer coefficient for gas interchange between the cloud and the emulsion:

$$W_{Ace} = K_{ce}(C_{Ac} - C_{Ae})$$

$$W_{Bce} = K_{ce}(C_{Be} - C_{Bc})$$
(R12.3-31)

where W_{Ace} is the moles of A transferred from the cloud to the emulsion per unit time per unit volume of bubble. Note that even though this mass transfer does not involve the bubble directly, it is still based on the bubble volume.

Using Higbie's penetration theory and his analogy for mass transfer from a bubble to a liquid, Kunii and Levenspiel[16] developed an equation for evaluating K_{ce}:

Mass transfer between cloud and emulsion

$$K_{ce} = 6.77\left(\frac{\varepsilon_{mf} D_{AB} u_b}{d_b^3}\right)^{1/2}$$
(R12.3-32)

where u_b is velocity of bubble rise in cm/s and the other symbols are as defined at Equation (R12.3-30). A typical value of K_{ce} is 1 s^{-1}. K_{ce} can also be thought of as the exchange volume between the cloud and the emulsion.

---

[14] D. Kunii and O. Levenspiel, *Fluidization Engineering* (New York: Wiley, 1968).
[15] D. Kunii and O. Levenspiel, *Fluidization Engineering* (New York: Wiley, 1968).
[16] D. Kunii and O. Levenspiel, *Fluidization Engineering* (New York: Wiley, 1968).

CD-Ch12FluidizedBed.doc

With knowledge of the mass transfer coefficients, the amount of gas interchange between the phases of a fluidized bed can be calculated and combined to predict the overall mass transfer behavior or reaction behavior of a fluidized-bed process.

R12.3.4   Reaction Behavior in a Fluidized Bed

To use the Kunii-Levenspiel model to predict reaction rates in a fluidized-bed reactor, the reaction rate law for the heterogeneous reaction per gram (or other fixed unit) of solid must be known. Then the reaction rate in the bubble phase, the cloud, and the emulsion phase, all per unit of bubble volume, can be calculated. Assuming that these reaction rates are known, the overall reaction rate can be evaluated using the mass transfer relationships presented in the preceding section. All this is accomplished in the following fashion.

We consider an nth order, constant-volume catalytic reaction. In the bubble phase

$$r_{Ab} = -k_b C_{Ab}^n$$

in which the reaction rate is defined per unit volume of bubble. In the cloud,

RATE LAWS

$$r_{Ac} = -k_c C_{Ac}^n$$

and similarly in the emulsion,

$$r_{Ae} = -k_e C_{Ae}^n$$

where k_e, k_c and k_b are the specific reaction rates in the emulsion cloud, and bubble respectively. In the latter two equations, the reaction rate is also defined per unit volume of bubble.

R12.3.5   Mole Balance on the Bubble, the Cloud, and the Emulsion

Material balances will be written over an incremental height Δz for substance A in each of the three phases (bubble, cloud, and emulsion) (Figure R12.3-7).
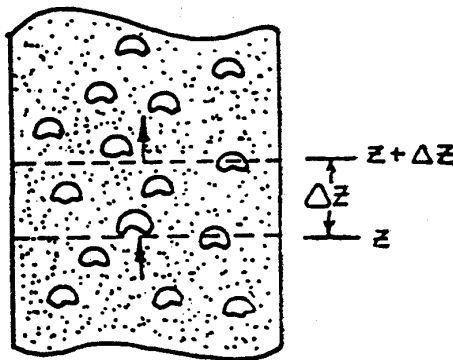

Figure R12.3-8 Section of a bubbling fluidized bed

CD-Ch12FluidizedBed.doc

R12.3.5A   Balance on Bubble Phase

The amount of A entering at z is the bubble phase by flow,

$$(u_b A_c C_{Ab})(\delta) \; = \; \begin{pmatrix} \text{Molar flow rate} \\ \text{of A assuming the} \\ \text{entire bed is filled} \\ \text{with bubbles} \end{pmatrix} \begin{pmatrix} \text{Fraction of the} \\ \text{bed occupied} \\ \text{by bubbles} \end{pmatrix}$$

A similar expression can be written for the amount of A leaving in the bubble phase in flow at z + Δz.

$$\underset{\text{In by flow}}{\;} \qquad \underset{\text{Out by flow}}{\;} \; + \; \underset{\substack{\text{Out by mass} \\ \text{Transport}}}{\;} \; + \; \underset{\text{Generation}}{\;}$$

$$(u_b A_c C_{Ab})(\delta)\big|_x \; - \; (u_b A_c C_{Ab} \delta)_{z+\Delta x} \; - \; K_{bc}(C_{Ab} - C_{Ac})A_c \Delta z \delta \; - \; k_b C_{Ab}^n A_c \Delta z \delta = 0$$

Dividing by $A_c \Delta z \delta$ and taking the limit as $\Delta z \to 0$

A balance on A in the bubble phase for steady state operation in section Δz.

Balance on
the bubble

$$u_b \frac{dC_{Ab}}{dz} = -k_b C_{Ab}^n - K_{bc}(C_{Ab} - C_{Ac}) \qquad \text{(R12.3-33)}$$

R12.3.5B   Balance on Cloud Phase

In the material balance on the clouds and wakes in the section Δz, it is easiest to base all terms on the volume of bubble. The material balance for the clouds and wakes is

Balance on
the clouds

$$u_b \delta \left[\frac{3(u_{mf}/\varepsilon_{mf})}{u_{br} - (u_{mf}/\varepsilon_{mf})} + \alpha \right] \frac{dC_{Ac}}{dz} = K_{bc}(C_{Ab} - C_{Ac}) - K_{ce}(C_{Ac} - C_{Ae}) - k_c C_A^n \qquad \text{(R12.3-34)}$$

R12.3.5C   Balance on the Emulsion

The fraction of the bed in the emulsion phase is $(1 - \delta - \alpha\delta)$. The material balance for A in the emulsion the following expression for the emulsion-phase material balance on A results in

Balance on
the emulsion

$$u_e \left(\frac{1 - \delta - \alpha\delta}{\delta} \right) \frac{dC_{Ae}}{dz} = K_{ce}(C_{Ac} - C_{Ae}) - k_e C_{Ae}^n \qquad \text{(R12.3-35)}$$

The three material balances thus result in three coupled ordinary differential equations, with one independent variable (z) and three dependent variables (C_{Ab}, C_{Ac}, C_{Ae}). These equations can be solved numerically. The Kunii-Levenspiel model simplifies these still further, by assuming that the derivative terms on the left-hand side of the material balances on the cloud and emulsion are negligible in comparison

CD-Ch12FluidizedBed.doc

with the terms on the right-hand side. Using this assumption, and letting $t = z/u_b$ (i.e., the time the bubble has spent in the bed), the three equations take the form:

$$\frac{dC_{Ab}}{dt} = -\left(k_b C_{Ab}^n\right) - K_{bc}\left(C_{Ab} - C_{Ac}\right) \tag{R12.3-36}$$

$$K_{bc}\left(C_{Ab} - C_{Ac}\right) = k_c C_{Ac}^n + K_{ce}\left(C_{Ac} - C_{Ae}\right) \tag{R12.3-37}$$

$$K_{ce}\left(C_{Ac} - C_{Ae}\right) = k_e C_{Ae}^n \tag{R12.3-38}$$

Note

or only one differential equation and two algebraic equations. *In all equations, kC_A^n is the g-moles per second reacted in the particular phase per volume of bubbles.*

R12.3.5D   Partitioning of the Catalyst

To solve these equations, it is necessary to have values of k_b, k_c, and k_e. Three new parameters are defined:

$$\gamma_b : \frac{\text{Volume of solid catalyst dispersed in bubbles}}{\text{Volume of bubbles}}$$

$$\gamma_c : \frac{\text{Volume of solid catalyst in clouds and wakes}}{\text{Volume of bubbles}}$$

$$\gamma_e : \frac{\text{Volume of solid catalyst in emulsion phase}}{\text{Volume of bubbles}}$$

First of all the specific reaction rate of solid catalyst, k_{cat} must be known. It is normally determined from laboratory experiments. The term $k_{cat} C_A^n$ is the g-moles reacted per volume of solid catalyst. Then

$$k_b = \gamma_b k_{cat}; \quad k_c = \gamma_c k_{cat}; \quad k_e = \gamma_e k_{cat} \tag{R12.3-39}$$

$$k_{cat} = \rho_c \times k' = \frac{\text{g cat}}{\text{cm}^3\text{cat}} \times \frac{\text{cm}^3}{\text{g cat} \cdot \text{s}}\left(\frac{\text{cm}^3}{\text{mol}}\right)^{n-1} = \frac{\text{cm}^3}{\text{cat} \cdot \text{s}}\left(\frac{\text{cm}^3}{\text{mol}}\right)^{n-1}$$

The term k' is the specific reaction rate per weight of catalyst.

The value of γ_b ranges between 0.001 and 0.01, with 0.005 being the more

typical number. The volume fraction of catalyst in the clouds and wakes is $(1 - \varepsilon_{mf})$. The volume of cloud and wakes per volume of bubble is

$$\frac{V_c}{V_b} = \frac{3\left(u_{mf}/\varepsilon_{mf}\right)}{u_b - \left(u_{mf}/\varepsilon_{mf}\right)}$$

so the expression for γ_c is

R12-22

CD-Ch12FluidizedBed.doc

$$\gamma_c = \left(1 - \varepsilon_{mf}\right) \left[\frac{3\left(u_{mf}/\varepsilon_{mf}\right)}{u_b - \left(u_{mf}/\varepsilon_{mf}\right)} + \alpha \right]$$

(R12.3-40)

It turns out that the value of α is normally far from insignificant in this expression for γ_c and represents a weakness in the model because there does not yet exist a reliable method for determining α. The typical values of γ_c ranges from 0.3 to 0.4. The value of γ_c can be quite incorrect on occasion, in particular, a value of $\alpha=1$.

The volume fraction of the solids in the emulsion phase is again $(1 - \varepsilon_{mf})$. The volume of emulsion per volume of bubble is

$$\frac{V_e}{V_b} = \frac{1-\delta}{\delta} - \left(\frac{\text{Volume of clouds and wakes}}{\text{Volume of bubbles}} \right)$$

and so the expression for γ_e is

| The value of catalysts in the emulsion is γ_e. |

$$\gamma_e = \left(1 - \varepsilon_{mf}\right)\left(\frac{1-\delta}{\delta}\right) - \gamma_c - \gamma_b$$

(R12.3-41)

Typical values of γ_b, γ_c, and γ_e are 0.005, 0.2, and 1.5, respectively. Using the expressions given above, the three balance equations become

| For reactors other than first or zero order, these equations must be solved numerically. |

Bubble balance $\quad \dfrac{dC_{Ab}}{dt} = -\left(\gamma_b k_{cat} C_{Ab}^n\right) - K_{bc}\left(C_{Ab} - C_{Ac}\right)$ (R12.3-42)

Cloud balance $\quad K_{bc}\left(C_{Ab} - C_{Ac}\right) = \gamma_c k_{cat} C_{Ac}^n + K_{ce}\left(C_{Ac} - C_{Ae}\right)$ (R12.3-43)

Emulsion balance $\quad K_{ce}\left(C_{Ac} - C_{Ae}\right) = \gamma_e k_{cat} C_{Ae}^n$ (R12.3-44)

R12.3.5E Solution to the Balance Equations for a First-Order Reaction

If the reaction is first order, then the C_{Ac} and C_{Ae} can be eliminated using the two algebraic equations, and the differential equation can be solved analytically for C_{Ab} as a function of t. An analogous situation would exist if the reaction were zero. Except for these two situations, solution to these two equations must be obtained numerically.

For first-order reactions, we can combine the three balance equations into one differential equation, which we can then solve to determine the conversion achieved in a fluidized-bed reactor. In addition, the closed form solution allows us to examine certain limiting situations in order to determine which operating parameters are most influential in dictating bed performance. Here we can pose and ask a number of "What if . . ." questions. To arrive at our fluidized-bed design equation for a first-order reaction, we simply express both the concentration of A in the emulsion, C_{Ae},

CD-Ch12FluidizedBed.doc

and in the cloud, C_{Ac}, in terms of the bubble concentration, C_{Ab}. First, we use the emulsion balance

$$K_{ce}(C_{Ac} - C_{Ae}) = \gamma_e k_{cat} C_{Ae}^n \qquad \text{(R12.3-45)}$$

to solve for C_{Ae} in terms of C_{Ac}.

    Rearranging (R12.3-45) for a first-order reaction (n = 1), we obtain

$$C_{Ae} = \frac{K_{ce}}{\gamma_e k_{cat} + K_{ce}} C_{Ac} \qquad \text{(R12.3-46)}$$

We now use this equation to substitute for C_{Ae} in the cloud balance

$$K_{bc}(C_{Ab} - C_{Ac}) = C_{Ac}\gamma_c k_{cat} + K_{ce}\left(C_{Ac} - \frac{K_{ce}C_{Ac}}{\gamma_e k_{cat} + K_{ce}}\right)$$

Solving for C_{Ac} in terms of C_{Ab}

$$C_{Ac} = \frac{K_{bc}}{\gamma_c k_{cat} + \left[\dfrac{K_{ce}\gamma_e k_{cat}}{\gamma_c k_{cat} + K_{ce}}\right] + K_{bc}} C_{Ab} \qquad \text{(R12.3-47)}$$

    We now substitute for C_{ac} in the bubble balance

$$\frac{dC_{Ab}}{dt} = \gamma_b k_{cat} C_{Ab} + \left[C_{Ab} - \frac{K_{bc}C_{Ab}}{\gamma_c k_{cat} + K_{bc} + \left[\dfrac{K_{ce}\gamma_e k_{cat}}{\gamma_e k_{cat} + K_{ce}}\right]}\right]$$

Rearranging

$$\frac{dC_{Ab}}{dt} = k_{cat} C_{Ab}\left[\gamma_b + \frac{\gamma_e \gamma_c k_{cat} K_{bc} + \gamma_c K_{bc} K_{ce} + K_{ce}\gamma_e K_{bc}}{\gamma_e \gamma_c k_{cat}^2 + K_{ce}\gamma_c k_{cat} + K_{bc}\gamma_e k_{cat} + K_{ce}K_{bc} + K_{ce}\gamma_e k_{cat}}\right]$$

After some further rearrangement,

$$-\frac{dC_{Ab}}{dt} = k_{cat} C_{Ab}\left(\gamma_b + \frac{1}{\dfrac{k_{cat}}{K_{bc}} + \dfrac{1}{\gamma_c + \dfrac{1}{\dfrac{1}{\gamma_e} + \dfrac{k_{cat}}{K_{ce}}}}}\right) \qquad \text{(R12.3-48)}$$

CD-Ch12FluidizedBed.doc

<table>
<tr><td>
The overall transport coefficient K_R for a first-order reaction.
</td><td>

$$K_R = \gamma_b + \cfrac{1}{\cfrac{k_{cat}}{K_{bc}} + \cfrac{1}{\gamma_c + \cfrac{1}{\cfrac{1}{\gamma_e} + \cfrac{k_{cat}}{K_{ce}}}}}$$

</td><td>(R12.3-49)</td></tr>
</table>

$$-\frac{dC_{Ab}}{dt} = k_{cat}K_R C_{Ab} \qquad (R12.3\text{-}50)$$

Expressing C_{Ab} as a function of X, that is,

$$C_{Ab} = C_{A0}(1 - X)$$

We can substitute to obtain

$$\frac{dX}{dt} = k_{cat}K_R(1 - X)$$

and integrating

<div>
The design equation
</div>

$$\boxed{ln\left(\frac{1}{1-X}\right) = k_{cat}K_R t} \qquad (R12.3\text{-}51)$$

The height of the bed necessary to achieve this conversion is

$$h = tu_b$$

$$\boxed{h = \frac{u_b}{k_{cat}K_R} \ ln \ \frac{1}{1-X}} \qquad (R12.3\text{-}52)$$

The corresponding catalyst weight is

$$W = \rho_c A_c h \left(1 - \varepsilon_{mf}\right)\left(1 - \delta\right) \qquad (R12.3\text{-}53)$$

$$W = \frac{\rho_c A_c u_b \left(1 - \varepsilon_{mf}\right)\left(1 - \delta\right)}{k_{cat}K_R} \ ln \ \frac{1}{1-X} \qquad (R12.3\text{-}54)$$

R12.3.5F   The Procedure

Unfortunately, one must use an iterative procedure to calculate the catalyst weight. This predicament is a consequence of the fact that both K_R and u_b depend upon the bubble diameter, which depends upon the bed height, Equation (R12.3-52). Consequently, one should check the estimated average bubble diameter using the value of h calculated from Equation (R12.3-52). A flow chart outlining this procedure is shown in Figure R12.3-9.

CD-Ch12FluidizedBed.doc
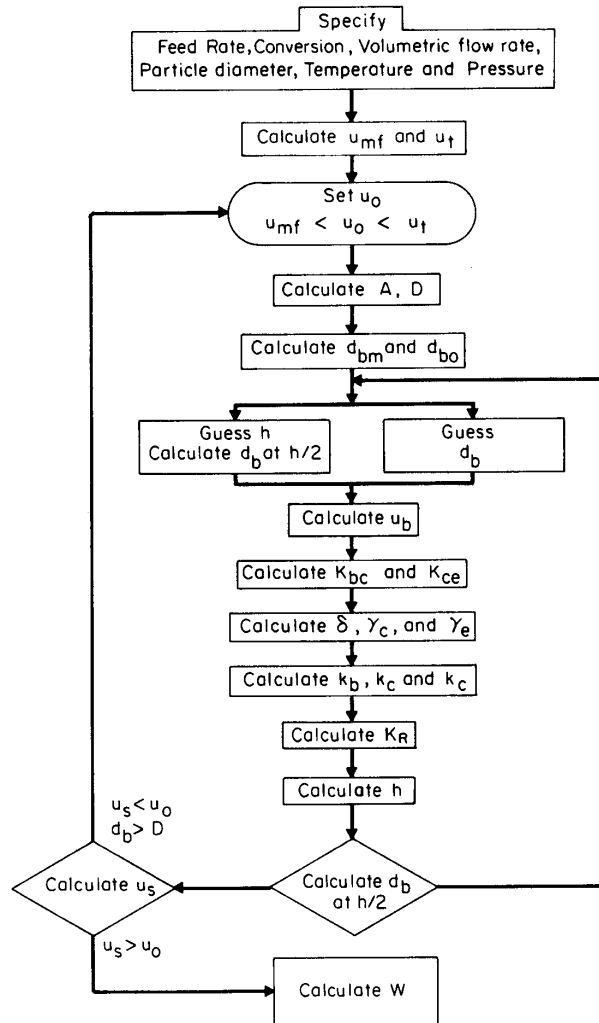
Figure R12.3-9   Computational algorithm for fluidized-bed reactor design. Reprinted with permission from Fogler and Brown, "Reaction Control and Transport," *Chemical Reactors*, ACS Symposium Series, vol. 168, 1981, H.S. Fogler, ed.

Example R12-2 Catalytic Oxidation of Ammonia

Massimilla and Johnstone[17] studied the catalytic oxidation of ammonia in a fluidized-bed reactor. Under their experimental conditions, the reaction was first-order, dependent only upon the ammonia concentration, and without a significant change in volumetric flow rate. In one of their runs, 4 kg of catalyst were used with a gas flow rate of 818 cm^3/s at reaction conditions. A conversion of 22% of the entering ammonia was obtained. Predict this conversion using the Kunii-Levenspiel model.

---

[17] L. Massimilla and R.F. Jornstone, *Chem. Eng. Sci.* <u>16</u>, (105) (1961).

CD-Ch12FluidizedBed.doc

Other data:

$P = 840$ torr $= 1.11$ atm

$T = 523$ K $(250°C)$

⎱ Operating conditions

$D_t = 11.4$ cm

Distributor plate is porous
stainless steel.

⎱ Reactor

$v_0 = 818$ cm$^3/$s @ reaction conditions

Composition : 10% NH_3, 90% O_2

⎱ Feed

$d_p = 105$ μm $(0.0105$ cm$)$

$\psi = 0.6$ (assumed)

$\rho_p = 2.06$ (g/cm^3)

$h_s = 38.9$ (cm)

⎱ Catalyst

$-r_A = kC_{NH_3}$ $\left(\text{gmoles } NH_3/(s)(cm^3 \text{ of catalyst })\right)$

$k_{cat} = 0.0858$ s^{-1} @ reaction conditions

⎱ Reaction rate

$\rho_g = 7.85 \times 10^{-4}$ g$/$cm^3

$\mu_g = 2.98 \times 10^{-4}$ g$/$cm $\cdot$ s

$D_{AB} = 0.618$ cm$^2/$s

⎱ Fluid properties

CD-Ch12FluidizedBed.doc

Solution

A. Mechanical Characteristics of Bed

Step 1. Gravitation term, η

$$\eta = g\left(\rho_c - \rho_g\right)$$

$$= 980 \ \text{cm/s}^2 \ \left(2.06 - 7.85 \times 10^{-4}\right) \text{g/cm}^3$$

$$= 2.02 \times 10^3 \ \text{g/(s)}^2 \text{(cm)}^2$$

Step 2. Porosity of bed a minimum fluidization, ε_{mf}

$$\varepsilon_{mf} = 0.586 \psi^{-0.72} \left(\frac{\mu^2}{\rho_g \eta d_p^3}\right)^{0.029} \left(\frac{\rho_g}{\rho_c}\right)^{0.021} \tag{R12.3-7}$$

$$= (0.586)(0.6)^{-0.72}\left\{\left(2.98 \times 10^{-4} \ \text{g/cm} \cdot \text{s}\right)^2 \right/$$

$$\left[\left(7.85 \times 10^{-4}\right)^2 \left(2.02 \times 10^3 \ \text{g/cm}^2 \cdot \text{s}^2\right)(0.0105 \ \text{cm})^3\right]\right\}^{0.029}$$

$$\times \left(7.85 \ \text{g/cm}^3 \times 10^{-4} / 2.06 \ \text{g/cm}^3\right)^{0.021}$$

$\varepsilon_{mf} \sim 0.65$ $\boxed{\varepsilon_{mf} = 0.657}$

Step 3. Gas velocity at minimum fluidization

$$u_{mf} = \frac{\left(\psi d_p\right)^2}{150\mu} \underbrace{\left[g\left(\rho_c - \rho_g\right)\right]}_{\eta} \frac{\varepsilon_{mf}^3}{1 - \varepsilon_{mf}} \tag{R12.3-5}$$

$$= \left[(0.6)(0.0105 \ \text{cm}^2)\right]\left(2.02 \times 10^{-3} \ \text{g/cm}^2 \cdot \text{s}^2\right)(0.657)^3 \right/$$

$$\left[(150)\left(2.98 \times 10^{-4} \ \text{g/cm} \cdot \text{s}\right)(1 - 0.657)\right]$$

$u_{mf} \sim 1.5 \ \text{cm/s}$ $\boxed{u_{mf} = 1.48 \ \text{cm/s}}$

Step 4. Entering gas velocity u_0

$$u_0 = v_0 / A_c = v_0 \left/ \left(\pi D_t^2 / 4\right)\right.$$

$$= 818 \ \text{cm}^3/\text{s} \left/ \left[(\pi)(11.4 \ \text{cm})^2 / 4\right]\right.$$

CD-Ch12FluidizedBed.doc

$u_o \sim 8$ cm/s

$\boxed{u_0 = 8.01 \text{ cm/s}}$

Step 5. Is u_0 within a reasonable operating range?

Check u_t.

$$u_t = \left(1.78 \times 10^{-2}\, \eta^2 / \rho_g \mu\right)^{1/3} \left(d_p\right) \quad\quad\quad (R12.3\text{-}11)$$

$$= \left[\left(1.78 \times 10^{-2}\right)\left(2.02 \times 10^{-3}\, \text{g/cm}^2 \cdot \text{s}^2\right)^2 \middle/ \right.$$

$$\left.\left(7.85 \times 10^{-4}\, \text{g/cm}^3\right)\left(2.98 \times 10^4\, \text{g/cm} \cdot \text{s}\right)\right]^{1/3} (0.0105)$$

$u_t \sim 70$ cm/s

$\boxed{u_t = 71.1 \text{ cm/s}}$ Maximum fluidization gas velocity
(Particle blown out of the bed)

Are N_{Re} in proper range for use of Equations (R12.3-6) and (R12.3-11)?

$$N_{Re} = \frac{d_p \rho_g u}{\mu}$$

At u_{mf}: $N_{Re} = \left(0.0105 \text{ cm}\right)\left(7.85 \times 10^{-4}\, \text{g/cm}^3\right)\left(1.48 \text{ cm/s}\right) \middle/$

$$\left(2.98 \times 10^{-4}\, \text{g/cm} \cdot \text{s}\right)$$

$$= 0.0409 \text{ (OK, since it is } < 10\text{)}$$

At u_t $N_{Re} = \left(0.0105 \text{ cm}\right)\left(7.85 \times 10^{-4}\, \text{g/cm}^3\right)\left(71.1 \text{ cm/s}\right) \middle/$

$$\left(2.98 \times 10^{-4}\, \text{g/cm} \cdot \text{s}\right)$$

$$= 1.97 \text{ (OK, since } 0.4 < N_{Re} < 500\text{)}$$

Thus u_0 is 5.4 times u_{mf}, and well below u_t.

Step 6. Bubble sizes, d_{bo}, d_{bm}, and d_b

$$d_{b0} = 0.00376\left(u_o - u_{mf}\right)^2, \text{ cm} \quad\quad\quad (R12.3\text{-}17)$$

$$= 0.00376 \left(8.01 \text{ cm/s} - 1.48 \text{ cm/s}\right)^2$$

$$d_b = 0.160 \text{ cm}$$

$$d_m = 0.652 \left[A_c\left(u_0 - u_{mf}\right)\right]^{0.4} \qu\quad\quad (R12.3\text{-}18)$$

CD-Ch12FluidizedBed.doc

$$= 0.652 \left\{ \pi(11.4)^2/4 \right] 8.01 \text{ cm/s} - 1.48 \text{ cm/s} \right\}^{0.4} \text{cm}$$

d_{bm} = 08.8 cm

$$\boxed{d_{bm} = 8.79 \text{ cm}} \quad \text{(Since this is smaller than column diameter,} \\ \text{slugging will not occur.)}$$

Step 7. Bubble sizes, d_{bo}, d_{bm}, and d_b

The unexpanded bed height is 38.9 cm. The expanded bed height will probably be 40 to 50% greater, say ~ 60 cm. We therefore will assume the average bubble size will be taken as the one calculated for (h/2) = 30 cm.

Step 8. Average bubble diameter

$$d_b = d_{bm} - (d_{bm} - d_{b0})e^{-0.3h/D_t} \quad \text{(From Equation R12.3-15)}$$

$$= 8.79 - (8.79 - 0.160)e^{-(0.3)(30)/11.4}$$

d_b ~ 5 cm

$$\boxed{d_b = 4.87 \text{ cm}}$$

Step 9. Rise velocity of single bubble

$$u_{br} = (0.71)(gd_b)^{1/2} = (0.71)\left[(980 \text{ cm/s}^2)(4.87 \text{ cm})\right]^{1/2} = 49.0 \text{ cm/s} \quad \text{(R12.3-13)}$$

Step 10. Rise velocity of a bubble when many bubbles are present

$$u_b = u_0 - u_{mf} + (0.71)(gd_b)^{1/2} \quad \text{(R12.3-14)}$$

$$= 8.01 - 1.48 + 49.0 = 55.6 \text{ cm/s}$$

u_b ~ 55 cm

$$u_b = 55.6 \text{ cm/s}$$

From Figure (R12.3-5) for glass spheres with d_p = 0.105 mm, then α = 0.4

Step 11. Fraction of bed in bubble phase

$$\delta = (u_o - u_{mf}) / \left[u_b - u_{mf}(1 + \alpha) \right] \quad \text{(R12.3-23)}$$

$$= (8.01 - 1.48) / \left[55.6 - 1.48(1 + 0.4) \right]$$

δ ~ 0.12

$$\boxed{\delta = 0.122}$$

Step 12. Bed height

$$\underbrace{(h A_c)}_{\substack{\text{Volume} \\ \text{of bed}}} \quad \underbrace{(1 - \delta)}_{\substack{\text{Volume in} \\ \text{emulsion,} \\ \text{clouds,} \\ \text{and wakes}}} \quad \underbrace{(1 - \varepsilon_{mf})}_{\substack{\text{Volume of solids} \\ \text{in emulsion,} \\ \text{clouds, and} \\ \text{wakes}}} \quad \rho_p = \text{mass of catalyst in bed}$$

CD-Ch12FluidizedBed.doc

$$h = \frac{W}{A_c(1-\delta)(1-\varepsilon_{mf})\rho_c}$$

$$= \frac{4000 \text{ g}}{\left[\pi(11.4 \text{ cm})^2/4\right](1-0.122)(1-0.657)(2.06 \text{ gm}/\text{cm}^3)} = 63.2 \text{ cm}$$

Since the estimated bed height of 60 cm is sufficiently close to the calculated value of 63.2 cm, one can proceed further in the calculations without making a new estimate of h.

Good Guess of h = 60 cm

C. Mass Transfer and Reaction Parameters:

Step 1. Bubble-cloud mass transfer coefficient

Order of magnitude parameters

⇓

$$K_{bc} = 4.5(u_{mf}/d_b) + 5.85(D^{1/2}g^{1/4}/d_b^{5/4}) \qquad \text{(R12.3-30)}$$

$$= 4.5(1.48\text{cm/s})/(4.87\text{cm}) + 5.85(0.61\text{cm}^2/\text{s})^{1/2}(980\text{cm/s}^2)^{1/4}/(4.87\text{cm})^{5/4}$$

$$= 1.37 \text{ s}^{-1} + 3.54 \text{ s}^{-1}$$

$$\boxed{K_{bc} = 4.92 \text{ s}^{-1}}$$

$K_{bc} \sim 5 \text{ s}^{-1}$

Step 2. Cloud-emulsion mass-transfer coefficient

$$K_{ce} = 6.78(\varepsilon_{mf}Du_b/d_b^3)^{1/2} \qquad \text{(R12.3-32)}$$

$$= 6.78\left[(0.657)(0.61\text{cm}^2/\text{s})(55.6\text{cm/s})/(4.87\text{cm})^3\right]^{1/2}$$

$$\boxed{K_{ce} = 3.00 \text{ s}^{-1}}$$

$K_{ce} \sim 3 \text{ s}^{-1}$

Step 3. Volume of catalysts in the bubble per volume of bubble.

$$\boxed{\gamma_b = 0.01 \text{ (assumed)}}$$

Step 4. Volume of catalyst in clouds and wakes/cm³ of bubbles

$$\gamma_c = (1-\varepsilon_{mf})\left\{3(u_{mf}/\varepsilon_{mf})/\left[u_b - (u_{mf}/\varepsilon_{mf})\right] + \alpha\right\}$$

$$= (1-0.657)\left\{(3)(1.48/0.657)/\left[49.0 - (1.48/0.657)\right] + 0.4\right\} \qquad \text{(R12.3-40)}$$

$\gamma_c \sim 0.2$

$$\boxed{\gamma_c = 0.187}$$

Step 5. Volume of catalyst in emulsion/cm³ of bubbles

$$\gamma_e = (1-\varepsilon_{mf})\left[(1-\delta)/\delta\right] - \gamma_c - \gamma_b$$

CD-Ch12FluidizedBed.doc

$$= (1 - 0.657)\left[(1 - 0.122/0.122)\right] - 0.187 - 0.005 \qquad \text{(R12.3-41)}$$

$\gamma_e \sim 2$ $\boxed{\gamma_e = 2.28}$

Step 6.   Calculate K_R and X from Equations (R12.3-49) and (R12.3-51)

$$X = 1 - \exp\left[-\frac{K_R k_{cat} h}{u_b}\right]$$

where

$$K_R = \gamma_b + \cfrac{1}{\cfrac{k_{cat}}{K_{bc}} + \cfrac{1}{\cfrac{1}{\cfrac{1}{\gamma_e} + \cfrac{k_{cat}}{K_{ce}}} + \gamma_c}} \qquad \text{(R12.3-49)}$$

$$K_R = 0.01 + \cfrac{1}{\cfrac{0.0858/s}{4.92/s} + \cfrac{1}{\cfrac{1}{\cfrac{1}{2.28} + \cfrac{0.0858/s}{3.0/s}} + .187}}$$

$K_R \sim 2$

$$K_R = 0.01 + \cfrac{1}{0.0174 + \cfrac{1}{.187 + 2.14}} = 2.23$$

$$\boxed{K_R = 2.23}$$

$$ln\left(\frac{1}{1-X}\right) = k_{cat} K_R t$$

$$= k_{cat} K_R \frac{h}{u_b}$$

Solving for X

$$X = 1 - \exp\left[-\frac{(2.23)(0.0858 \ s^{-1})(63.2 \ cm)}{55.6 \ cm/s}\right]$$

$$X = 0.20$$

This is close to the observed value of 22% conversion.

R12.3.6   Limiting Situations

As engineers, it is important to deduce how a bed will operate if one were to change operating conditions such as gas flow rate or catalyst particle size. To give

CD-Ch12FluidizedBed.doc

some general guides as to how changes will affect bed behavior, we shall consider the two limiting circumstances of reaction control and transport control.

In the K-L bubbling bed model, reaction occurs within the three phases of the bed, and material is continuously transferred between the phases. Two limiting situations thus arise. In one, the interphase transport is relatively fast, and transport equilibrium is maintained, causing the system performance to be controlled by the rate of reaction. In the other, the reaction rate is relatively fast, and the performance is controlled by interphase transport between the bubbles, clouds, and emulsions. It will be shown that the ammonia oxidation example used earlier is essentially a reaction-limited system.

The overall reaction rate in the bed is proportional to K_R, so the reciprocal of K_R can be viewed as an overall resistance to the reaction. The different terms and groups on the right-hand side of Equation (R12.3-49) can be viewed as individual resistances,zs which can be arranged in series or parallel to give the overall resistance.

$$R_0 = \frac{1}{K_R} = \cfrac{1}{\cfrac{1}{\cfrac{1}{\gamma_b}} + \cfrac{k_{cat}}{K_{bc} + \cfrac{1}{\cfrac{1}{\cfrac{1}{\gamma_c}} + \cfrac{1}{\cfrac{1}{\gamma_e} + \cfrac{k_{cat}}{K_{ce}}}}}} \tag{R12.3-55}$$

$$R_0 = \cfrac{1}{\cfrac{1}{R_{rb}} + \cfrac{1}{R_{tbc} + \cfrac{1}{\cfrac{1}{R_{rc}} + \cfrac{1}{R_{re} + R_{tce}}}}} \tag{R12.3-56}$$

in which:

$R_{rb} = \dfrac{1}{\gamma_b}$ = Resistance to reaction in the bubble

$R_{tbc} = \dfrac{k_{cat}}{K_{bc}}$ = Resistance to transfer between bubble and cloud

$R_{rc} = \dfrac{1}{\gamma_c}$ = Resistance to reaction in cloud

$R_{re} = \dfrac{1}{\gamma_e}$ = Resistance to reaction in the emulsion

$R_{tce} = \dfrac{k_{cat}}{K_{ce}}$ = Resistance to transfer between cloud and emulsion

CD-Ch12FluidizedBed.doc

Example R12-3 Calculation of Resistances

Calculate each of the resistances to reaction and transfer, and the relationship between C_{Ab}, C_{Ac} and C_{Ae} for the ammonia oxidation reaction described in Example R12-2. Assume $\gamma_b = 0.01$.

Solution

$$R_{rb} = \frac{1}{\gamma_b} = \frac{1}{0.01} = 100$$

$$R_{tbc} = \frac{k_{cat}}{K_{bc}} = \frac{0.0858}{4.92} = 0.0174$$

$$R_{re} = \frac{1}{\gamma_e} = \frac{1}{2.28} = 0.439$$

$$R_{rc} = \frac{1}{\gamma_c} = \frac{1}{0.187} = 5.35$$

$$R_{tcb} = \frac{k_{cat}}{K_{ce}} = \frac{0.0858}{3.0} = 0.0286$$

To relate C_{Ae} and C_{Ac}, we rearrange Equation (R12-67) for a first-order reaction as

$$C_{Ae} = \left(\frac{K_{ce}}{\gamma_e + k_{cat} + K_{ce}}\right) C_{Ac} = \frac{3.00}{(2.28)(0.0858) + 3.00} C_{Ac}$$

$$C_{Ae} = 0.939 \, C_{Ac}$$

The analog electrical resistance for the system is shown in Figure R12.3-10 along with the corresponding resistances for this reaction. As with its electrical analog, the reaction will pursue the path of least resistance, which in this case is along the right hand-side branch of Figure R12.3-10. If the major resistance in this side, the resistance to reaction in the emulsion R_{re}, could be reduced, a greater conversion could be achieved for a specific catalyst weight. To reduce R_{re}, one needs to look for ways of increasing γ_e.
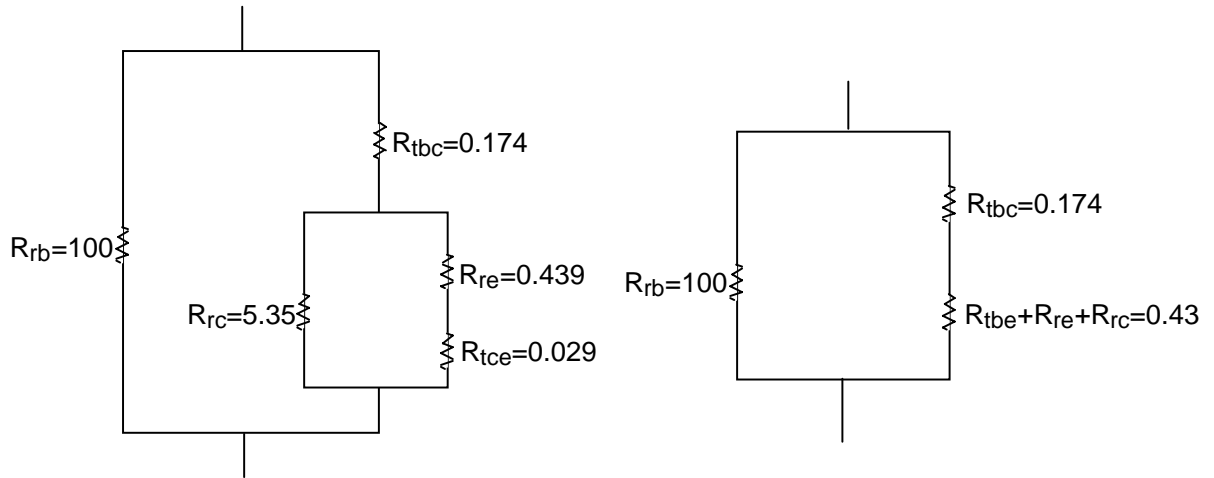
CD-Ch12FluidizedBed.doc

Electrical Analog

$R_{tbc}=0.174$

$R_{rb}=100$

$R_{rc}=5.35$

$R_{re}=0.439$

$R_{tce}=0.029$

$R_{tbc}=0.174$

$R_{rb}=100$

$R_{tbe}+R_{re}+R_{rc}=0.43$

Figure R12.3-10 Electrical analog.

$$\gamma_e = \left(1 - \varepsilon_{mf}\right)\left[\frac{1-\delta}{\delta} - \frac{3u_{mf}/\varepsilon_{mf}}{\left(0.71\, d_b g\right)^{1/2} - \left(u_{mf}/\varepsilon_{mf}\right)} - \alpha\right] \qquad (R12.3\text{-}57)$$

Examination of Equation (R12.3-57) shows that decreasing the bubble fraction, δ, and the minimum fluidization velocity would increase γ_e and hence the conversion. The minimum fluidization velocity could be decreased by decreasing the particle size. We now will investigate how the various parameters will affect the conversion for different limiting situations.

R12.3.6A   The Slow Reaction

In addition to the obvious way of increasing the temperature to increase the conversion, and perhaps some unwanted side reactions, there are other ways the conversion may be increased when the reaction is slow. From Equation (R12.3-31) we know the conversion depends upon h, k_{cat}, u_b, and K_R. We will first determine K_R under this situation. For a slow reaction, k_{cat} is small when compared to K_{bc} and K_{ce} so that resistance to transport is essentially zero, that is,

$$\frac{k_{cat}}{K_{bc}} \approx 0 \qquad (R12.3\text{-}58)$$

and

$$\frac{k_{cat}}{K_{ce}} \approx 0 \qquad (R12.3\text{-}59)$$

then

$$K_R = \gamma_b + \cfrac{1}{0 + \cfrac{1}{\gamma_c + \cfrac{1}{\cfrac{1}{\gamma_e} + 0}}} = \gamma_b + \gamma_c + \gamma_e \qquad (R12.3\text{-}60)$$

R12-35

Using Equation (R12-64) to substitute for γ_e, we have

$$K_R = \gamma_b + \left(1 - \varepsilon_{mf}\right)\left(\frac{1-\delta}{\delta}\right) \qquad \text{(R12.3-61)}$$

neglecting γ_b, with respect of the second term yields

$$K_R = \left(1 - \varepsilon_{mf}\right)\left(\frac{1-\delta}{\delta}\right) \qquad \text{(R12.3-62)}$$

Consequently, we see that K_R can be increased by decreasing δ the volume fraction of bubbles. For the ammonia oxidation example, this would give

$$K_R \approx 2.47$$

or about 11% higher than the value obtained by the more elaborate calculations which included the transport. This would predict a conversion of 21.4%, very close to the 20% given by the method which includes the transport limitations. Thus the ammonia oxidation system of Massimilla and Johnstone is essentially a reaction-limited system. The conversion and catalyst weight are related by

$$W = A_c h\rho_c\left(1 - \varepsilon_{mf}\right)\left(1 - \delta\right) = \frac{A_c u_b \rho_c \left(1 - \varepsilon_{mf}\right)\left(1 - \delta\right)}{k_{cat}K_R} \ln\frac{1}{1-X} \qquad \text{(R12.3-63)}$$

Substituting for K_R,

$$W = \frac{A_c \rho_c u_b \delta}{k_{cat}} \ln\left(\frac{1}{1-X}\right) \qquad \text{(R12.3-64)}$$

Recalling Equation (R12.3-23),

$$\delta = \frac{u_o - u_{mf}}{u_b - u_{mf}\left(1+\alpha\right)} \qquad \text{(R12.3-23)}$$

In almost all instances, u_b is significantly greater than $u_{mf}(1+\alpha)$ so that Equation (R12.3-45) is approximately

$$\delta = \frac{u_0 - u_{mf}}{u_b} \qquad \text{(R12.3-65)}$$

Combining Equations (R12.3-64) and (R12.3-65) gives

Approximate catalyst weight for slow reactions

$$\boxed{W = \frac{A_c \rho_c \left(u_o - u_{mf}\right)}{k_{cat}} \ln\frac{1}{1-X}} \qquad \text{(R12.3-66)}$$

Therefore one observes that to reduce the catalyst weight for a specified conversion, u_0 and u_{mf} should be as close as possible. One can now ask in what ways the catalyst

"What if . . ." questions

weight may be reduced for a specified conversion. The answer to this question is the

CD-Ch12FluidizedBed.doc

same as to the question, "How may one increase the conversion for a fixed catalyst weight?"

Example R12-4 Effect of Particle Size on Catalyst Weight for a Slow Reaction

Suppose you are operating at five times the minimum fluidization velocity, $u_0 = 5u_{mf}$. What would be the effect of doubling the particle diameter on the catalyst weight for the same throughput and conversion?

Solution

Substitution for u_0, into Equation (R12.3-66) gives

Case 1
$$W_1 = \frac{A_c \rho_c \, 4u_{mf1}}{k_{cat1}} \ln \frac{1}{1-X_1} \qquad \text{(RE12-7.1)}$$

Case 2
$$W_2 = \frac{\rho_c A_c \left(u_{o2} - u_{mf2}\right)}{k_{cat2}} \ln \frac{1}{1-X_2} \qquad \text{(RE12-7.2)}$$

Since the temperature remains constant and there are no inter- and intra-particle resistances, $k_{cat1} = k_{cat2}$, the throughput ($u_{01} = u_{02}$), and conversion ($X_1 = X_2$) are the same for Cases 1 and 2. The ratio of Equation (E4-1) and (E4-2) yields

$$\frac{W_2}{W_1} = \frac{u_{o1} - u_{mf2}}{4u_{mf1}} = \frac{5u_{mf1} - u_{mf2}}{4u_{mf1}} \qquad \text{(RE12-7.3)}$$

Recalling Equation (R12.3-5),

$$u_{mf} = \frac{(\psi d_p)^2}{150\mu} \underbrace{\left[g(\rho_c - \rho_g)\right]}_{\eta} \frac{\varepsilon_{mf}^3}{1 - \varepsilon_{mf}} \qquad \text{(R12.3-5)}$$

and neglecting the dependence of ε_{mf} on d_p we see that the only parameters that vary between Case 1 (d_p) and Case 2 ($d_{p2} = 2d_{p1}$) are u_{mf} and W. Taking the ratio of u_{mf2} to u_{mf1} and substituting for d_{p2} in terms of d_{p1} we obtain

$$\frac{u_{mf2}}{u_{mf1}} = \left(\frac{d_{p2}}{d_{p1}}\right)^2 = \left(\frac{2d_{p1}}{d_{p1}}\right)^2 = 4 \qquad \text{(RE12-7.4)}$$

and therefore

$$\frac{W_2}{W_1} = \frac{5u_{mf1} - 4u_{mf1}}{4u_{mf1}} = 0.25 \qquad \text{(RE12-7.5)}$$

CD-Ch12FluidizedBed.doc

Thus in the situation we have postulated, with a first-order reaction and reaction limiting the bed behavior, doubling the particle size will reduce the catalyst by approximately 75% and still maintain the same conversion.

R12.3.6B   The Rapid Reaction

To analyze this limiting situation, we shall assume the particles are sufficiently small so that the effectiveness factor is essentially one and that the rate of transfer from the bulk fluid to the individual catalyst particles is rapid in comparison with the rate of transfer between the fluidization phases. For the case of rapid reaction,

$$\frac{k_{cat}}{K_{bc}} \text{ and } \frac{k_{cat}}{K_{ce}} >> 1$$

Using these approximations in the equation for K_R, which is

$$K_R = \gamma_b + \cfrac{1}{\cfrac{k_{cat}}{K_{cb}} + \cfrac{1}{\gamma_c + \cfrac{1}{\cfrac{k_{cat}}{K_{ce}} + \cfrac{1}{\gamma_e}}}}$$

one observes the first term to be neglected is γ_b, and we also note that because the reaction is rapid k_{cat}/K_{ce} is a large number.

$$K_R = \cfrac{1}{\cfrac{k_{cat}}{K_{ce}} + \cfrac{1}{\gamma_c + \cfrac{1}{(\text{Large No. })+ \cfrac{1}{\gamma_e}}}}$$

Then neglecting the reciprocal of γ_e with respect to k_{cat}/K_{cb}, K_R becomes

$$K_R = \gamma_b + \cfrac{1}{\cfrac{k_{cat}}{K_{cb}} + \cfrac{1}{\gamma_c}} \approx \gamma_b + \frac{K_{cb}}{k_{cat}} \qquad (R12.3\text{-}67)$$

There are two situations one can analyze here

Situation 1: $\quad \gamma_b << \dfrac{K_{bc}}{k_{cat}}$ Resistance to transport small wrt resistance to reaction inside the bubble

Situation 2: $\quad \gamma_b >> \dfrac{K_{bc}}{k_{cat}}$ Resistance to transport large wrt resistance to reaction inside the bubble

CD-Ch12FluidizedBed.doc

Only situation 1 will be analyzed in the text; the analysis of situation 2 is left as an exercise.

Assuming very few particles are present in the bubble phase

$$K_R \cong \frac{K_{bc}}{k_{cat}} \qquad \text{(R12.3-68)}$$

The catalyst weight is given by combining Equations (R12.3-54) and (R12.3-68)

$$W = \frac{A_c u_b \rho_c (1-\delta)(1-\varepsilon_{mf})}{K_{bc}} ln\left(\frac{1}{1-X}\right) \qquad \text{(R12.3-69)}$$

Neglecting δ with respect to 1 in the numerator

Approximate catalyst rate for a rapid reaction

$$W = \frac{A_c u_b \rho_p (1-\varepsilon_{mf})}{k_{cat} K_{bc}} ln\left(\frac{1}{1-X}\right) \qquad \text{(R12.3-70)}$$

On observing that the equation for K_{bc}, Equation (R12.3-30), is the sum of two terms A_0 and B_0

$$K_{bc} = 4.5\left(\frac{u_{mf}}{d_b}\right) + 5.85\left(\frac{D_{AB}^{1/2} g^{1/4}}{d_b^{5/4}}\right) \qquad \text{(R12.3-30)}$$

$$K_{bc} = A_0 + B_0$$

one finds the problem can be further divided.

Case A: $\qquad\qquad A_0 \gg B_0$

Case B: $\qquad\qquad B_0 \gg A_0$

Only Case A will be considered here; Case B again will be left as an exercise.

For Case A

$$K_{bc} \cong 4.5\frac{u_{mf}}{d_b} \qquad \text{(R12.3-71)}$$

Then

$$W = \frac{u_b d_b}{4.5 u_{mf}} \rho_c A_c \left(1-\varepsilon_{mf}\right) ln\left(\frac{1}{1-X}\right) \qquad \text{(R12.3-72)}$$

Recalling the equation for u_b and neglecting other terms in the equation with respect to the velocity of rise of a single bubble, that is,

$$u_b \approx u_{br}$$

and

CD-Ch12FluidizedBed.doc

$$u_{br} = 0.71g^{1/2}d_b^{1/2}$$

$$W = \frac{0.71g^{1/2}d_b^{3/2}}{4.5u_{mf}} A_c\rho_c\left(1 - \varepsilon_{mf}\right)\ln\left(\frac{1}{1-X}\right)$$

$$W = 4.9\frac{d_b^{3/2}}{u_{mf}} A_c\rho_c\left(1 - \varepsilon_{mf}\right)\ln\left(\frac{1}{1-X}\right) \tag{R12.3-73}$$

The average bubble diameter is a function of the tower diameter (thus the tower cross-sectional area A_c), height, u_0, and u_{mf}. As a first approximation, we assume the average bubble diameter is some fraction, (say 0.75) of the maximum bubble diameter.

$$d_b = 0.75 \, d_{bm} \tag{R12.3-74}$$

Then, from Equation (R12.3-16), we have

$$d_{bm} = (0.75)(0.652)\left[A_c\left(u_o - u_{mf}\right)\right]^{0.4} \tag{R12.3-75}$$

which is substituted into Equation (R12.3-73) to give

$$\boxed{\text{One Approximation for fast reactions}}$$

$$W = 1.69\frac{A_c^{1.6}\left(u_o - u_{mf}\right)^{0.6}}{u_{mf}}\rho_c\left(1 - \varepsilon_{mf}\right)\ln\left(\frac{1}{1-X}\right) \tag{R12.3-76}$$

Example R12-5 Effect of Catalyst Weight on Particle Size for a Rapid Reaction

We again consider the effect of doubling particle size while keeping all other variables the same. Case 1: $d_{p1} = d_{p1}$, Case 2: $d_{p2} = 2\,d_{p1}$.

Solution

Using Equation (R12.3-76) and taking the ratio of Case 1 to Case 2

$$\frac{W_2}{W_1} = \frac{\left(u_{02} - u_{mf2}\right)^{0.6}}{\left(u_{01} - u_{mf1}\right)^{0.6}}\frac{u_{mf1}}{u_{mf2}} \tag{RE12-6.1}$$

Recalling from previous examples

$$u_{o2} = u_{o1} = 5u_{mf1}$$

$$u_{mf2} = 4u_{mf1}$$

then

$$\frac{W_2}{W_1} = \left(\frac{5u_{mf1} - 4u_{mf1}}{5u_{mf1} - u_{mf1}}\right)^{0.6}\frac{u_{mf1}}{4u_{mf1}} = \left(\frac{1}{4}\right)^{0.6}\frac{1}{4} \tag{RE12-6.2}$$

or

R12-40

$$\frac{W_2}{W_1} = 0.11 \qquad\qquad \text{(RE12-6.3)}$$

In this case, we see that doubling the particle diameter decreases the catalyst weight by 89% while maintaining the same conversion. However, for a fast reaction, a significant decrease in effectiveness factor could offset this advantage.

SUMMARY

1. Minimum fluidization velocity

$$u_{mf} = \frac{(\psi d_p)^2 \, \eta \, \varepsilon_{mf}^3}{150 \, \mu \, (1 - \varepsilon_{mf})}$$

(S12.3-1)

2. Porosity at minimum fluidization

$$\varepsilon_{mf} = \frac{0.586}{\psi^{0.72}} \left[\frac{\mu^2}{\rho_g \, \eta \, d_p^3} \right]^{0.029} \left[\frac{\rho_g}{\rho_c} \right]^{0.021}$$

(S12.3-2)

or

$$\varepsilon_{mf} = \frac{0.415}{\psi^{0.33}}$$

(S12.3-3)

3. Bubble size

$$d_b = d_{bm} - (d_{bm} - d_{bo}) e^{-0.3 \, h/D_t}$$

(S12.3-4)

where

$$d_{bm} = 0.652 \left[A_c (u_o - u_{mf}) \right]^{0.4}, \ cm$$

(S12.3-5)

For porous plates

$$d_{b0} = 0.00376 (u_o - u_{mf})^2, \ cm$$

(S12.3-6)

4. Velocity of bubble rise

$$u_b = u_0 - u_{mf} + 0.71 (g d_b)^{1/2}$$

(S12.3-7)

5. Bed height - conversion in first order reaction

$$h = \frac{u_b}{k_{cat} K_R} \ ln \ \frac{1}{1 - X}$$

(S12.3-8)

$$K_R = \gamma_b + \cfrac{1}{\cfrac{k_{cat}}{k_{bc}} + \cfrac{1}{\gamma_c + \cfrac{1}{\cfrac{1}{\gamma_e} + \cfrac{k_{cat}}{K_{ce}}}}}$$

(S12.3-9)

6. Mass Transfer Parameters

    a. Between the bubble and the cloud

$$K_{bc} = 4.5 \left[\frac{u_{mf}}{d_b} \right] + 5.85 \frac{D^{1/2} g^{1/4}}{d_b^{5/4}}$$

(S12.3-10)

    b. Between the cloud and the emulsion

CD-Ch12FluidizedBed.doc

$$K_{ce} = 6.78\left[\frac{\varepsilon_{mf}\,D\,u_b}{d_b^3}\right]^{1/2}$$

(S12.3-11)

7. The reaction rate parameters

$$k_{cat} = \rho_p k$$

(S12.3-12)

a. Bubble

$$0.001 < \gamma_b < 0.01$$

(S12.3-13)

b. Cloud

$$\gamma_c = \left(1 - \varepsilon_{mf}\right)\left[\frac{3\left(u_{mf}/\varepsilon_{mf}\right)}{u_{br} - \dfrac{u_{mf}}{\varepsilon_{mf}}} + \alpha\right]$$

(S12.3-14)

c. Emulsion

$$\gamma_e = \left(1 - \varepsilon_{mf}\right)\frac{(1-\delta)}{\delta} - \gamma_c$$

(S12.3-15)

$$\delta = \frac{u_0 - u_{mf}}{u_b - u_{mf}\left(1+\alpha\right)}$$

(S12.3-16)

where α is given by Figure 12.3-5.

8. Procedure

See flow chart in Figure R12.3-9.

Supplementary Reading

1.   Anonymous, *Chem. Eng. Prog.*, <u>53</u> (10), 50 (1957).

2.   Blanding, F. H., *Ind. Eng. Chem.*, <u>45</u>, 1186 (1953).

3.   Carlsmith, L. E., and F. B. Johnson, *Ind. Eng. Chem.*, <u>37</u>, 451 (1945).

4.   Davidson, J. F., and D. L. Keairns, *Fluidization*. Proceedings of the Second Engineering Foundation Conference, Cambridge: Cambridge University Press, 1978.

5.   Grace, J. R., and J. M. Matsen, *Fluidization*. New York: Plenum Press, 1980.

6.   Keavins, D. L., ed. *Fluidization Technology*, vol. I and II. Washington, D.C.: Hemisphere Publishing Co. in association with McGraw-Hill I(1975), II(1976).

7.   Kunii, D., and O. Levenspiel, *Ind. Eng. Chem. Process Design Devel.*, <u>7</u>, 481 (1968).

8.   Kunii, D., and O. Levenspiel, *Fluidization Engineering*, 2nd Ed., (Boston: Butterworth, 1991).

9.   Mathur, R. B., and N. Epstein, *Spouted Beds*, (New York: Academic Press, 1974).

10.   Weekman, V. W., Jr., *Ind. Eng. Chem. Process Design Devel.* <u>7</u>, 91 (1968).

11.   Wen, C. Y., and Y. H. Yu, *AIChE J.*, <u>12</u>, 610 (1966).

12.   Zenz, F. A., *Ind. Eng. Chem. Fund.*, <u>3</u>, 65 (1964).

13.   Zenz, F. A., *Ind. Chem. E. Symposium Series*, No. 30, 136 (1968).

14.   Zenz, F. A., and N. A. Weil, *AIChE J.*, <u>4</u>, 472 (1958).

Multiphase reactors

Slurry reactors

The catalytic reaction can also be carried out in two–phase or three –phase stirred tank reactors also known as slurry reactors. In three –phase reactor, gas and liquid reactants are brought into contact with solid catalyst particles. In two–phase reactor, fluid phase is usually liquid reactant in contact with the solid catalyst. The reaction of gaseous reactant with catalyst is usually carried out in fixed bed reactor. In three –phase slurry reactor the gaseous reactant and solid catalysts are dispersed in continuous liquid phase by mechanical agitation using stirrer. The efficient stirring ensures nearly uniform composition throughout the reactor. This kind of reactor is used in hydrogenation, oxidation, halogenations and fermentation process. The advantages include nearly isothermal operation and good heat and mass transfers. The use of powder catalysts having high activity minimizes the intraparticle diffusion limitation. The reactors can be operated in batch, semi batch or continuous mode. In three – phase system bubbles of gas rise through agitated slurry. Solid particles are in size range of 0.01to 1.0 mm. The solid concentration can be up to 30 vol. %. Lower concentration is also used. In hydrogenation of oil with nickel catalyst, the solid content is 0.5 vol. %. The external transport effects are important in slurry reactors and details are discussed in lecture no. 30. Hydrogenation of oils is carried out in slurry of nickel catalyst particles. Industrial hydrogenation reactors are usually of the size in the range of 500-200 L. The reactors are operated up to pressure of 200 atm and temperature of 350°C. The reactors are equipped with internal agitator, gas inlet, facility for insitu sampling and heater or cooler for temperature control.
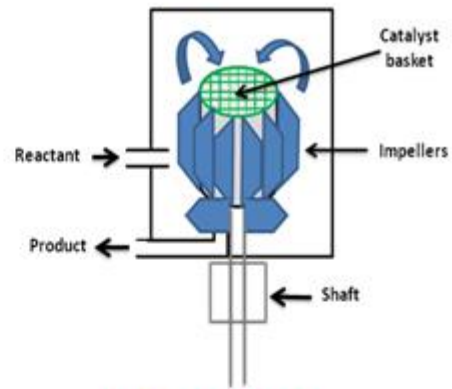
Trickled bed reactors

In trickled bed reactor gaseous and liquid reactants flow co-currently downward over a packed bed of solid catalyst particles. The liquid is distributed across the reactor cross section by a distributor plate. The gas enters at the top and distributed along with the liquid. The liquid flows downward by gravity and drag of the gas. For low liquid flow rates and low to moderate gas flow rates, the gas phase is continuous with liquid trickling down forming film over the solid catalyst. The thickness of the liquid film has been estimated to vary between 0.01 and 0.2 mm. This flow regime is known as a trickle flow regime. The fluid approaches plug flow leading to higher conversion than slurry reactors

for the same reactor volume. Other advantages include ease of installation, minimal catalyst handling and low catalyst attrition as in packed bed reactor. Disadvantages include maldistribution of flow resulting in channeling or bypassing, possibility of non uniformity in packing, incomplete contacting or wetting and intraparticle diffusion resistance. Catalyst bed depth is limited by pressure drop, catalyst crush strength and maximum adiabatic temperature increase for stable operation. The reactor length to diameter ratio can vary between 1 and 10 depending on the allowable pressure drop. Other parameters important for trickled bed include void fraction of bed, holdup for phases, wetting efficiency (fraction of catalyst wetted by liquid), gas – liquid mass transfer coefficient, liquid–solid mass transfer coefficient, liquid and gas mixing, pressure drop and heat transfer coefficients. The wetting efficiency of the catalyst is important for reaction rate and increases with increasing liquid rate. The trickle bed reactor is most commonly used for hydrogenation and hydrodesulfurization reactions.

In trickled bed reactor gaseous and liquid reactants flow co-currently downward over a packed bed of solid catalyst particles. The liquid is distributed across the reactor cross section by a distributor plate. The gas enters at the top and distributed along with the liquid. The liquid flows downward by gravity and drag of the gas. For low liquid flow rates and low to moderate gas flow rates, the gas phase is continuous with liquid trickling down forming film over the solid catalyst. The thickness of the liquid film has been estimated to vary between 0.01 and 0.2 mm. This flow regime is known as a trickle flow regime. The fluid approaches plug flow leading to higher conversion than slurry reactors for the same reactor volume. Other advantages include ease of installation, minimal catalyst handling and low catalyst attrition as in packed bed reactor. Disadvantages include maldistribution of flow resulting in channeling or bypassing, possibility of non uniformity in packing, incomplete contacting or wetting and intraparticle diffusion resistance. Catalyst bed depth is limited by pressure drop, catalyst crush strength and maximum adiabatic temperature increase for stable operation. The reactor length to diameter ratio can vary between 1 and 10 depending on the allowable pressure drop. Other parameters important for trickled bed include void fraction of bed, holdup for phases, wetting efficiency (fraction of catalyst wetted by liquid), gas – liquid mass transfer coefficient, liquid–solid mass transfer coefficient, liquid and gas mixing, pressure drop and heat transfer coefficients. The wetting efficiency of the catalyst is important for reaction rate and increases with increasing liquid rate. The trickle bed reactor is most commonly used for hydrogenation and hydrodesulfurization reactions.
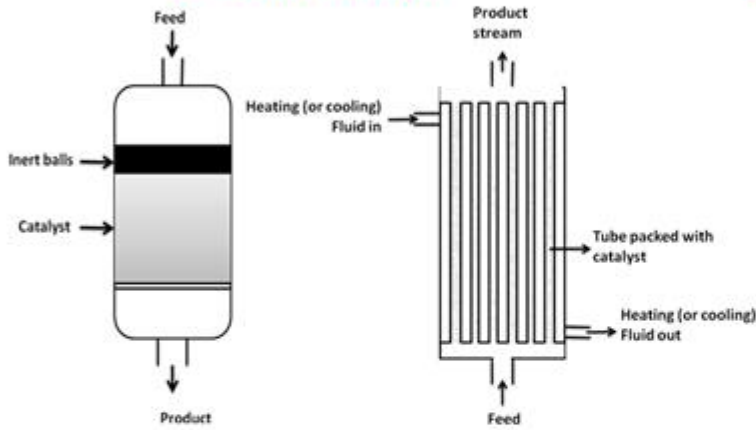
Bioreactors

In bioreactor live cells or enzymes are used as catalyst to perform the biochemical reactions. Bioreactor operations are limited by the conditions favorable for the biological systems. Most living cells can tolerate only mild conditions of temperature and pH. Hence in bioreactors stringent control of temperature, pH or any contamination is needed. Bioreactor may have two phases, liquid-solid as in anaerobic process or three phases, gas, liquid and solid as in aerobic process. The solid phase typically contains the cells (bacteria, fungi, algae etc.) that serve as biocatalyst. The density of biocatalytic phase is close to water. The biocatalyst can also be used in immobilized form in which cells are trapped within solid or semi solid structure such as porous particles or gel. Liquid is primarily water with dissolves the feed and products. In aerobic bioreactor the gas phase consists of primarily air and product gas CO_2. Bioreactors are mainly operated in batch or semi batch mode allowing better control of process parameters. Increasing number of bioreactor is operated in continuous mode such as in wastewater treatment, lactic acid production, production of human insulin etc.
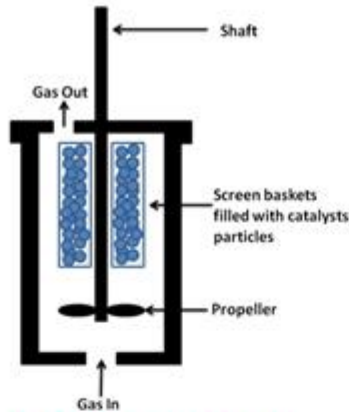
a) Carberry reactor

b) Berty reactor

c) Packed bed reactor

d) Multi tubular reactor
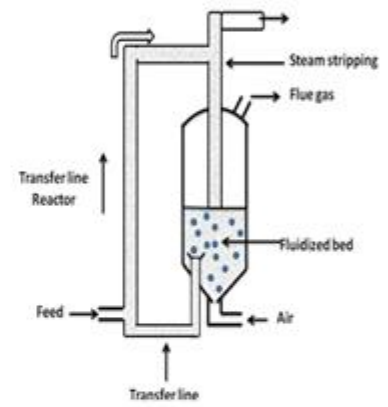
e) Fluidized bed reactor
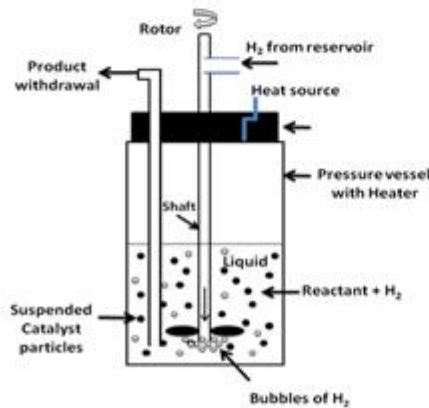
g) Agitated slurry reactor
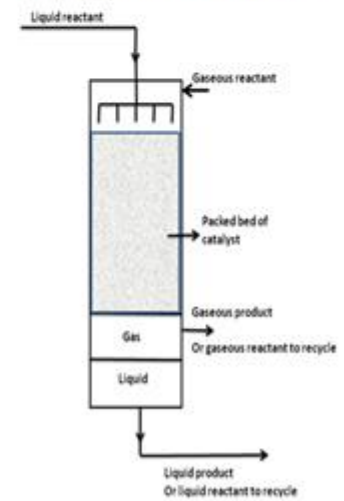
f) Trickled bed reactor

Fig. 1. Schematic diagram of different type of reactors

are $D_{eff} = 2 \times 10^{-5}$ cm²/s, $\lambda = 3 \times 10^{-4}$ cal/s cm°K. ΔT becomes 0.33°C.

If pores are filled with vapor, however, temperature differences in the hundreds of degrees are quite possible, because values of D_{eff} for vapors are 3 to 4 orders of magnitude greater than for solutes and gas phase concentrations are not lowered by as large a factor. The key limiting component will then usually be vaporized reactant rather than hydrogen. Representative conditions are as follows: $-\Delta H = 5 \times 10^4$ cal/mole (this is now per mole of vaporized reactant), $D_{eff} = 10^{-2}$ cm²/s, $c_s = 3 \times 10^{-5}$ g-mol/cm³, representing vaporized reactant present in small mole fraction but superatmospheric total pressure, and λ as before. ΔT becomes 50°C. This situation will not develop, of course, if the reactant does not have an appreciable vapor pressure.

If a reaction is substantially diffusion-limited when pores are filled with liquid reactant, then circumstances causing the pores to become instead filled with vaporized reactant can cause a marked increase in reaction rate, associated with the marked increase in diffusivity. This, of course, cannot happen if the reactant has insignificant vapor pressure. In an early study by Ware (1959) of the hydrogenation of benzene at 70° to 100°C and 7 to 34-atm pressure the rate varied by a factor of 5 to 10 depending upon the startup conditions. The higher rate was interpreted as a system in which pores were filled with benzene vapor and hydrogen and diffusion limitations were negligible; the lower rate was interpreted as involving diffusional resistance inside liquid-filled pores. More recently the same effect was reported by Sedricks and Kenney (1972, 1973) in a well-defined study of the hydrogenation of crotonaldehyde. In both cases, however, a highly exothermic and rapid reaction was being studied at a low liquid flow rate (about 0.15 kg/m² s in Ware's work and 0.045 kg/m² s in that of Sedricks and Kenney). Liquid phase reaction could presumably switch to vapor phase reaction at a critical value of the local liquid flow rate below which the heat evolved could no longer be carried away by the flowing liquid. This effect could interact with liquid flow to cause temperature instabilities in various ways. Germain et al. (1974) describe a cyclic and irregular performance of a trickle bed using countercurrent flow of gas against downflowing α-methyl styrene which was hydrogenated to cumene at liquid flow rates of 0.08 to 1.6 kg/m² s, but here the erratic behavior may have stemmed in substantial degree from the use of countercurrent flow which could have substantially altered the flow and mixing patterns from those obtained with concurrent trickle flow at the same gas and liquid flow rates. Quantitative analysis of coupling effects between heat release on catalyst pellets and dissipation to the flowing fluids might be very helpful in revealing possible causes of instabilities in trickle bed reactors in general.

4. MODELS FOR DESIGN AND ANALYSIS

4.1 The Ideal Trickle Bed Reactor

The analysis of trickle bed performance under ideal circumstances and assuming simple first-order kinetics provides a point of departure for analysis of real cases. We assume the following:

1. Plug flow of liquid, that is, no dispersion in the axial or radial direction.
2. No mass or heat transfer limitations between gas and liquid, between liquid and solid catalyst or inside catalyst particles. The liquid is saturated with gas at all times.

3. First-order isothermal, irreversible reaction with respect to the reactant in the liquid. Gaseous reactant present in great excess.
4. Catalyst pellets are completely bathed with liquid.
5. Reaction occurs only at the liquid-catalyst interface.
6. No vaporization or condensation occurs.

Consider a differential volume element across the reactor and set the rate of reaction in that element equal to the disappearance of reactant as the liquid passes through the element: Then

$$Fc_{in}dx = r\,dV \tag{21}$$

where c_{in} = concentration of reactant in entering liquid, moles/cm³

x = fractional conversion of reactant

dV = reactor volume in slice under consideration, cm³

If the reaction is first order,

$$r = k_v c(1 - \epsilon) \tag{22}$$

where $k_v = \dfrac{\text{cm}^3 \text{ of liquid}}{(\text{cm}^3 \text{ of cat. pellet vol.}) \, (\text{s})}$

Substituting Equation (22) in (21), we obtain

$$Fc_{in}dx = k_v(1 - \epsilon)\, c\,dV$$
$$c = c_{in}^{(1-x)}$$

resulting in

$$F \int \frac{dx}{x} = k_v(1 - \epsilon) \int dV$$

or

$$\ln \frac{c_{in}}{c_{out}} = \frac{V}{F} k_v(1 - \epsilon) = \frac{k_v(1 - \epsilon)}{L_v/h} = \frac{3600 k_v(1 - \epsilon)}{\text{LHSV}} \tag{23}$$

where V is the volume of the trickle bed packed with catalyst.

4.2 Comparison with Autoclave Measurements

If the same simplifying assumptions again hold, one should be able to obtain the same values of the reaction rate constant k_v from studies in a stirred autoclave. In the autoclave, one measures change in concentration with time, whereas in the trickle-bed reactor we have change in concentration with distance, but the autoclave and the trickle-bed reactor should give the same value of k_v because there is a one-to-one correlation between time in the autoclave and distance traversed in the trickle bed. (For a specified flow rate the distance traversed is inversely proportional to the dynamic liquid holdup, but it is unnecessary to know this in the ideal case—see Section 5.5). In the autoclave,

$$\frac{dc}{dt} = \frac{r(v_{cat} + v_{liq})}{v_{liq}} \tag{24}$$

Here r is moles/(s) (cm³ of liquid plus cm³ of catalyst in the autoclave)

v_{cat} = volume of catalyst pellets in autoclave, cm³
v_{liq} = volume of liquid in autoclave, cm³
t = time, s

Substituting Equation (22) in Equation (24), where $(1 - \epsilon)$ is now the volume fraction of solid catalyst in the liquid slurry in the autoclave,

$$\frac{dc}{dt} \frac{v_{liq}}{v_{cat}} = k_v c$$

Synopsis

- **Introduction to Slurry Reactors**

- **Types & Construction**

- **Operation and Working**

- **Start up and Shut down**

- **Trouble shooting**

- **Advantages & disadvantages**

- **Applications**

- **Incident**

What is Slurry ??

- Any mixture of solid liquid or a gas gas is called **slurry.**

- Sloppy mud, cement or mixture of additives in petrochemicals.

Slurry Reactors

- Slurry reactors are three-phase reactors, meaning they can be used to react solids, liquids, and gases simultaneously.

- They usually consist of a solids suspended in a liquid, through which a gas is bubbled. They can operate in either semi-batch or continuous mode.

SLURRY PHASE REACTOR

Source: Sasol Ltd.
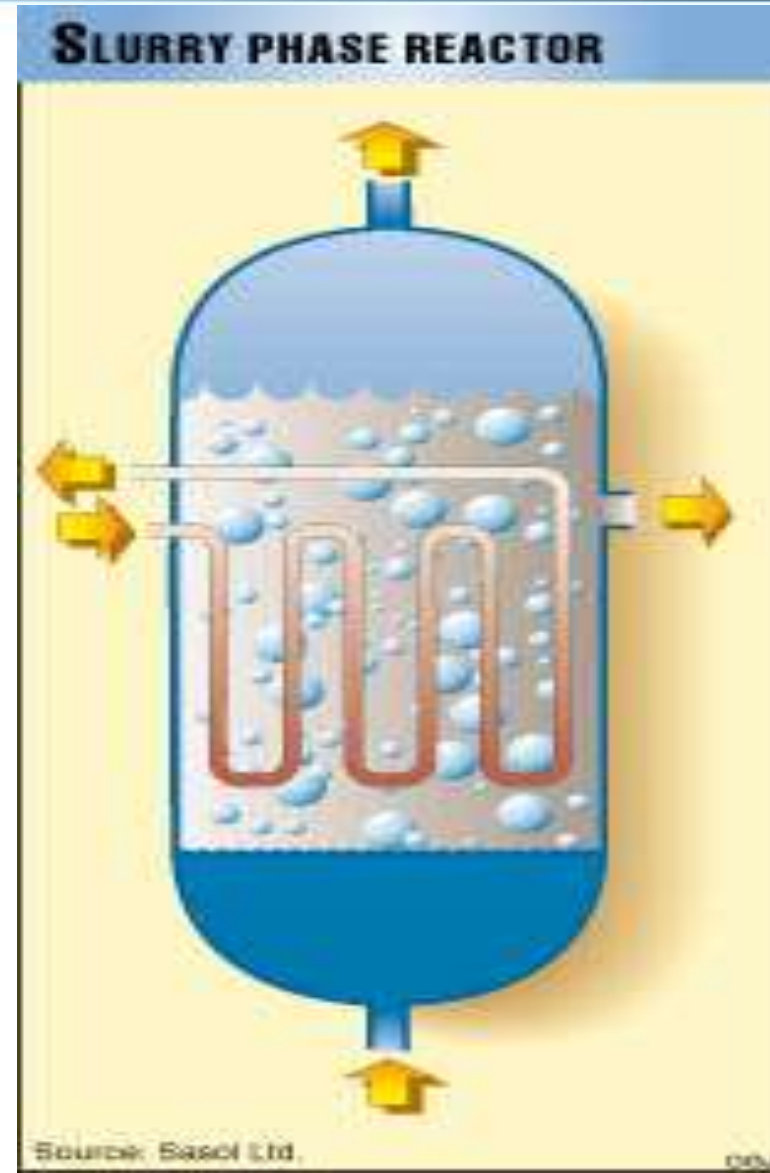
Types

- Types Of Slurry Reactors are :

- Bubble Column Reactor

- Fischer Tropsch Reactor

- Slurry Batch Reactor

Bubble Column Reactor
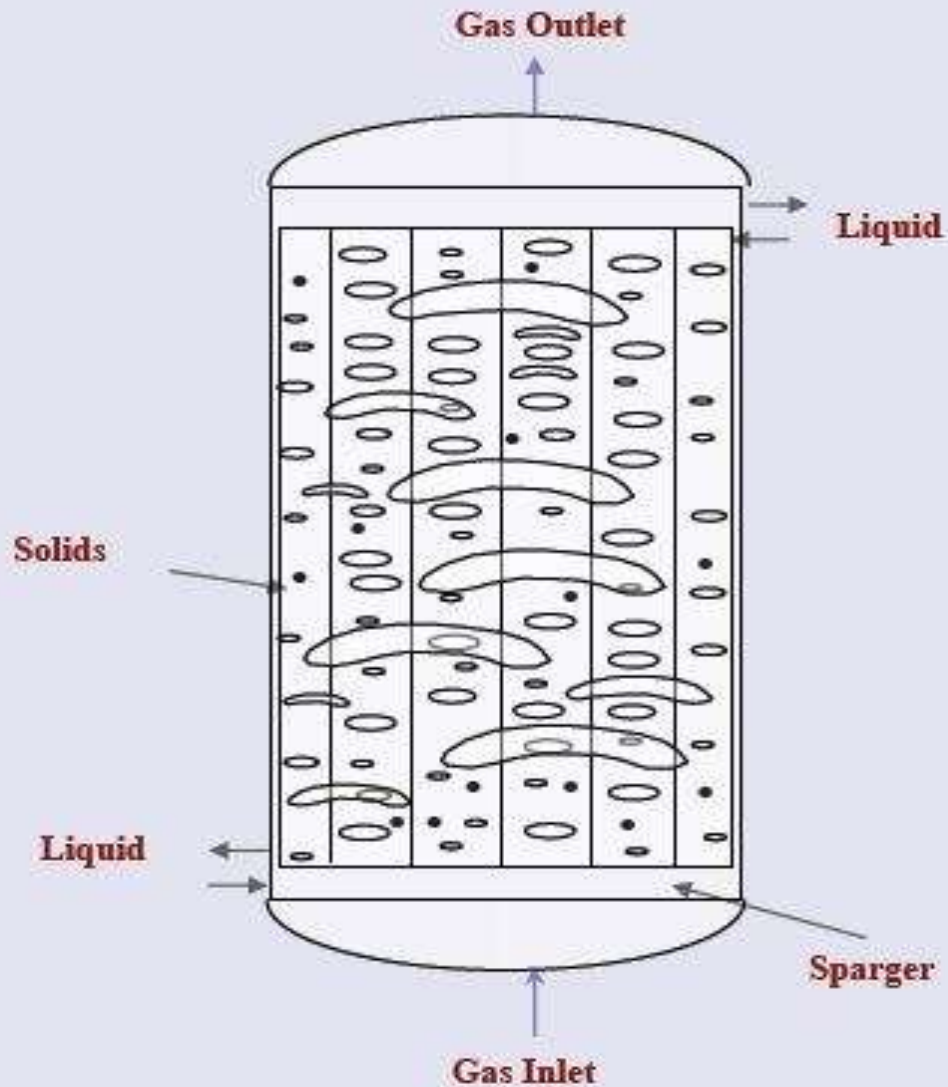
F-T Tubular Slurry Reactor
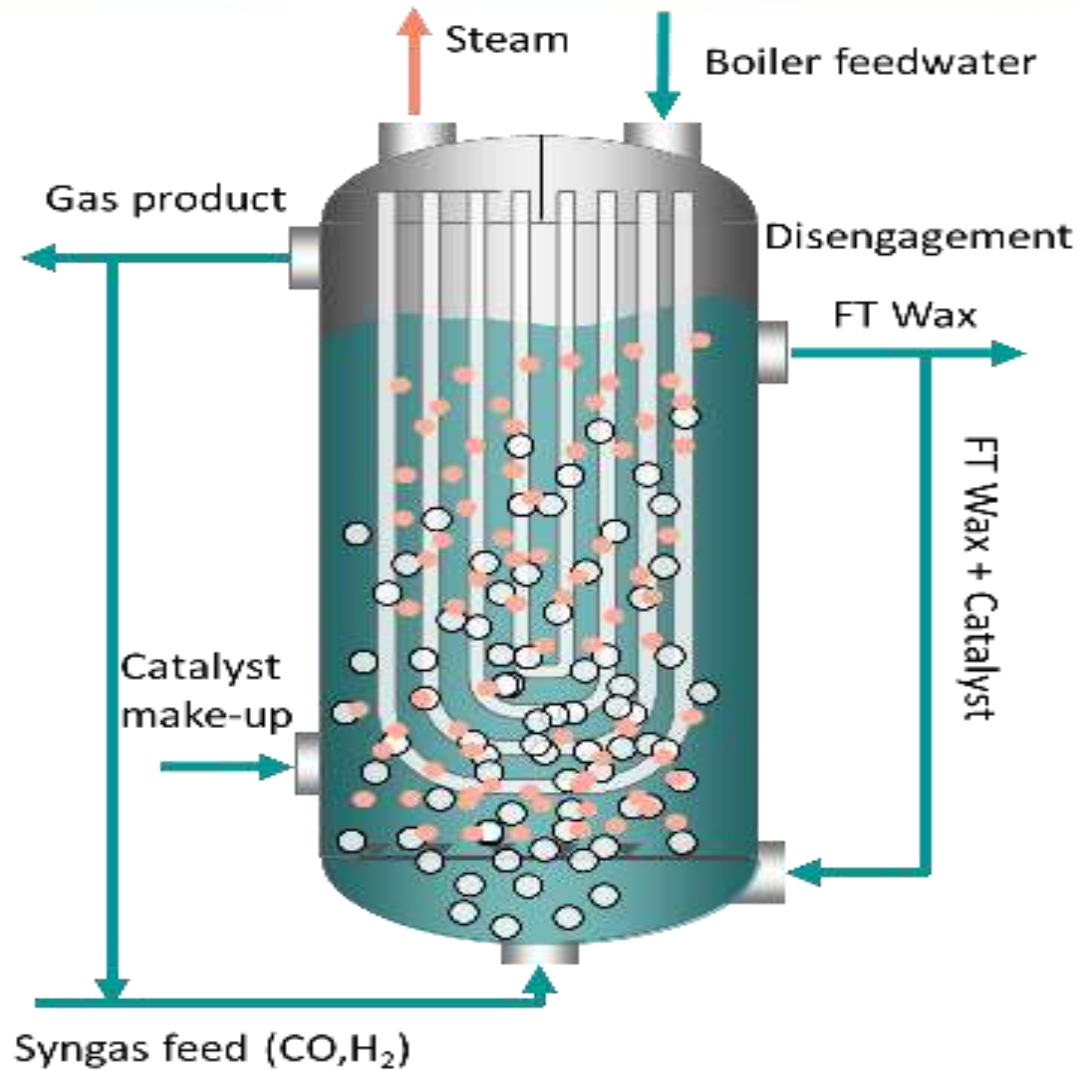
Slurry Batch Reactor for Hydrogenation
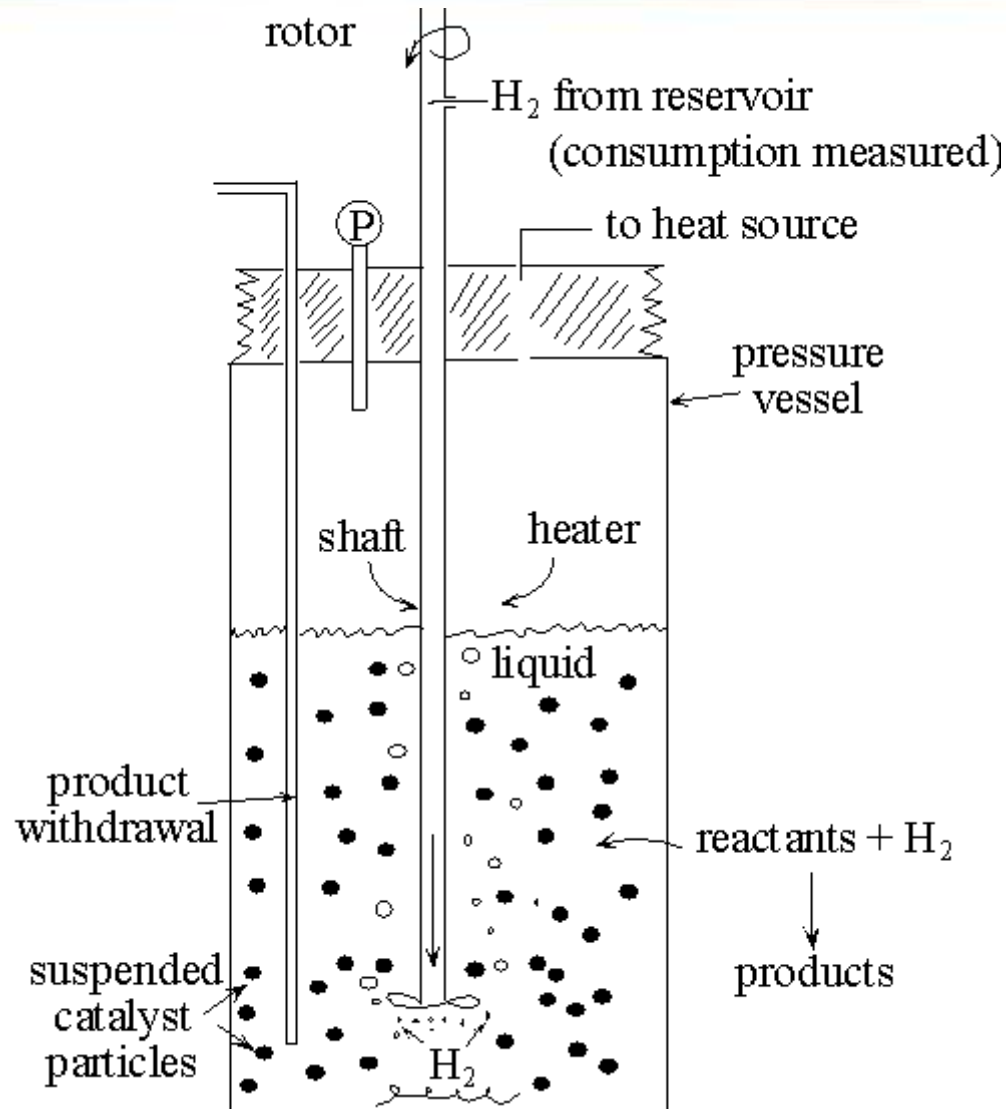
Construction

- **Reaction tank**

- Made of glass or steel.

- Hold Media and catalyst.

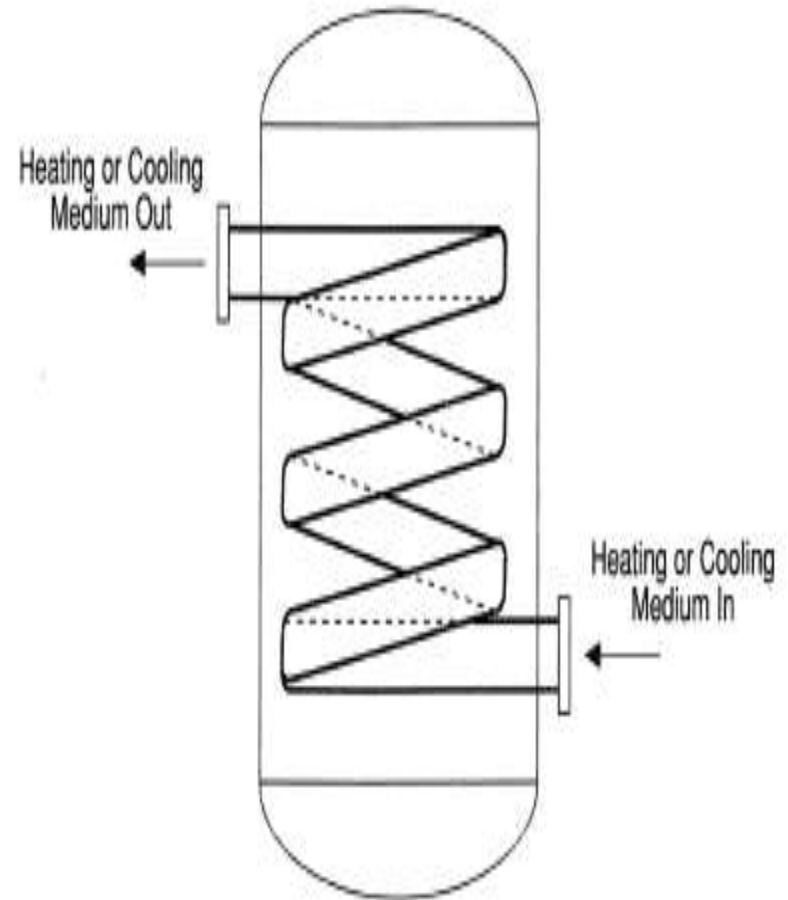- Additional parts are mounted on it.
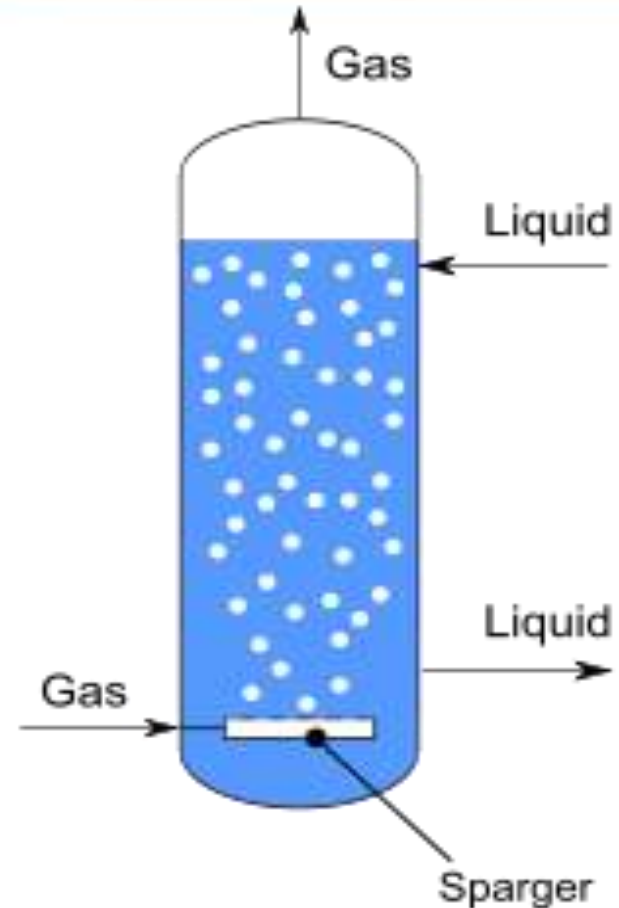
Construction

- **Sparger**
- Used to introduce air in reactor.
- Install at the bottom, consist of tube and holes for escape air and gases.
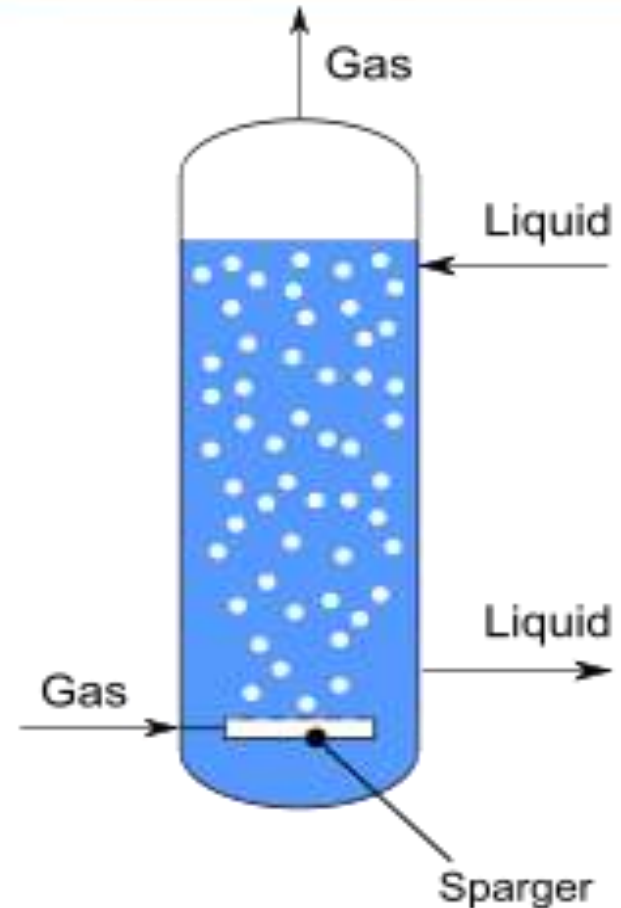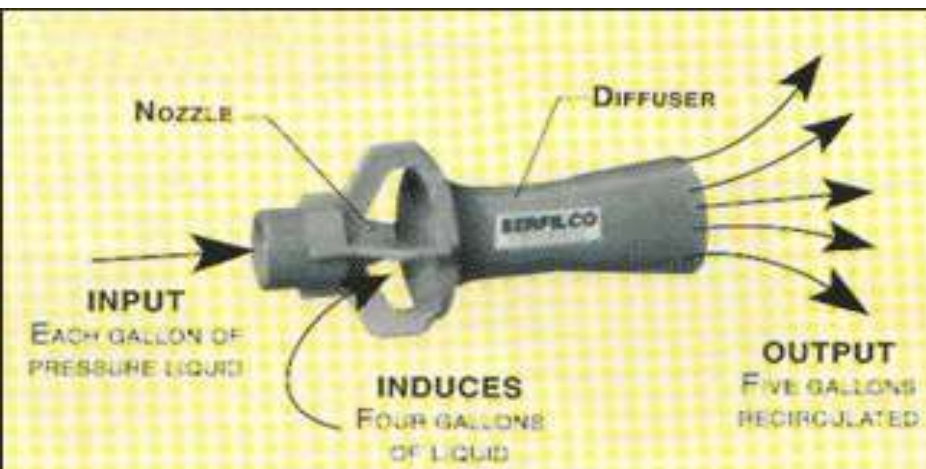
Construction

- **Cooling Coils**

- Water is circulated through these coils to lower the temperature inside the reaction vessel.

Heating or Cooling Medium Out

Heating or Cooling Medium In

Construction

- **Probes**

- Heat transfer probes

- Mass Transfer Probes

- Bubble size measurement probe
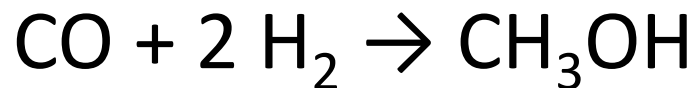
- Temperature probe

Construction

- **Hydro-cloning Section**
- Hydro-cloning section is attached separate to the vessel.

- A Hydro-clone is a static device that applies centrifugal force to a liquid mixture so as to promote the separation of heavy and light components.
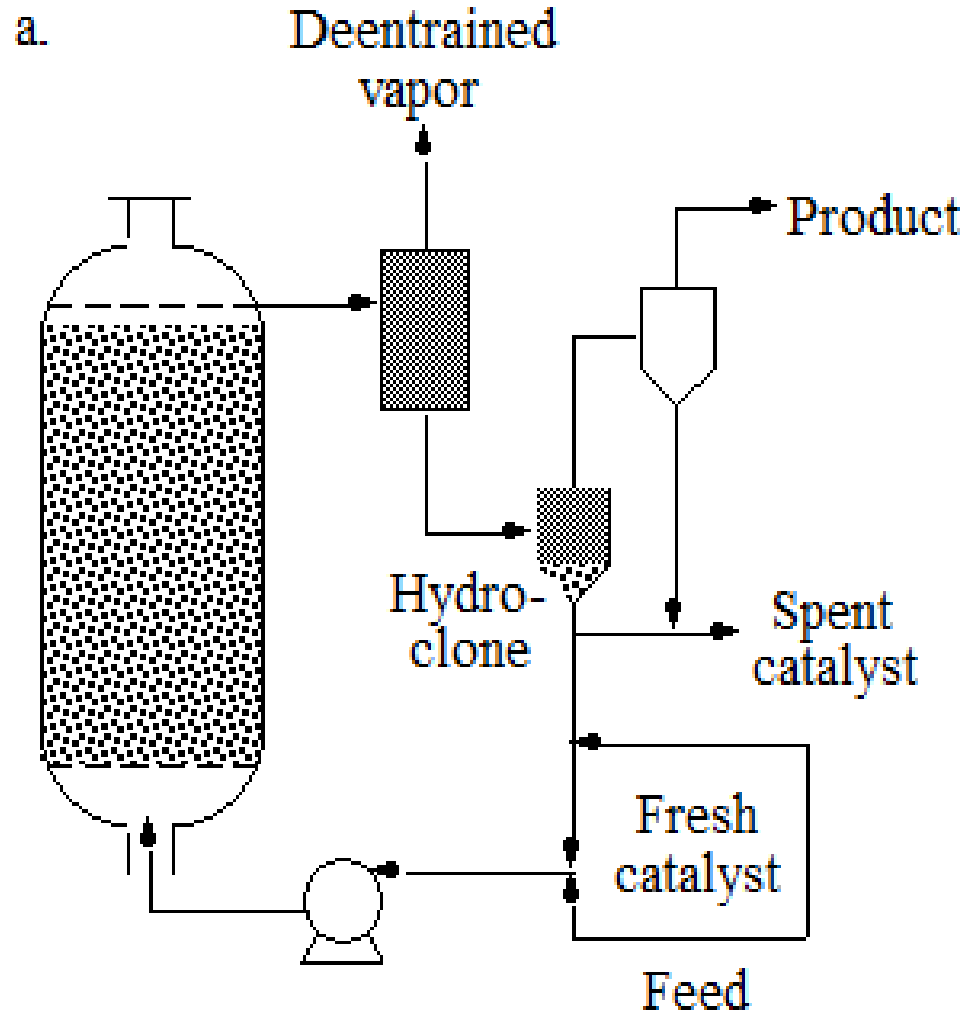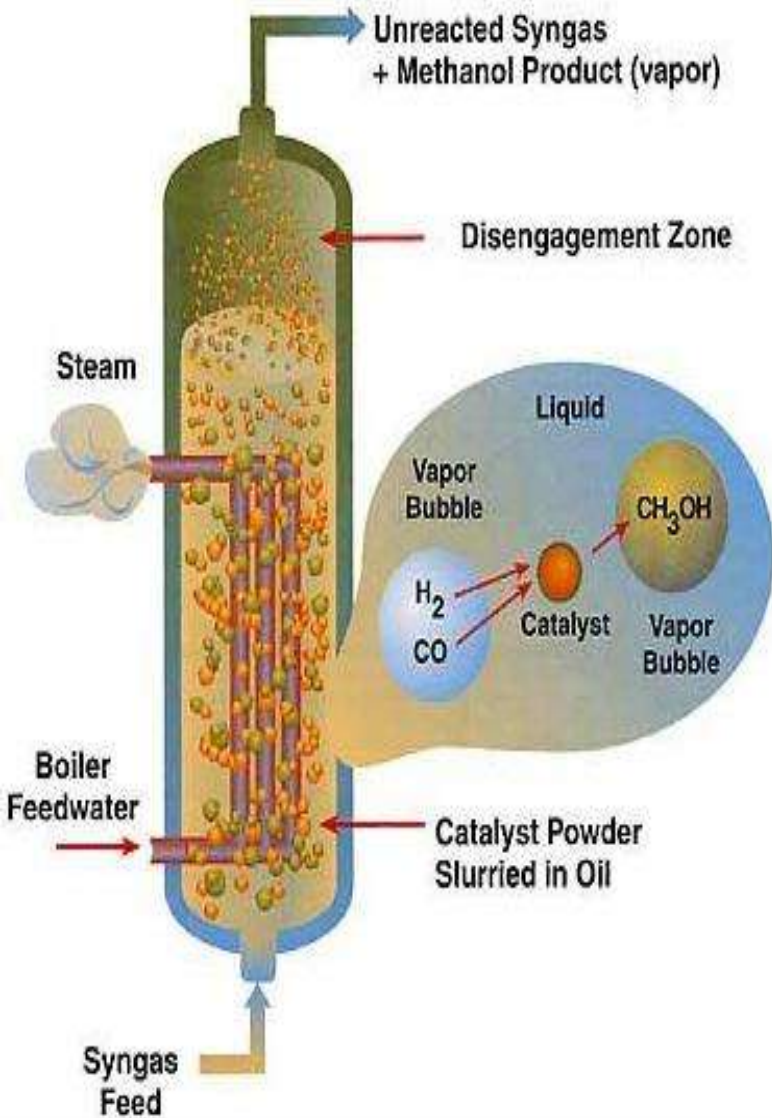
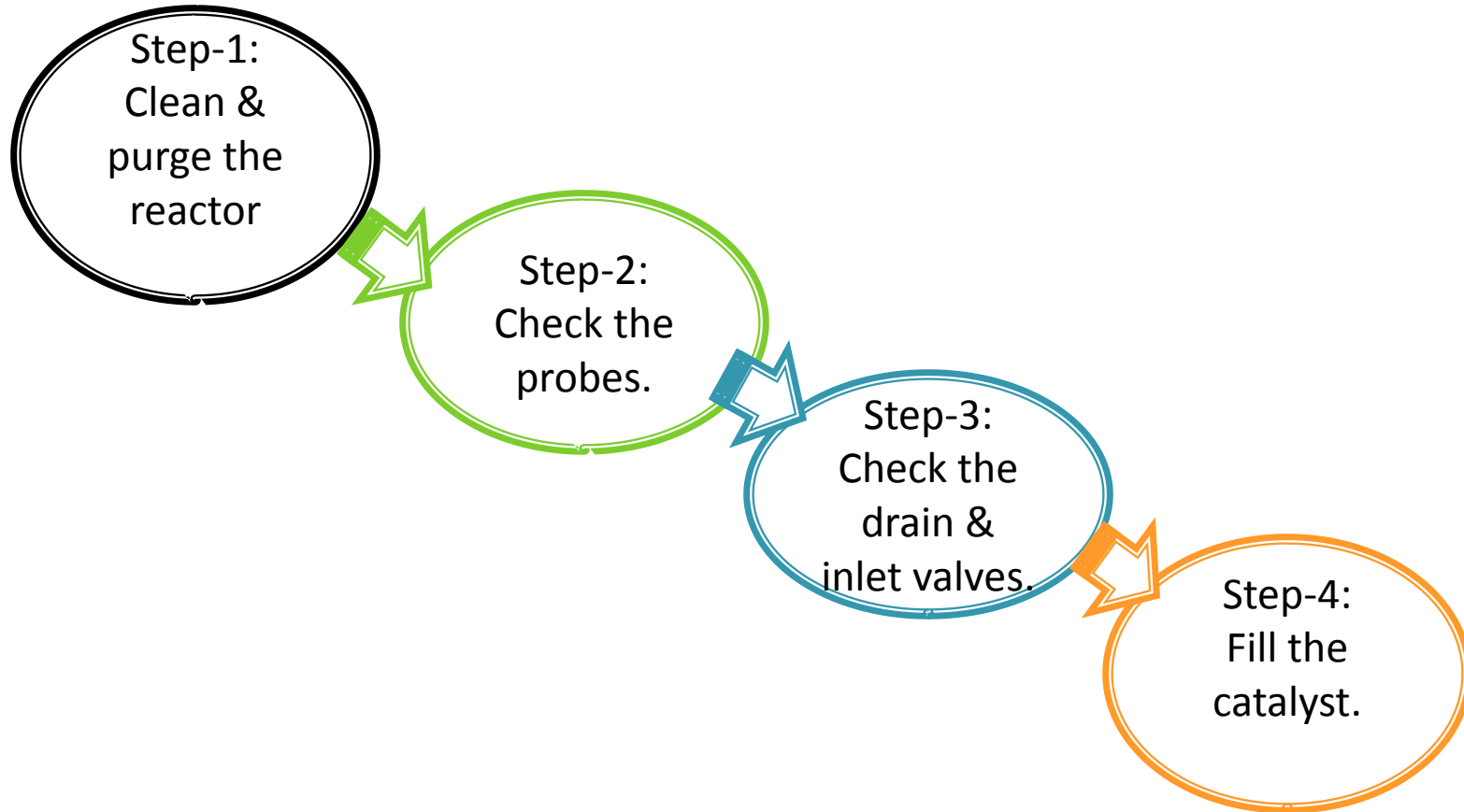# Production of methanol by Bubble column reactor

- Carbon monoxide and hydrogen react over a catalyst to produce methanol.

- Catalyst is a mixture of copper, zinc oxide, and alumina.
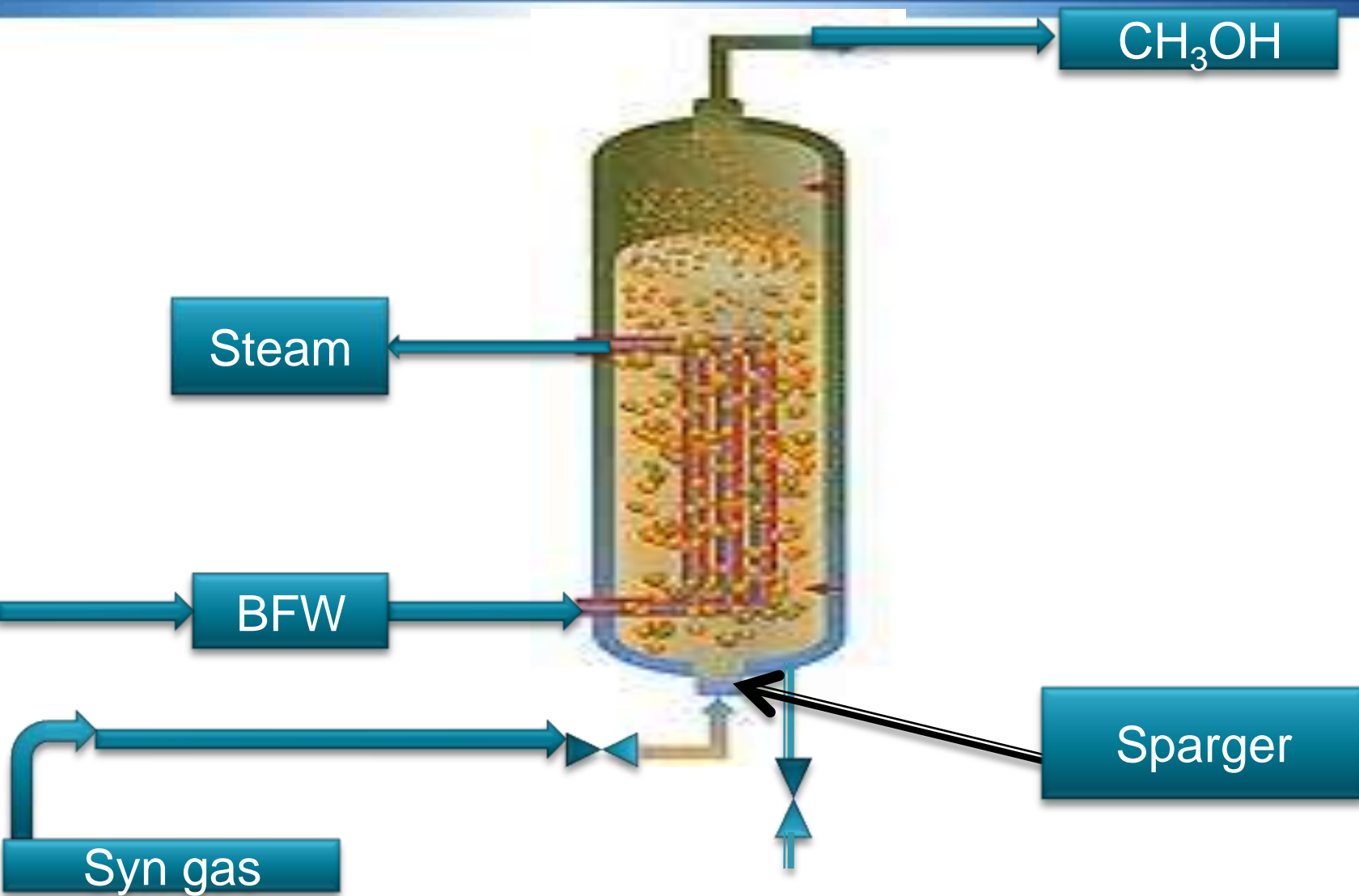
- At 5–10 MPa (50–100 atm) and 250 °C.

$$CO + 2\ H_2 \rightarrow CH_3OH$$

Operation and Working

Unreacted Syngas + Methanol Product (vapor)

Disengagement Zone

Steam

Liquid

Vapor Bubble

CH_3OH

H_2

CO

Catalyst

Vapor Bubble

Boiler Feedwater

Catalyst Powder Slurried in Oil

Syngas Feed

a.

Deentrained vapor

Product

Hydro-clone

Spent catalyst

Fresh catalyst

Feed

Pre-Start up

Step-1: Clean & purge the reactor

Step-2: Check the probes.

Step-3: Check the drain & inlet valves.

Step-4: Fill the catalyst.

CH$_3$OH

Steam

BFW

Syn gas

Sparger

Shut Down

CH$_3$OH

Steam

BFW

Syn gas

Sparger

Shut down

Step-1:
Open the
drain valve.

Step-2:
Remove
the catalyst

Step-3:
Clean the
reactor.

Troubleshooting

problem	cause	consequence	solution
Hot spot formation.	Due to non uniform temperature distribution.	Catalyst will deactivate. Decrease product selectivity.	Rapid removal of large heat of a reaction.
Agglomeration	Uneven distribution of feed gas. Very high superficial velocity of the gas feed.	Mass transfer rate will decrease. product selectivity will decreases.	Change the type of sparger. Low the velocity of gas .
Sparger is not working	Nozzle may be choked	Very low flow rate of syn gas	Clean or replace the sparger

Troubleshooting

problem	cause	consequence	solution
Coagulant formation of solid catalyst in the liquid oil.	Very high temperature.	Agitation will not be done properly.	Regenerate the catalyst.
Orifice of the sparger damage.	Over time	Fine particles of catalyst will enter in the sparger and chock the sparger.	Change the orifice and clean the sparger.

Advantages

- High heat capacity to provide good temperature control.

- Potentially high reaction rate per unit volume of reactor if the catalyst is highly active.

- Easy heat recovery.

- Adaptability to either batch or flow processing.

- The catalyst may readily be removed and replaced if its working life is relatively short.

- Because of high intraparticle diffusion rate, small particles can be used.

Disadvantages

- Generation of fine particles by abrasion of the catalyst.

- Catalyst removal by filtration may provoke problems with possible plugging difficulties on filters, further time of operation, and the costs of filtering systems may be a substantial portion of the capital investment.

- Higher catalyst consumption than that of fixed - bed reactors.

- Back mixed flow and the volume of the reactor are not fully utilized.

Applications

- Stack gas scrubbing with lime or magnesia.
- Waste water treatment.
- Ethylene oxychlorination.
- Oxidation of toluene to benzoic acid.
- Ethylene oxidation to acetaldehyde.
- Olefin polymerization using catalyst suspension.
- Fatty oil hydrogenation with catalytic suspension.

Methanol tank explosion and fire

- On January 11, 2006, an explosion and fire occurred at the City of Daytona Beach, Bethune Point WWTP in Daytona Beach, Florida. Two employees died and one was severely burned after.

- a worker using a cutting torch accidentally ignited vapors coming from the methanol storage tank vent.

- An explosion inside the tank followed, causing the attached piping to fail and release about 3,000 gallons of methanol, which burned.

Reference

- Gandhi, B.; Prakash, A.; Bergougnou, M. A. Hydrodynamic Behavior of Slurry Bubble Column at High Solids Concentrations. *Powder Technol. **1999, 103, 80.***

- Sherwin, M. B.; Frank, M. C. Make Methanol by Three Phase Reaction. *Hydrocarbon Process. **1976, 55, 122.***

- BAHA E. ABULNAGA, P.E. Slurry systems handbook. **1990**

- Deckwer, W.-D.; Bubble Column Reactors; Wiley, 1985. Shimizu K, Takada S, Minekawa K, Kawase Y. Phenomenological model for bubble column reactors: prediction of gas holdups and volumetric mass transfer coefficients. Chem Eng **J 2000;78:21–8.**

Q1: What is trickle bed reactor?

A1: Trickle-bed reactors is most widely used type of three-phase reactors. The gas and liquid co-currently flow downward over a fixed bed of catalyst particles. Concurrent down-flow of gas and liquid over a fixed-bed of catalyst. Liquid trickles down, while gas phase is continuous
In a trickle-bed, various flow regimes are distinguished, depending on gas and liquid flow rates, fluid properties and packing characteristics. Approximate dimensions of commercial trickle-bed reactors are a height of 10 m and a diameter of 2 m.

Q2: What is fluidised bed reactor?

A2: A fluidized bed reactor (FBR) is a type of reactor device that can be used to carry out a variety of multiphase chemical reactions. In this type of reactor, a fluid (gas or liquid) is passed through a granular solid material (usually a catalyst possibly shaped as tiny spheres) at high enough velocities to suspend the solid and cause it to behave as though it were a fluid. This process, known as fluidization, imparts many important advantages to the FBR. As a result, the fluidized bed reactor is now used in many industrial applications

Q3: What are the advantages of fluidised bed reactor?

A3: Advantages of fluidised bed reactor are
 • The smooth, liquid-like flow of particles allows continuous automatically controlled operations with ease of handling.
 • The rapid mixing of solids leads to nearly isothermal conditions throughout the reactor, hence the operation can be controlled simply and reliably.
 • It is suited to large-scale operations.

Q4: What are the disadvantages of fluidised bed reactor?

A4: Disadvantages of fluidised bed reactor are
- The difficult-to-describe flow of gas, with its large deviation from plug flow and the bypassing of solids by bubbles, represents an inefficient contacting system.
- The rapid mixing of solids in the bed leads to non-uniform residence times of solids in the reactor.
- Friable solids are pulverized and entrained by the gas.
  Erosion of pipes and vessels from abrasion by particles

Q5: What are the different types of fluidised bed reactor?
A5: There are different type of FBR such as Fix fluidised bed reactor.circulating fluidised bed reactor.